

**REMOVAL OF ORGANIC COMPOUNDS
FROM AQUEOUS SOLUTIONS
BY ELECTRON RADIATION TECHNIQUE**

by

Piotr R. Lubicki

A thesis

presented to the University of Waterloo

in fulfillment of the

thesis requirement for the degree of

Doctor of Philosophy

in

Electrical Engineering

Waterloo, Ontario, Canada, 1998

© Piotr R. Lubicki 1998



**National Library
of Canada**

**Acquisitions and
Bibliographic Services**

**395 Wellington Street
Ottawa ON K1A 0N4
Canada**

**Bibliothèque nationale
du Canada**

**Acquisitions et
services bibliographiques**

**395, rue Wellington
Ottawa ON K1A 0N4
Canada**

Your file Votre référence

Our file Notre référence

The author has granted a non-exclusive licence allowing the National Library of Canada to reproduce, loan, distribute or sell copies of this thesis in microform, paper or electronic formats.

The author retains ownership of the copyright in this thesis. Neither the thesis nor substantial extracts from it may be printed or otherwise reproduced without the author's permission.

L'auteur a accordé une licence non exclusive permettant à la Bibliothèque nationale du Canada de reproduire, prêter, distribuer ou vendre des copies de cette thèse sous la forme de microfiche/film, de reproduction sur papier ou sur format électronique.

L'auteur conserve la propriété du droit d'auteur qui protège cette thèse. Ni la thèse ni des extraits substantiels de celle-ci ne doivent être imprimés ou autrement reproduits sans son autorisation.

0-612-30623-2

The University of Waterloo requires the signatures of all persons using or photocopying this thesis. Please sign below, and give address and date.

ABSTRACT

Electron beam water treatment is a new, advanced oxidation technology, which is used for decomposition of organic contaminants in water. Very little has been done to estimate an effect of electron radiation parameters on efficiency of the decomposition. The objective of this thesis is to investigate the influence of accelerating voltage, beam current and electron beam power utilization on the removal rate of the compounds, such as: trichloroethylene, benzene, toluene, chloroform and nitrobenzene.

The thesis describes the experiment concerning low and medium energy electron beam water treatment. The design and construction of the lab scale electron beam water treatment apparatus, which has unique features that enable to decompose water contaminants even for low energy of the beam electrons, are explained. The electron beam is generated in high vacuum, pressure is less than 10^{-5} Pa, obtained by the system of rotary, sorption and diffusion pumps. The electron beam is then accelerated and injected into water through electron permeable membrane (transparent window). In the setup the treated water is also used as the window coolant. This provides an opportunity to operate at a relatively high power density of the incident beam (more than about 500 W/cm²). The irradiator can utilize two types of the electron permeable windows: 1. 15 μm and 25 μm titanium foils (measured current transmission at 100 kV is 57% and 25%, respectively), 2. 10 μm boron nitride ceramic window (measured current transmission at 100 kV is 95%).

The dependence of relative concentration of the contaminants on radiated and absorbed dose of electron radiation is presented. Additionally, by-products and intermediates distribution depending on the absorbed dose during benzene removal is analyzed. The absorbed dose was calculated on the basis of the measured power loss occurring while the electron beam passes through the transparent window. The obtained results suggest that the relative content of organic contamination decreases exponentially with an increase in the absorbed dose. It has been found that a substantial removal of the investigated contaminants (80-99%) can be obtained for relatively low accelerating voltages range (100-180 kV). The use of such a low voltage level can result in a significant simplification of X-ray shielding and insulation systems that further would allow to design and build an energy efficient, portable water irradiation apparatus.

The closed water circulation system enables to adjust the dose of electron radiation, not only by the beam power and flow rate of the treated water, but also by varying the total treatment time. In this case, the dose of radiation needed for required removal of a given contaminant can be calculated on the basis of low voltage and low current measurements. The dose can then be converted into a high power commercial system, provided that the power absorbed per unit volume is the same, so that the beam power and flow rate can be adjusted in order to obtain the required decomposition of the contaminant.

ACKNOWLEDGEMENTS

I would like to thank my supervisors Professor James D. Cross and Professor Shesha Jayaram for their support throughout this study. Without their advice this thesis could not have been written.

I would like to express my appreciation to the faculty staff of the Water Research Group, Civil Engineering Department of the University of Waterloo, for their assistance and help in the field of Water Treatment Technology.

I am also thankful to Mr. Terry Weldon of the High Voltage Laboratory and Mr. Mark Sobon of the Civil Engineering Department for their technical help.

I am grateful to Dr. Arnold Kelly of Charged Injection Corporation for his help in providing electron permeable membranes and for sharing the knowledge about the boron nitride layers.

Financial assistance provided by Electrical and Computer Engineering Department and by my supervisors through grants awarded by Natural Sciences and Engineering Research Council of Canada is greatly appreciated.

Special thanks are due to Professor Boleslaw Mazurek of Wroclaw University of Technology, Wroclaw, Poland, for suggesting to work with Professor James D. Cross on the interesting and exciting project.

Finally, I would like to express my deep appreciation to my wife Danuta for her patience and unconditional support.

Dedicated to dear son, Robert

TABLE OF CONTENTS

Author's declaration	(ii)
Borrower's page	(iii)
Abstract	(iv)
Acknowledgments	(vi)
Dedication	(vii)
Table of contents	(viii)
List of Tables	(x)
List of Figures	(xii)
CHAPTER 1. INTRODUCTION	1
CHAPTER 2. ELECTRON BEAM WATER TREATMENT	6
2.1. Electron beam water treatment - radiation technology	6
2.2. Electron beam water treatment - radiation chemistry of aqueous solutions	17
2.3. Electron beam water treatment - energy efficiency and cost	28
CHAPTER 3. AIM OF THE PRESENT STUDY	38
CHAPTER 4. EXPERIMENTAL SETUPS	40
4.1. Electron gun and cathode system	40
4.2. Isolating transformer and filament heating	48
4.3. Vacuum chamber and high vacuum system	53
4.4. Anode (window housing) and water flow system	56

4.5. Titanium and boron nitride electron permeable windows	59
4.6. Electron beam laboratory scale apparatus for water purification	69
CHAPTER 5. RESULTS - REMOVAL OF	
VOLATILE ORGANIC COMPOUNDS	74
5.1. Removal of benzene, toluene and trichloroethylene	74
5.1.1. Effect of beam power utilization	76
5.1.2. Effect of accelerating voltage and electron beam current	80
5.2. Removal of chloroform	84
5.3. Removal of volatile organic compounds depending on absorbed dose	86
5.4. By-products and intermediates during e-beam benzene removal	94
CHAPTER 6. RESULTS - REMOVAL OF NITROBENZENE	100
CHAPTER 7. DISCUSSION AND CONCLUSION	103
REFERENCES	111

LIST OF TABLES

<u>Table 1.1.</u> Typical organic contamination found in different water treatments [1,3].	2
<u>Table 2.1.</u> Existing electron beam water treatment facilities - based on work [22].	8
<u>Table 2.2.</u> Fundamental radiochemical reactions [27].	18
<u>Table 2.3.</u> Estimated amount (in millimoles) of reactive species generated at different absorbed doses using high-energy electron beam irradiation [19].	21
<u>Table 2.4.</u> Rate constants (in moles ⁻¹ x second ⁻¹) of selected organic chemicals and the free radicals formed in irradiated aqueous solution [9,12,54].	25
<u>Table 2.5.</u> Summary of electron beam removal of various organic compounds [13,14,19].	27
<u>Table 4.1.</u> Work function and melting point of materials used for electron emitters [58]	41
<u>Table 4.2.</u> Physical properties of titanium and boron nitride [85-94].	62

Table 4.3. Power density at the time of window implosion

for four different membranes.

66

Table 7.1. Estimated values of the rate constant k for the

investigated contaminants.

104

LIST OF FIGURES

- Figure 2.1.** Penetrated mass per unit area as a function of electron energy [33]. 10
- Figure 2.2.** Dependence of the power $p_v(z)$ per unit volume absorbed at a distance z from the surface referred to the maximum value of $p_{v,max}$ for polyethylene ($d=0.94 \text{ g/cm}^3$) - energy $E=1.5 \text{ MeV}$: 1. measured; 2. approximation according to eqn. 2.5 [27]. 12
- Figure 2.3.** Sequence of events in radiation chemistry of pure water [42]. 20
- Figure 2.4.** Electron transmission at normal angle of incidence through $25 \mu\text{m}$ Al and Ti foils as a function of electron energy - beam current losses and energy losses [28,59]. 29
- Figure 2.5.** Determination of dose depth distribution and absorption fractions in the irradiated matter for the: a) single sided radiation - 300 keV ; b) double sided radiation - 500 keV [28]. 31

<u>Figure 4.1.</u> Saturation current density of some customary cathode materials versus cathode temperature: I. LaB₆ on carbonized tantalum; II. tantalum solid; III. tungsten solid. Operating ranges are indicated by bold lines [27].	43
<u>Figure 4.2.</u> Hairpin filament electron gun with Wehnelt electrode and self-biasing circuit.	44
<u>Figure 4.3.</u> Commercial dispenser cathode electron gun.	46
<u>Figure 4.4.</u> Isolating transformer.	50
<u>Figure 4.5.</u> Self-oscillating inverter filament heating circuit.	51
<u>Figure 4.6.</u> Filament heating circuit utilizing function generator and amplifier.	52
<u>Figure 4.7.</u> Vacuum chamber and X-ray shielding.	54
<u>Figure 4.8.</u> Vacuum system for electron beam water treatment apparatus.	55
<u>Figure 4.9.</u> The hairpin filament (made of 0.5 mm wire) lifetime vs. pressure.	57
<u>Figure 4.10.</u> Anode with window housing and water flow system.	59

<u>Figure 4.11.</u> Current transmission fraction vs. accelerating voltage for three types of windows: 15 and 25 μm thick titanium, and 10 μm thick boron nitride.	64
<u>Figure 4.12.</u> Energy loss of electron beam for 10 μm thick boron nitride window.	65
<u>Figure 4.13.</u> Methods of mounting 10 μm thick boron nitride membranes in anode: a) windows with diameter less than 5 mm; b) windows with diameter greater than 5 mm.	68
<u>Figure 4.14.</u> The schematic diagram of electron beam water treatment apparatus.	70
<u>Figure 4.15.</u> The photograph of electron beam apparatus used for water purification.	73
<u>Figure 5.1.</u> Relative concentration of TCE vs. radiated dose for three different types of windows.	77
<u>Figure 5.2.</u> Relative concentration of toluene vs. radiated dose for three different windows.	78
<u>Figure 5.3.</u> Relative concentration of benzene vs. radiated dose for three different windows.	79

Figure 5.4. Relative concentration of benzene vs. radiated dose for two different values of accelerating voltage: 125 kV ($C_0=9.5$ ppm) and 175 kV ($C_0=10.1$ ppm). 82

Figure 5.5. Relative concentration of benzene vs. radiated dose for two different values of incident electron beam current: 0.8 mA ($C_0=12.9$ ppm) and 1.12 mA ($C_0=13.0$ ppm). 83

Figure 5.6. The dependence of the relative content of chloroform on the radiated dose for 25 μm thick Ti window using electron beam at $V_A=170$ kV and $I=1.1$ mA. 85

Figure 5.7. The dependence of the relative concentration of trichloroethylene vs. the estimated absorbed dose for two kinds of electron permeable windows. 89

Figure 5.8. The dependence of the relative content of chloroform on absorbed dose for two different values of the incident beam powers: $P_0=63$ W, $V=115$ kV, $I=0.55$ mA, and $C_0=49.8$ ppm; and $P_0=187$ W, $V=170$ kV, $I=1.1$ mA, and $C_0=89.1$ ppm. 90

<u>Figure 5.9.</u> Relative content of toluene vs. absorbed dose of electron radiation.	91
<u>Figure 5.10.</u> Relative concentration of benzene vs. absorbed dose of electron radiation.	92
<u>Figure 5.11.</u> The dependence of benzene and total phenol concentrations on the estimated absorbed dose of electron beam radiation.	95
<u>Figure 5.12.</u> The dependence of the concentrations of benzene and total aldehydes on the estimated absorbed dose of electron beam radiation.	97
<u>Figure 5.13.</u> The dependence of the concentrations of benzene and total carboxylic acids intermediates on the estimated absorbed dose of electron beam radiation.	98
<u>Figure 6.1.</u> The dependence of the relative concentration of nitrobenzene vs. the estimated absorbed dose for 10 μm thick BN window and incident beam power $P=40\text{ W}$ (accelerating voltage $V_A=100\text{ kV}$ and electron beam current $I_B=0.4\text{ mA}$).	102

CHAPTER 1

INTRODUCTION

In the last three decades very rapid industrial growth has been a major cause of contamination of ground and surface water sources. Recently, it has been realized that even trace quantities of organic contaminants in drinking water are hazardous, in particular aromatic and aliphatic hydrocarbons and their halogenated compounds. Many of these chemicals are proven or suspected carcinogens [1,2]. As a result of increased industrialization, a lack of relatively clean drinking water sources requires contaminated water sources to be used after purification treatment. The above mentioned difficulties, along with increasingly strict local and global regulations (maximum contaminant level - MCL - has been constantly lowered as the knowledge about hazardous contaminants has been increasing [3]) enacted to limit the concentration of hazardous compounds in a final water product, have led to a search for new efficient technologies to remove or avoid such a contamination.

The contamination of drinking and waste water by organic hydrocarbons can generally take place in two different ways: 1. the compounds can arise from industrial wastes, and 2. can be formed during chemical disinfection of water by means of either chlorine or ozone. Hydrocarbons, such as toluene, benzene, xylene, nitrobenzene, phenols, trichloroethylene (TCE), and tetrachloroethylene (PCE), and many others can be introduced to the ground and surface waters as industrial waste. Halogenated

hydrocarbons can be found in drinking water as a consequence of disinfection with chlorine, which has been the most common way to disinfect drinking water in North America since the beginning of the 20th century. Disinfection with ozone, the technique which has commonly been utilized in Europe, can cause the formation of formaldehydes, bromate BrO_3^- , and organic compound peroxides. Table 1.1 shows organic contaminants that can be found in water in different kinds of treatments. All these contaminants pose a potential health threat to human populations - most of them are fairly resistant to chemical or biological degradation.

Table 1.1. Typical organic contamination found in different water treatments [1,3].

Kind of Treatment	Typical Contaminants
Drinking Water Treatment	trihalomethanes, bromate
Wastewater/Groundwater Treatment	trichloroethylene, tetrachloroethylene, hexachloroethane, carbon tetrachloride, methylene chloride
Groundwater Treatment	benzene, toluene, chlorobenzene, total phenol, ethylbenzene, xylene

The chlorination of drinking water may lead to the formation of various halogenated hydrocarbons (trihalomethanes - THM) as a reaction with chlorine by-products [1-5]. The primary use of chlorination in water treatment is disinfection, with a

secondary role being taste and odor control by water oxidation. When waters containing naturally occurring humic substances are chlorinated, chloroform (CHCl_3) is formed, and in the presence of even trace quantities of bromide ions, bromodichloromethane, chlorodibromomethane, and bromoform (CHBr_3) may result [1-3]. All of the THM are known to be carcinogens and a total amount of four THM in drinking water has been regulated at a maximum contaminant level (MCL) of $100 \mu\text{g/l}$ [3]. It is probable that either MCL will be established in the future for the individual compounds or will be lowered to $10\text{-}25 \mu\text{g/l}$ in North America [1,3]. The content of THM has been controlled by removal of either precursor chemicals, i.e. humic substances, or THM after their formation. Lately, attention has been focused on possibilities of THM removal, because precursor removal, the most common approach, is not economically feasible [1].

The degradation of most of the above mentioned contaminants is often not very sufficient with the use of common water treatment techniques [1,3]. The decomposition of these contaminants in water necessitates the development of treatment technologies capable of degrading these compounds from a variety of matrices, as the total amount of THM formed during chlorination depends on physico-chemical properties of a water source. One potentially efficient method of destroying hydrocarbons is through the chemical oxidation by hydroxyl radicals (OH^\cdot) [2,4-8]. These are commonly generated by ozonation and even more effectively by ozonation combined with ultraviolet radiation and hydrogen peroxide treatment [1,9-12]. Recently, it has been found that electron beam water treatment is also a very effective way to generate a relatively high

amount of hydroxyl radicals [13-25]. Conventional methods that have been used for the removal of the THM from water are air stripping, activated carbon adsorption, and oxidation with ozone [2,4-6].

Air-stripping offers a relatively inexpensive way to remove volatile contaminants; however, the pollutants are simply transferred to another medium. Activated carbon, although studied extensively, does not destroy the compounds - they are also transferred to activated carbon which may pose a problem with its disposal after the use - and if the MCL are to be lowered, this equilibrium-controlled method will become rather expensive (cost of activated carbon per year could reach as much as one million US dollars) [1,3]. Ozonation may be combined with ultraviolet light or hydrogen peroxide to ultimately remove THM. However, in order for this technique to be effective and efficient, long reaction times are necessary [1,3]. Additionally, the ozonation is not energy efficient, because of a relatively low efficiency of ozone production using ac high voltage methods [2] and a limited solubility of this gas in water [4].

It has recently been shown that high-energy electron beam irradiation in combination with ozone is effective for THM precursors removal [3]. It has also been shown that the electron beam process alone is effective in removing various organic contaminants from water sources as well as in removing THM and bromate contained in drinking water [1,3,11,13,14,18,24]. The high energy electron beam irradiation technique in which the electrons initiate chain reactions that further decompose toxic

molecules into other products, has been found to be the most promising technology for degradation of hydrocarbons in drinking, ground, and waste water treatment.

CHAPTER 2

ELECTRON BEAM WATER TREATMENT

2.1. Electron beam water treatment - radiation technology

In the last few decades electron beam technology has become substantially more important all over the world. This development is a result of the new possibilities in the face of environmental constraints and generally highly productive processes that are amenable to automation. Low, medium and high voltage electron beam facilities have been widely used in thermal techniques, such as: evaporation, welding, melting, electron beam machining, treatment for refining and hardening, annealing of implantation damages, and heat treatment of metal strips [26,27]. The electron beam has also been used in radiation techniques, for instance: cross-linking of polymers, vulcanization of natural and synthetic rubber, paint curing, polymerization and depolymerization, sterilization of food, medical products, and municipal sewage [22,23,26-30]. Most recently, electron beam radiation has been used within a scope of advanced oxidation technologies for radiation purification of water [18-23,31,32] and flue gases [22,31,32]. The dominating applications in the electron beam radiation field are: cross-linking of cable insulation, electronic treatment of plastic films and tubes, and sterilization of medical products and food [22,27]. The electron beam treatment of sewage sludge, water and flue gases has still been in a developmental stage [22,23]. In

all of the above mentioned cases, processing at a high rate, low processing temperatures, and the low specific energy expenditure can be seen as benefits of electron beam radiation. Since the reaction process in electron beam radiation technology requires no catalysts and activators, or any other additives, the relatively pure final product may be obtained. In all of the cases where thickness of the irradiated matter does not require an application of γ - or X-rays, the use of electron beam is advantageous. In general, the advantages of electron beam application in radiation processing can be summarized as follow [27]: 1. ability to direct radiation exactly to the point of action; 2. free choice of electron energy and power and thus facility for matching processing requirements; 3. implementation of high dose rates; 4. controlling and disconnecting of radiation source; 5. availability of high beam powers (1 kW of beam power corresponds to the activity of 70 kCi - kilocurie - for common source of γ radiation Cobalt-60). The above mentioned advantages and the recent increase in the beam power of irradiation facilities have caused the increasing use of electron beam irradiation techniques over the other kinds of radiation.

Although pilot facilities utilizing electron beam (see Table 2.1), and γ -ray radiation (Moscow 1973 [22, 33]), for radiolytical oxidation of sewage sludge and aqueous animal wastes existed in laboratory scale as early as in the 70s and 80s, the interest in the use of electron beam for killing of septics and for decomposing of chemical contaminants in water has grown significantly since 1989. At this time the largest test facility for electron beam water treatment in North America, the Electron

Beam Research Facility (EBRF) at the Virginia Key Wastewater Treatment Plant in Miami, Florida, started being utilized. This 1.5 MeV unit (beam current up to 50 mA) has been used for a range of experiments and these have led to a still increasing interest in this topic [3,10,13-21].

Table 2.1. Existing electron beam water treatment facilities - based on work [22].

Facility	Energy [MeV]	Power [kW]	Treatment
Deer Island Electron Research Facility, Boston, USA	1.5	225	Drinking Water Sewage Sludge
Takasaki Radiation Chemistry Establishment, Takasaki, Japan	2.0	100	Drinking Water Sewage Sludge
EOL-400 Facility, Moscow, Russia	1.0	28	Liquid Animal Waste
ELV Facility, Voronezh, Russia	1.0	50	Industrial Waste (emulsifiers)
Electron Beam Research Facility, Virginia Key Plant, Miami, USA	1.5	75	Sewage Sludge Industrial Waste Drinking Water

The three main areas of interest in the purification of water and wastewater by means of electron beam radiation have been so far [22,31,32]: 1. electron beam treatment of natural and polluted drinking water; 2. radiation purification of industrial

liquid wastes; 3. radiation treatment of sewage sludge. For drinking water, attention has been directed toward the radiation-chemical decomposition of halogenated hydrocarbons, in particular trihalomethanes. The possibility of a decomposition of aromatic and aliphatic hydrocarbons and their compounds has been used in electron beam purification of industrial wastes. To inactivate microorganisms and to accelerate sedimentation and filtration - it facilitates dewatering - have been the main advantages of electron beam treatment of sewage sludge [23]. In all of the above mentioned cases, electron radiation has also been used in combination with other techniques, such as ozonation and biodegradation [31,32].

In drinking and wastewater treatment, the energy of the electrons used for irradiation is within the range of 1.0-2.0 MeV [18,22,23]. The suitable adjustment of water layer thickness and flow velocity can provide one with a radiation dose determined experimentally, that is high enough for decomposition of the chemicals. The penetration depth or electron range (R_e) of electrons into an irradiated matter depends mainly on kinetic energy (accelerating voltage V_A) of electrons and on mass density (d) of an irradiated material. The dependence of the penetration depth on the accelerating voltage is non-linear due to secondary processes, such as backscattering and emission of secondary electrons, and can be approximated using the following equations [27]:

$$R_e \approx 2.1 \times 10^{-12} \frac{V_A^2}{d} \quad [\text{cm}] \quad \text{for } 10 \text{ keV} < eV_A < 100 \text{ keV}, \quad (2.1)$$

$$R_e \approx 6.67 \times 10^{-11} \frac{V_A^{5/3}}{d} \quad [\text{cm}] \quad \text{for } 100 \text{ keV} < eV_A < 1 \text{ MeV}, \quad (2.2)$$

$$R_e \approx \frac{1}{d} (5.1 \times 10^{-7} V_A - 0.26) \quad [\text{cm}] \quad \text{for } eV_A > 1 \text{ MeV.} \quad (2.3)$$

where V_A is in [V] and d is in [g/cm^3]. As can be seen in Fig. 2.1, the utilized accelerating voltages in pilot plants can allow electrons to penetrate the water (mass density of $1 \text{ g}/\text{cm}^3$) within the range of 0.3-1 cm [22,23,33,34].

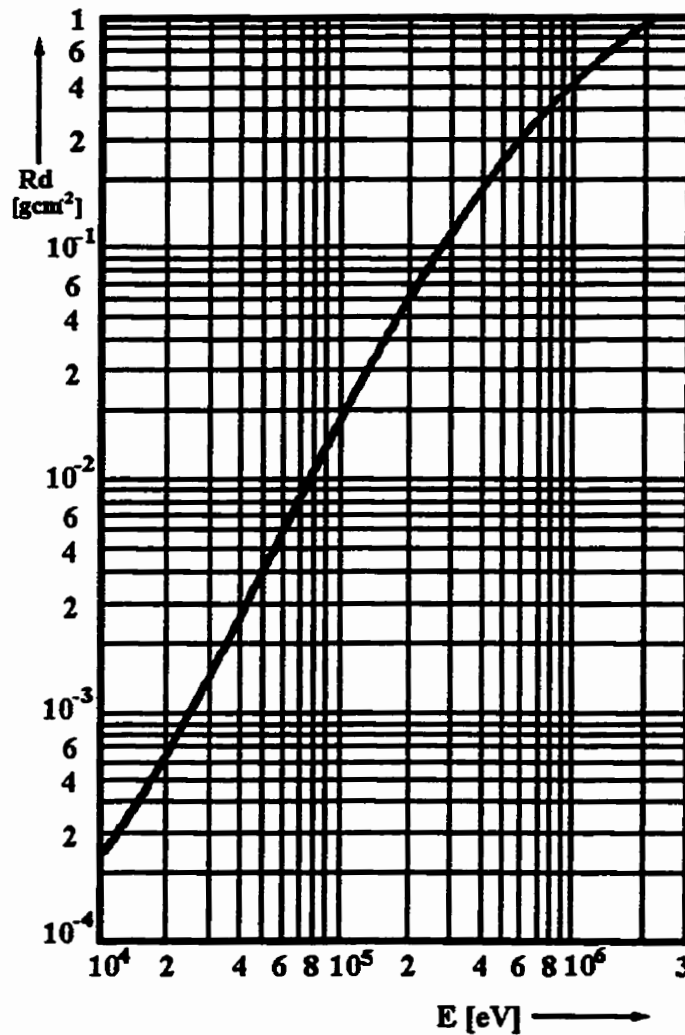


Figure 2.1. Penetrated mass per unit area as a function of electron energy [33].

In electron beam radiation techniques, the absorbed dose A is used as a measure of the radiation energy required to produce important radiochemical changes. Its commonly used units are gray, Gy, (1 Gy=1J/1kg) and rad (1 Gy=100 rad). As practicable quantities, the megarad (Mrad), kilorad (krad) and kilogray (kGy) are usually used. The dose rate A_t is the dose absorbed per unit time. The dose and the dose rate are related to absorbed energy e_v per unit volume or to power absorbed p_v per unit volume by means of mass density d of an irradiated material:

$$e_v = d A \quad [\text{J/m}^3], \quad p_v = d A_t \quad [\text{W/m}^3] \quad (2.4)$$

In general the absorbed dose and dose rates are described by time-dependent, three-dimensional position functions [26,27]. The dose distribution to be implemented depends on the irradiation problem, such as the kind of contamination to be decomposed in the case of water treatment.

The energy absorption over the electron range shows non-uniform distribution [22,27,36,37]. This means that the absorbed power per unit volume is a function of distance from the hit surface. This relation shown in Fig. 2.2 is almost independent on beam energy and can be approximated by equation 2.5 [27]:

$$\frac{p_v(z)}{p_{v,max}} = 1 - \frac{9}{4} \left(\frac{z}{R_e} - \frac{1}{3} \right)^2 \quad (2.5)$$

where $p_v(z)$ is the power absorbed per unit volume at a distance z from the irradiated surface; $p_{v,max}$ is the maximum value of the power absorbed per unit volume at a distance $z=R_e/3$ from the incident beam surface; z is the distance coordinate pointing

from the incident beam surface into the matter. The absorbed power reaches maximum at about one-third of the electron range.

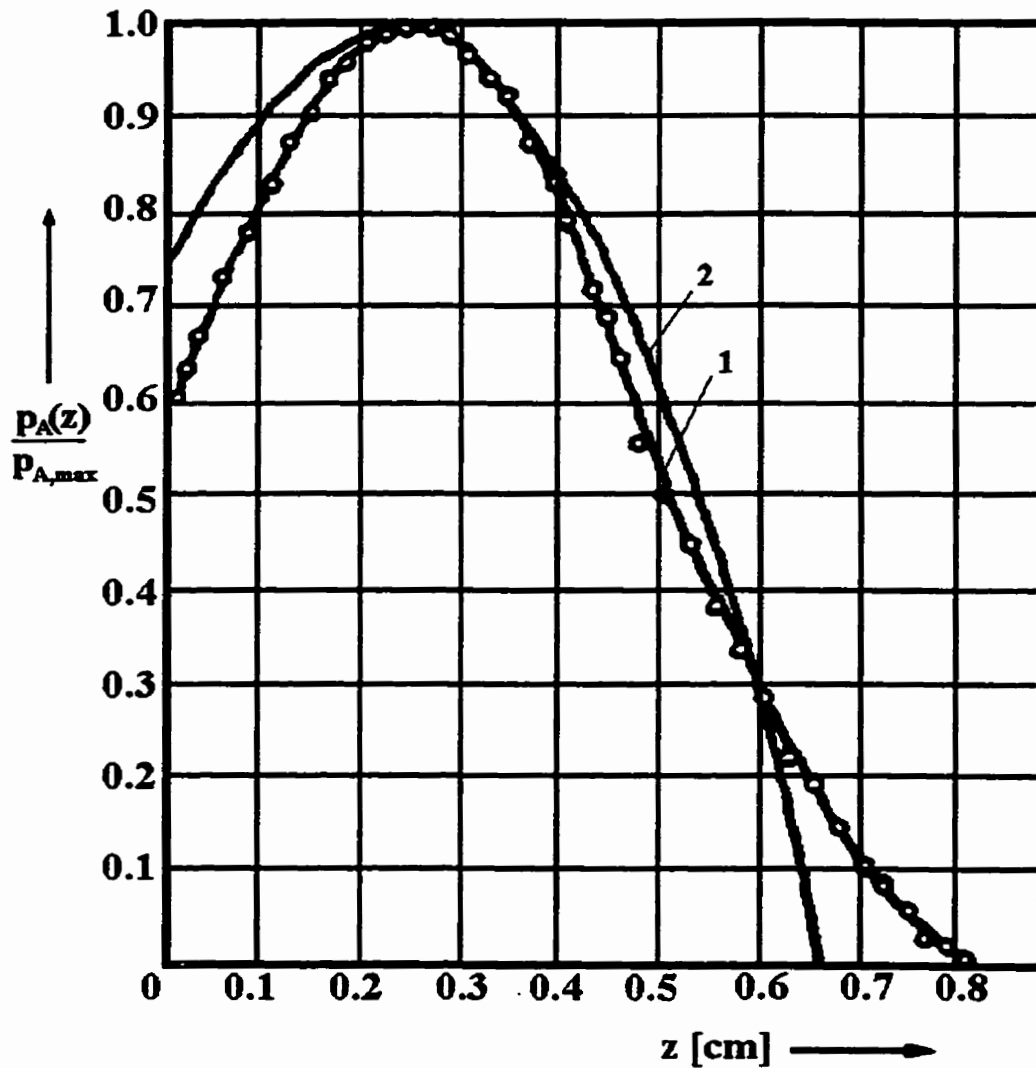


Figure 2.2. Dependence of the power $p_V(z)$ per unit volume absorbed at a distance z from the surface referred to the maximum value of $p_{V,max}$ for polyethylene ($d=0.94$ g/cm³) - energy $E=1.5$ MeV: 1. measured; 2. approximation according to eqn. 2.5 [27].

This irregularity does not have a substantial effect on the electron beam processing in the case of thermal techniques, such as welding and melting, because the

temperature differences over the electron range are compensated by thermal conduction. In electron beam non-thermal and irradiation processes; where the desired effect is closely related to the radiation energy absorbed per unit volume, such an energy-depth dependence is likely to have a strong effect on the final product. This relationship must also be taken into account in the design of electron permeable windows.

Types of electron beam devices used in electron beam radiation processing require that the beam pass out of a vacuum chamber in which the electron beam is generated. The vacuum chamber or electron gun housing is provided with a window for passage of the electron beam, so that the beam can be directed toward the workpiece positioned outside of the chamber. The window must be covered with a membrane which permits passage of the electron beam to the outside of the chamber, but which blocks passage of air or other fluids into the chamber so as to preserve the vacuum within the housing. Especially in the case of high-power and low- and medium-energy electron beams, it is the transparent window that is of special importance, because of a relatively high beam power absorption in the window [22,32]. Dynamic pressure stages can not be used due to a big exit surface requirement for a high throughput capacity of the processing, although the attempts have been made to develop the aerodynamic window system to be used with differential pumping [32]. The membrane material for an electron transparent window must have the following characteristics [27,38]:

1. high tearing strength to density ratio - this means that the window material must permit the electrons to pass with a little attenuation (low density gives a high electron

range at a decent accelerating voltage) and at the same time must have a high mechanical strength to withstand a differential pressure encountered in service;

2. availability as a foil or layer material - the requirement for low absorption of the electrons within the window material leads to a strong preference for very thin membranes. If the membrane absorbs a substantial fraction of the electrons in the beam, the energy imparted may heat the membrane and eventually cause a destruction of the membrane. At the same time, the membranes must be robust enough to enable mounting them in a whole device without damages or a loss of mechanical strength;

3. dense structure and thus impermeable to gases - a high vacuum inside the chamber must be preserved for long period of time;

4. high-temperature stability in the irradiation atmosphere - because there is always some power that is absorbed in the membrane, even for the cooled windows, the temperature rise may be significant and it remarkably affects mechanical properties of the material. Furthermore, especially when metal foils are used, the lifetime of the window may be strongly affected by hydrogen diffusion from irradiation atmosphere causing an embrittlement of the foil [27].

The lifetime of the window is affected when these requirements are not met. In commercial electron beam radiation facilities, which utilize electron energies above approximately 300 keV, the requirements can best be satisfied by titanium and aluminum foils or by their alloys [27,32]. The usual thickness of the foil is about 25 μm which enables to build big air-cooled windows (up to 1 m long and up to 0.1 m wide) for

scanned electron beams [26,27]. In the case of low electron energies, very thin membranes formed from materials having inherently low electron absorptivity - typically boron, silicon, aluminum and their hydrides, carbides, or nitrides - are preferred [38,39]. These materials however are inorganic ceramics and can only be used for small electron permeable windows due to their brittleness. Generally, the efficiency of electron beam transfer through the window depends on the accelerating voltage; the higher the voltage, the lower the relative losses in the window material. Although the use of high electron energies enables to obtain relatively high penetration depth of electrons, it must be noted that the increase in accelerating voltage does not cause an increase in radiation power absorbed per unit volume.

Above all, characteristic performance parameters of the various electron beam processes are [27]: 1. beam power - P_0 ; 2. accelerating voltage - V_A ; 3. surface power density - p_0 and 4. beam diameter - ϕ_0 , both at the point of action. Derived from the accelerating voltage, V_A , and beam current, I_B , the beam power is:

$$P_0 = V_A \cdot I_B, \quad (2.6)$$

and the beam power density at the point of action is:

$$p_0 = \frac{V_A \cdot I_B \cdot 4}{\pi \cdot \phi_0^2} = V_A \cdot j, \quad (2.7)$$

where j is current density in the point of action. Then, the power absorbed per unit volume is described by:

$$p_A = \frac{P_0}{\text{Volume}} = \frac{\eta \cdot V_A \cdot j}{R_e}, \quad (2.8)$$

where p_A is power absorbed per unit volume; η is ratio of absorbed beam power to incident beam power, η is always less than 1 and it includes among others energy and current losses of the electrons in the window material; R_e - penetration depth of electrons. Substituting equations 2.1, 2.2 and 2.3 for electron range, one can finally get the expressions for power absorbed per unit volume for three different ranges of electron energies:

$$p_A = \frac{\eta \cdot V_A \cdot j}{R_e} = \frac{\eta \cdot d}{2.1 \times 10^{-12}} \cdot \frac{j}{V_A} \quad \text{for } 10 \text{ keV} < eV_A < 100 \text{ keV} \quad (2.9)$$

$$p_A = \frac{\eta \cdot V_A \cdot j}{R_e} = \frac{\eta \cdot d}{6.67 \times 10^{-11}} \cdot \frac{j}{V_A^{2/3}} \quad \text{for } 100 \text{ keV} < eV_A < 1 \text{ MeV} \quad (2.10)$$

$$p_A = \frac{\eta \cdot V_A \cdot j}{R_e} = \eta \cdot d \cdot \frac{j \cdot V_A}{5.1 \times 10^{-7} \cdot V_A - 0.26} \quad \text{for } eV_A > 1 \text{ MeV} \quad (2.11)$$

where d is mass density of an irradiated material. From the above equations, it can clearly be seen that the power absorbed per unit volume can only be increased by means of increasing the current density at the point of action, but never by a rise in accelerating voltage. This is especially important in the case of low and medium energies of

electrons. The density of power absorbed in matter plays a major role in non-thermal electronic processes that include electron beam radiation [27].

2.2. Electron beam water treatment - radiation chemistry of aqueous solutions

In the electron beam radiation processes, among others in water treatment, an electron beam is used for inducing chemical reactions to produce chemical and physical changes in the irradiated matter. The action of electron beams on chemical compounds causes interactions owing to the excitation or ionization of molecules. Thus, chemical reactions may occur that are capable of producing new compounds or bonding types. The irradiated matter then exhibits new or quantitatively changed chemical and physical properties. Table 2.2 shows fundamental radiochemical reactions taking place while the electrons are acting on the irradiated matter. The beam electrons first produce primary reactions for the excitation or ionization of molecules taking place at comparable rates. The first reaction step is usually finished in 10^{-10} seconds after the moment of irradiation [22,40-42]. The moderated electrons - i.e. not only electrons from the beam but also those liberated in the ionization process - being incapable of further excitation,

Table 2.2. Fundamental radiochemical reactions [27].

Primary reaction step	<u>Fast (beam) electrons</u> 1. Ionization $AB \rightarrow AB^+ + e^-$ 2. Excitation $AB \rightarrow AB^*$	<u>Thermal electrons</u> 1. Dissociative ionization $AB \rightarrow A^+ + B + e^-$
Secondary reaction step	<u>Ion- or electron- excited molecules</u> 1. Ion-electron recombination $AB^+ + e^- \rightarrow AB^*$ 2. Ion-molecule reactions $A^+ + CB \rightarrow AC^+ + D$ or $AB^+ + CB \rightarrow AB_2^+ + C$, where A, B, C and D - stable molecules, and A^+, B^+, C^+ - positive ions 3. Formation of free radicals $AB^* \rightarrow A^\cdot + B^\cdot$, where A^\cdot and B^\cdot - free radicals, B^* - excited molecule 4. Formation of stable molecules $AB^* \rightarrow C + D$	
Further reaction steps	<u>Examples of radical reactions</u> 1. Dehydration $R_1^\cdot + R_2H \rightarrow R_1H + R_2^\cdot$ 2. Addition to double bonds $R^\cdot + \dots -CH=CH- \dots \rightarrow \dots -CH-CH- \dots R$ 3. Recombination $R_1^\cdot + R_2^\cdot \rightarrow R_1R_2$ 4. Disproportionation $R_1^\cdot + R_2-CH_2-CH_2 \rightarrow R_1H + R_2-CH=CH_2$	

are finally captured by the molecules. Because of the excess of their energy, the excited molecules or produced ions are not stable and therefore can produce either stable

molecules or free radicals and ions in the subsequent reaction steps (Table 2.2). In the first case, the reaction ends. In the latter case, the formation of free radicals (which usually occurs in 10^{-14} seconds and is finished in approximately 10^{-7} seconds after the moment of irradiation [22,42,43]) and ions results in further reaction steps, and can initiate chemical chain reactions in some systems (e.g. water solutions) which lead to the chemical turnover [9,22,23,27,44-46]. The radical-induced reactions may result in:

1. molecular degradation, e.g. depolymerization;
2. substitution, e.g. dechlorination and dehydration;
3. molecular build-up, e.g. polymerization.

These reactions depend mainly on physical and chemical properties of irradiated matter and on the external conditions, such as pressure and temperature [22,27,44].

The radical-induced reactions are the most important in water treatment. Because they initiate chemical reactions that eventually lead to decomposition of organic contaminants in electron beam water treatment, they must be properly recognized. Figure 2.3 shows the sequence of events that follows the absorption of radiation energy in water. The radiation chemistry of water is complete in 10^{-7} seconds in the sense that by this time species from the same spur* are so far apart that their chances of reacting together are negligible [40]. After that time, the process can be schematically presented by the following reaction [9,19,22,40-43]:



* There are two distinguishing features of radiation chemistry: the first is the non-selective absorption of energy, so that in moderately dilute solutions (<0.1 mole/liter) energy is absorbed mainly by the water; the second is the high energy involved, resulting in the formation of ions and highly excited molecules in spatially isolated volume elements, called SPURS, along the track of the ionizing particle [40].

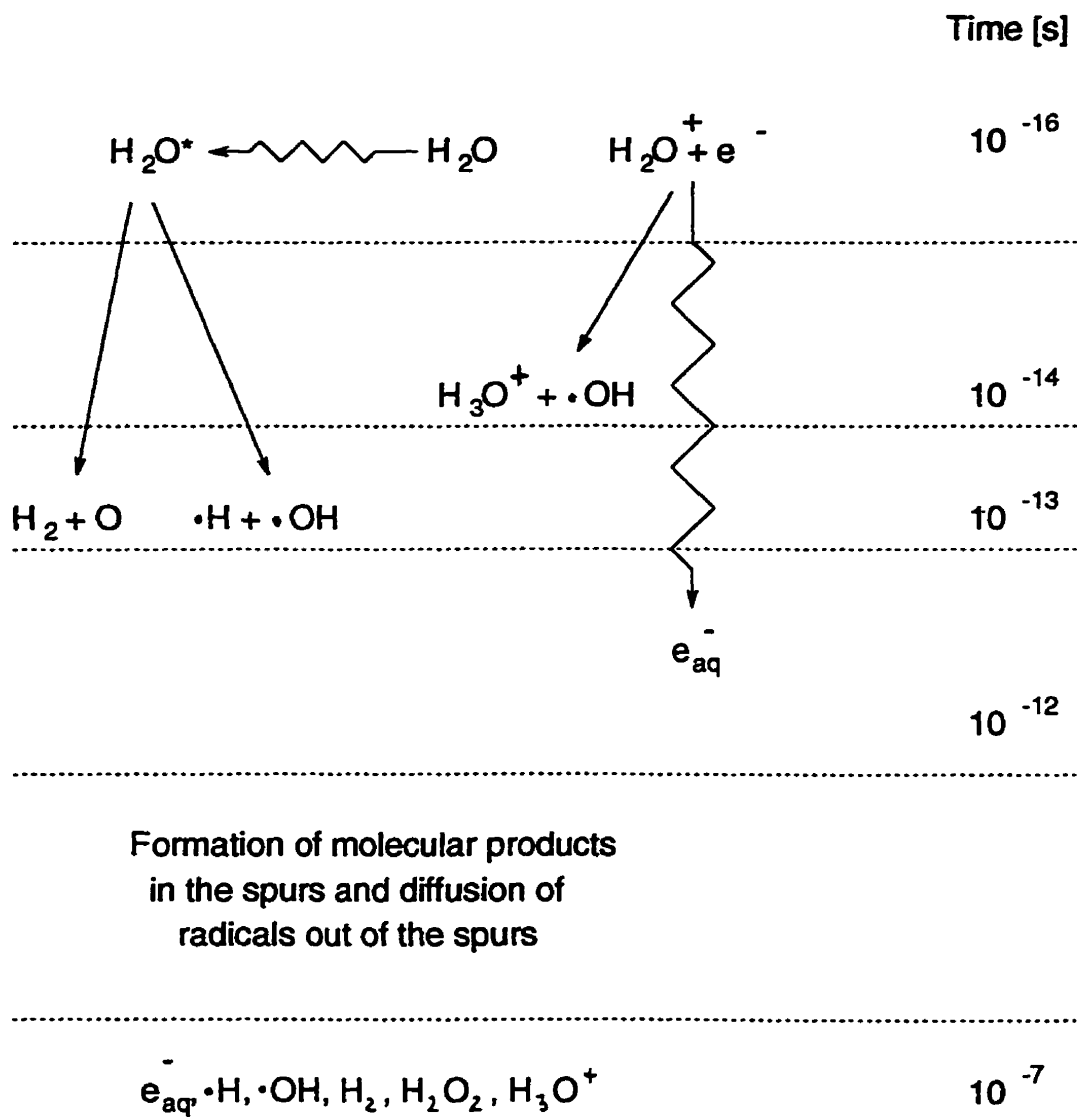


Figure 2.3. Sequence of events in radiation chemistry of pure water [42].

The numbers in brackets in equation 2.12 are defined as G values which represent radiation-chemical yield. It is defined as the number of species formed or destroyed per 100 eV of energy absorbed. G values are used to determine the concentrations of the radical species in solutions available for reaction with contaminants. Typical yields

depending on the absorbed dose are shown in Table 2.3. It is claimed that no other oxidation process has the capability of generating as high an overall free radical concentration mixture as electron beam treatment [19].

Table 2.3. Estimated amount (in millimoles) of reactive species generated at different absorbed doses using high energy electron beam irradiation [19].

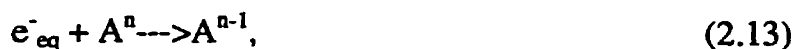
DOSE [krad]	e^-_{aq} [mM]	$H\cdot$ [mM]	$OH\cdot$ [mM]	H_2O_2 [mM]
100	0.27	0.06	0.28	0.07
500	1.4	0.3	1.4	0.4
1000	2.7	0.6	2.8	0.7

The efficiency of organic hydrocarbons removal by high energy electron radiation is relatively high [1,3,10,11,13-22,31,32]. The high efficiency of the electron beam removal of a variety organic substances results from the mechanism of an electron beam interaction with the treated water which is non-selective in the destruction of organic chemicals. This is because, according to equation 2.12 and Table 2.3, reducing reactive species - hydrated electron e^-_{aq} , hydrogen radical $H\cdot$ and molecular hydrogen H_2 ; and oxidizing reactive species - hydroxyl radical $OH\cdot$ and hydrogen peroxide H_2O_2 , are formed at the same time (10^{-7} s) and in approximately the same concentration in irradiated water. The appearance of H_3O^+ ion in Figure 2.3 shows that, during electron radiation, we also have an ionization process of treated water resulting in its

dissociation [40,47-53]. This ion is a main free charge carrier in pure water under low electric field conditions [47]. Its concentration increases significantly with an increase in electric field and reaches the maximum during pre-breakdown and breakdown phenomena in water [47-53]. The formation of H_3O^+ ions indicates that typical electric field-related water dissociation is also a part of the chemistry of water radiolysis.

The hydrated electron, hydrogen radical and hydroxyl radical are the most reactive species formed during water radiolysis. According to the chemistry of electron radiation of water, these radicals are mainly responsible for decontamination of water [1,3,10,11,13-22,31,32].

The aqueous electron (or hydrated electron) is a very reactive reducing radical, the life of which is very short (fraction of microseconds) [40]. Its lifetime depends also on impurities in the solution, especially on molecular oxygen that is a very efficient scavenger of hydrated electron [22,40]. The lifetime of the hydrated electron is also affected by its concentration: the higher the concentration, the shorter the lifetime, because of recombination [40]. All hydrated electron reactions are by definition electron-transfer reactions. In all cases, the primary product of the electron-transfer reaction acquires an additional electron [9,22,40,54]:



where A^n is an element with oxidation state n . The hydrated electron reacts with numerous organic chemicals. It plays an important role in the dehalogenation of

aliphatic halogen compounds, i.e. RX where X = Cl, Br, or I. The example of such an reaction is the dechlorination of a synthetic organochlorine compound [1,19,22,]:



This means that the reactions involving the hydrated electron may result in the dechlorination of halogenated compounds of organic contaminants. It is the main radical responsible for removal of trihalomethanes from drinking water.

The hydrogen radical (or hydrogen atom) (H \cdot) plays a lesser role in the radiolysis of aqueous solution than the hydrated electron. It results from the facts that the concentration of hydrogen radicals is substantially less than that of hydrated electrons, and that their reducing reactivity is in general weaker than that in the case of the hydrated electron [9,40,54]. The hydrogen atom undergoes two general types of reactions with organic compounds [1,9,11,22,23,54]:

1. with saturated organic compounds, it abstracts hydrogen to give an organic radical and H₂, and 2. addition reactions occurring with unsaturated and aromatic compounds. It is claimed that the high energy electron beam treatment is the only one oxidation process in which the H \cdot is generated [3,9,11,13,14,19,54].

The hydroxyl radical (OH \cdot) is one of the most powerful oxidizing short-living species. It is the main oxidizing radical formed when aqueous solutions are irradiated by electron beam, X- rays, γ -rays and ultra-violet light. Electron transfer is the most frequent mechanism of hydroxyl radical induced oxidation of both organic and inorganic cations [40]. Organic compounds containing aromatic systems or carbon-

carbon multiple bonds undergo addition reactions with OH[·] in a similar manner to H[·] addition with those compounds [1,9,19,54,55]. The typical examples of the reactions with OH[·][19] are:



It has to be noted that the other products of radiolysis are also involved in organic contamination removal, but their role is remarkably smaller than the above characterized free radicals. The recombination of hydrated electrons results in formation of reducing molecular hydrogen, and the recombination of hydroxyl radicals results in the formation of oxidizing hydrogen peroxide. Significant concentrations of this oxidant are likely to remain in solution and, if its amount produced during the reaction is possible to be controlled, it might be providing a microbial disinfection. If it is not needed, H₂O₂ will just have to be removed in further treatment [14,19]. It is known that adding H₂O₂ to influent water may lead to an increase in the overall hydroxyl radical concentration [54]. Hydrogen peroxide would therefore play a significant role in the case of a solute primarily removed by reactions with this radical.

For the technical utilization of the radiochemical processes, reaction kinetics are of great significance. The attempts to develop a quantitative description of electron beam radiation removal efficiency of organic contaminants in water have recently been made [9,54]. However, it must be noted that the calculations use data obtained in

laboratory experiments and they are strictly applicable to only pure water. If we assume that the only processes responsible for the removal of an organic solute, R, from an irradiated solution are reactions with the three reactive species e_{aq}^- , $H\cdot$, and $OH\cdot$, then the overall removal of any solute can be described by the following reaction kinetics expression [9,19,54]:

$$-d[R]/dt = k_1 [R] [OH\cdot] + k_2 [R] [e_{aq}^-] + k_3 [R] [H\cdot] \quad (2.17)$$

where, k_1 , k_2 , k_3 , are the respective second order rate constants in $(\text{mole s})^{-1}$. The relative concentrations of each of the three reactive species in pure aqueous solution are given by the G value. Selected values of the rate constants are shown in Table 2.4. The values of rate constants are very high - up to $10^{10} (\text{mole s})^{-1}$, it means that the free radical reactions occurring in water after electron irradiation are enormously fast.

Table 2.4. Rate constants (in $\text{moles}^{-1} \times \text{second}^{-1}$) of selected organic chemicals and the free radicals formed in irradiated aqueous solution [9,12,54].

COMPOUND	e_{aq}^-	$H\cdot$	$OH\cdot$
Benzene	9.0×10^6	9.1×10^8	7.8×10^9
Toluene	1.4×10^7	2.6×10^9	3.0×10^9
Chlorobenzene	5.0×10^8	1.4×10^9	5.5×10^9
Chloroform	3.0×10^{10}	1.1×10^7	5.5×10^6
Phenol	2.0×10^7	1.7×10^9	6.6×10^9
Trichloroethylene	1.9×10^9	----	4×10^9

The reaction rates presented in Table 2.4 have been estimated under ideal conditions for pure water. However, the extensions of these calculations to natural waters will have to involve additional steps to take into account the dependence of radiation-chemical yields and therefore reaction rate constants on the several factors, such as [19,40]: 1. reactions of the transient species with naturally occurring scavengers, e.g. oxygen, carbonate/bicarbonate etc.; 2. effect of extreme values of pH; 3. influence of alkalinity; 4. non-linear effects of dose rate - non-linear energy transfer; 5. temperature; 6. pressure; and 7. reversibility of the reactions.

Table 2.5 shows a summary of the removal percentages for organic compounds that have been investigated in the EBRF in Miami for water flow rate being equal to 380 l/min. It has been found that the doses of 50-800 krad (0.5-8 kJ/kg) effectively remove most of the compounds (initial concentration was always lower than 1500 µg/l, because then the efficiency does not depend on the initial concentration), although the experiments were carried out with contaminants dissolved in waters of varying qualities (potable water, chlorinated and raw wastewater) [3,10,13-21,54]. The absorbed dose was estimated on the basis of the measured temperature of the treated water [3,10,13-21,54]. On the basis of the results obtained, the EBRF research group has also attempted the estimation of the reaction kinetics models for several contaminants [56].

The features of the physico-chemical action of a high energy electron beam on water can be summarized as follows: 1. Ability to destroy organic contaminants in slurries containing up to 10% of solids (sludge) [14]; 2. The presence of both aqueous

electron and hydroxyl radical in aqueous solution at similar steady state concentrations [19]; 3. In the presence of common radical scavengers, hydrogen radical would be present in high enough concentrations to facilitate contaminant destruction [13,14,19]; 4. The capability to disinfection, but a disadvantage is that the reduction of coliforms, coliphage and total number of bacteria is barely 2 log cycles for up to 8 kGy of absorbed dose [21]; in order to decrease survival rate of bacteria, very high doses would be required.

Table 2.5. Summary of electron beam removal of various compounds [13,14,19].

Compound	Percent removal	Required dose [krad]	Compound	Percent removal	Required dose [krad]
DRINKING WATER			GROUNDWATER TREATMENT		
Chloroform	83-99	650	Benzene	>99	650
Bromodichloromethane	>99	80	Toluene	97	45-600
Dibromochloromethane	>99	80	Phenol	88	37-800
Bromoform	>99	80	m-Xylene	91	650
WASTEWATER/GROUNDWATER TREATMENT			o-Xylene	92	650
Trichloroethylene (TCE)	>99	500	Chlorobenzene	97	650
Methylene chloride	77	800	Ethylbenzene	92	650
Carbon tetrachloride	>99	80	1,2-Dichlorobenzene	88	650
Tetrachloroethylene (PCE)	>99	241-500	1,4-Dichlorobenzene	84	650

2.3. Electron beam water treatment - energy efficiency and cost

The cost of the treatment using the electron beam radiation technology depends on many factors, such as the dose required to obtain the desired detoxification, the volume of waste (water flow rate) to be treated, the size of the treatment facility (electron beam energy utilized), the time utilization of the facility, the efficiency of beam utilization, and the efficiency of high voltage dc power supply.

For economical reasons, the generated beam energy has to be utilized in the irradiated matter at the highest possible degree to produce the desired irradiation effects. Various losses, however, must inevitably occur in a facility and in a process. The most important losses are the following.

1. Power losses on the path of the beam from the cathode to the window. They occur because of the residual gas scattering, especially at the vicinity of the window surface. Depending on the pressure inside the chamber (usually 10^{-6} - 10^{-5} Pa), the relative losses referred to the incident beam power are within the range 5-10%.
2. Absorption losses in the window material and the following gas gap (if there is any) to the irradiated matter. Under given conditions, they depend mainly on the accelerating voltage. Figure 2.4 shows electron beam transmission for 25 μm Al and Ti foils as a function of electron energy. This losses are within the range 5-50% for the voltages commonly utilized in electron beam technology.

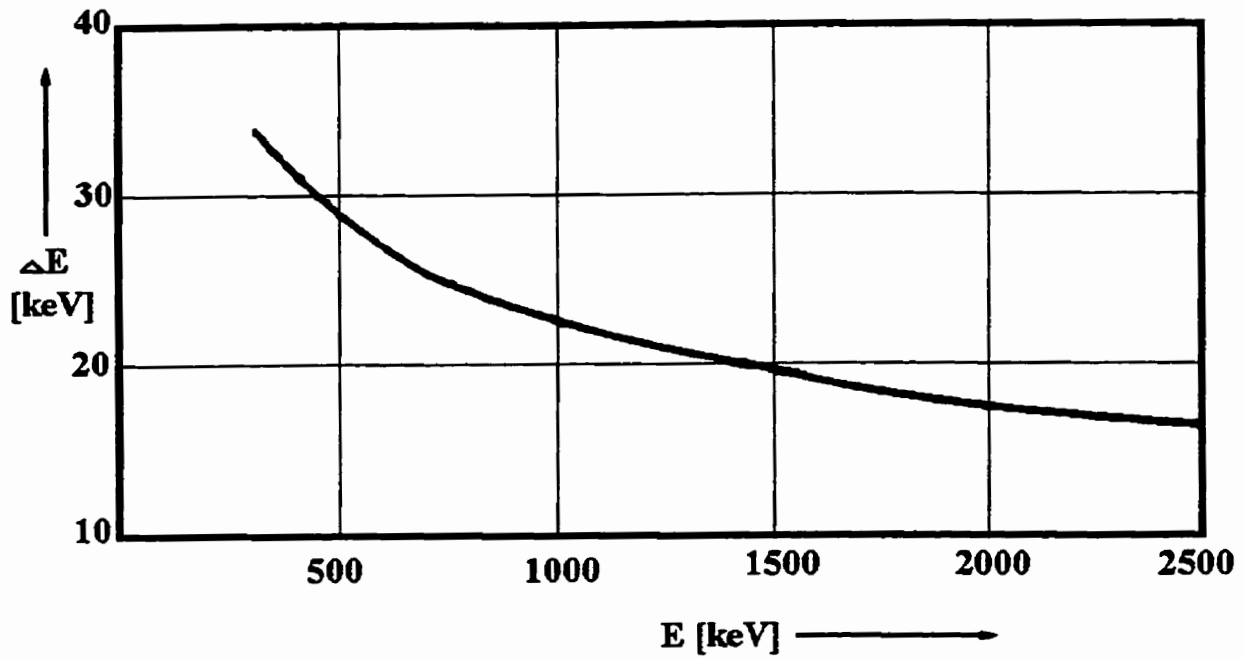
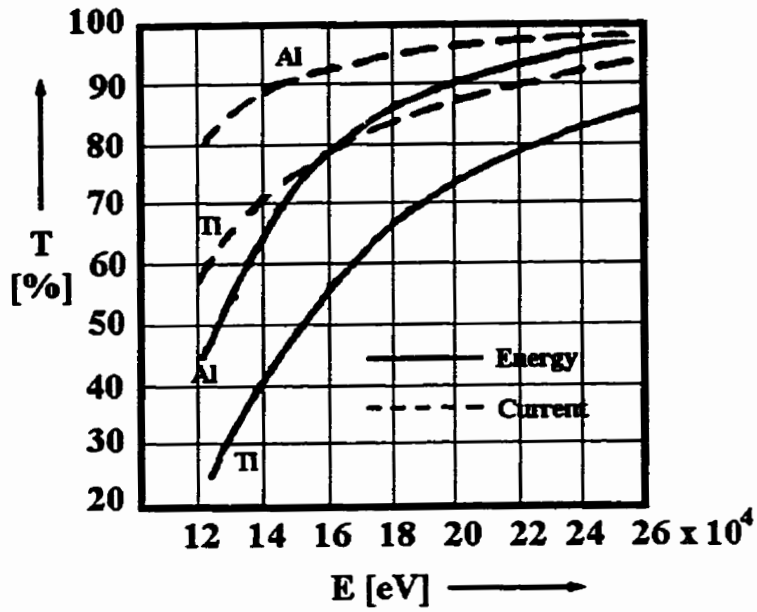


Figure 2.4. Electron transmission at normal angle of incidence through 25 μm Al and Ti foils as a function of electron energy - beam current losses and energy losses [28,59].

3. Losses due to overscan (beam deflection beyond the irradiated matter). They usually amount to 10-20%.

4. Losses due to overdoses and the unused dose tail of the dose depth distribution. This portion depends substantially on the irradiation conditions (Fig. 2.5). It depends on the use of either single-sided or double-sided irradiation (from both sides of water stream or film to be processed). Their usual relative values are within the range of 5-20%.

5. Losses caused by incomplete utilization of the irradiation area (about 2%). This component is associated with an incomplete utilization of the window area.

According to the above, the useful portion of the generated beam power converted in the electron beam radiation process essentially depends on the kind of job to be performed. With non-vacuum radiation (work-piece outside the vacuum chamber), it usually covers a range of $\eta=0.2-0.8$ and with vacuum radiation (work-piece is inside the vacuum, e.g. electron lithography, electron beam measurement techniques [26,27,57,58]), it is close to 0.9 [27].

For an overall energetic estimation of the irradiation technique, it is further necessary to consider additional loss components, such as: losses in high voltage generation; energy needed for the evacuation of the beam generating and guidance system; energy expenditure for cathode heating, beam deflection, and for powering other electronic and electrical equipment of the irradiation facility, such as vacuum system, hydrogen evacuation system (in electronic treatment of plastic films), SF₆ pressurizing and SF₆ reclaiming (compressing) systems.

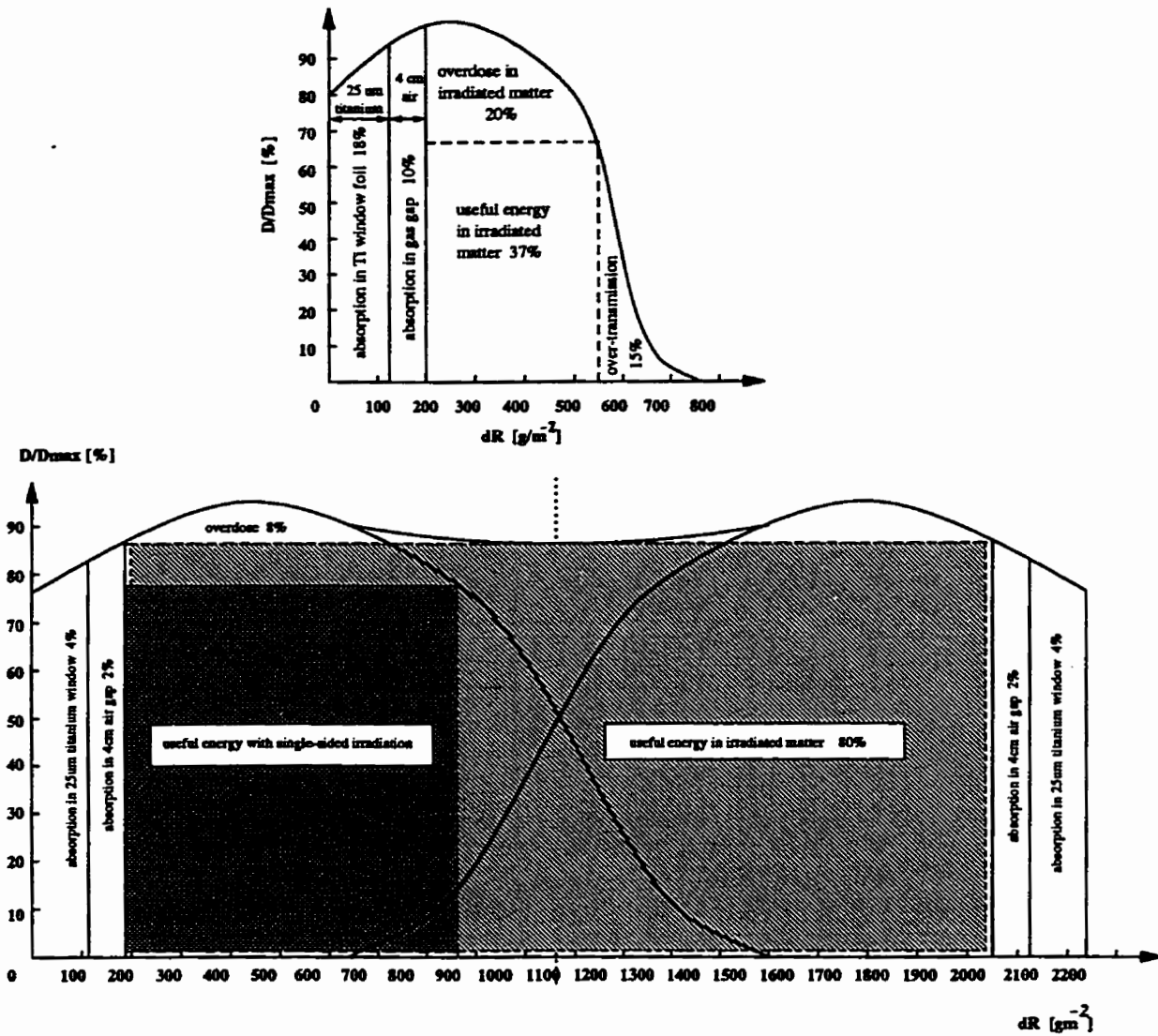


Figure 2.5. Determination of dose depth distribution and absorption fractions in the irradiated matter for the: a) single sided radiation - 300 keV; b) double sided radiation - 500 keV [28].

Considering these additional energy requirements among which the dc high voltage generation requires the most, it is estimated that in high-power irradiation facilities, i.e. above 100 kW, about 50-75% of the input power is converted into actual beam power [27]. For lower range of power, this efficiency is even lower. Taking into account that only a part of the generated beam power is utilized in the radiation process, the efficiency of electron beam facilities is within the range of 20-50%.

As an example of the efficiency of the electron beam water treatment facility, one can consider the EBRF in Miami. According to works [3,10,13-21,54,56] it can be concluded that the absorbed dose used in the EBRF facility in Miami never exceeds 8 kGy in continuous treatment. For the maximum water flow of 380 kg/min (6.3 kg/s) utilized in this facility, simple calculation can show that the conversion of the generated beam power into absorbed dose - beam utilization factor - is about 67% (power radiated=accelerating voltage x beam current, power absorbed=water flow x absorbed dose; efficiency=power absorbed/power radiated). It means that although a high accelerating voltage is used, over 30% of radiated power is lost during passage of the electron beam from electron gun to the treated water. The following mainly causes these losses: 1. use of a relatively thick and dense - 25 μm , 4.5 g/cm^3 , respectively - titanium window as an electron permeable membrane; 2. the exterior surface of the window is not directly exposed to the treated water and, therefore, there is an air gap between the window and water surface which causes an attenuation of beam energy; 3. the window is air cooled and the power density of electrons injected through the window is lower by

approximately one order of magnitude [32] than that in the case of water cooled windows, i.e. while the exterior surface of an electron permeable membrane is exposed to the treated water. The total efficiency however must be even lower, because the above does not include the other energy requirements, mainly efficiency of dc high voltage power generation. The supply used in the EBRF in Miami is the most commonly utilized in industry electron accelerator produced by Radiation Dynamics, Incorporated in the USA, called Dynamitron [60-64]. It is designed to work at a high frequency capacitive coupling as an insulating core transformer (ICT). A substantial number of these supplies has been utilized in industry for electron beam accelerators and the dc High Voltage power generation efficiency (line to beam) in this kind of the power supplies is about 50% [60-64]. Combining this efficiency with the 67% of electron beam utilization, one can conclude that the total efficiency of the EBRF in Miami must be only about 34%, which is rather low. This fact has a significant effect on the cost per unit volume of the water treated by electron beam radiation.

For most of the substances presented in the Table 2.5, the dose required for their decomposition is relatively high (>5 kJ/kg=500 krad). In the case of a high water flow rate the power radiated must be also quite high. This fact influences the cost of the facilities used for water and wastewater treatment. According to the estimation in [19], the capital cost of 1.5 MeV, 50 mA facility and its installation with support facility, such as water delivery system, is about US\$2.4 million. This cost consists mostly of the cost of the vacuum system for big vacuum chambers, electron gun and electron optics,

x-ray shielding, and dc high voltage supply and its insulation (SF_6 under high pressure). This part of the total cost will have to be limited, when one thinks about wide use of this kind of water treatment.

Utilizing very high energies of electron beam in water treatment process causes the safety problems with X-radiation. Energy losses on the work site caused by X-radiation are on the order of 1% or less [27]. They depend on the accelerating voltage V_A and on the atomic number Z of the matter hit by the beam. Although the portion of the beam energy η_X converted into X-radiation is rather small (it can be expressed by $\eta_X \approx 10^{-9} V_A Z$, where V_A is in volts [27,35]) X-ray shielding is a decisive factor determining the plant's dimensions. Because the penetrability of X-rays increases with quantum energy, and thus with the electron energy, shielding measures are determined mainly by the maximum accelerating voltage to be used in a particular electron beam processing plant. It should be pointed out that shield gaps in the direction of the primary X-rays must be avoided. For electron beam accelerators working above 500 keV, the X-ray shield is usually built of concrete and is the size of a small building with three- to 6-foot-thick walls and 3-inch-thick interlocked lead doors [19,27]; therefore, the high energy electron beam facilities are simply devoted to a treatment of only one water source. Due to their huge size, high energy electron beam plants have also a relatively high cost of maintenance. In the case of the energies up to about 300 keV it is common to provide just a local radiation protection by covering the unit with lead which lowers

the maintenance cost and increases portability of such facilities, so that they can be transported to different water sources.

Another factor that influences the size of electron beam radiation facilities, is a high voltage insulation system. Usually, electro-negative gas, sulfur hexafluoride SF₆, under pressure of up to 6 atmospheres is used for this purpose [60-64]. Although such an insulation has a high dielectric strength, dimensions for very high accelerating voltages are still substantial (about 2.6 meters in diameter by 6.8 meters long in the case of Dynamitron [60-64]). The cost of the gas then is very high, even if it is reclaimed if the chamber must be open. Again, lowering the operating voltage down to or even below 300 keV would substantially lower the size and cost of the insulation system.

In the case of the EBRF in Miami, the treatment cost has been estimated to be about US\$2.5 per 1000 gallons based on the 99% percent of TCE removal for absorbed dose of 500 krad, at a flow rate of 160 gallons per minute, energy cost of US\$0.07 per kWh, power of the beam 75 kWh and efficiency of dc high voltage power supply of 50% [19]. In the case of UV treatment combined with hydrogen peroxide, the reported cost was estimated at a similar level of US\$2.6 per 1000 gallons [65]. The hourly operating cost was estimated to be about US\$41 [19]. The cost estimation for electron beam water treatment based on the EBRF in Miami can not be taken as a measure of effectiveness of electron beam water treatment in industrial application, because at least two electron guns and accelerators - because of conservation, limited time of filament work and repairing in a case of failure - would have to be utilized and maintained in

order to provide a continuous water treatment. This would increase the total cost of the plant, especially the cost of equipment and maintenance, and therefore the cost per unit volume of water would also be higher. Recently, attempts have been made to develop a transportable electron beam system intended for treatment of water streams [66,67]. Although the removal of volatile organic compounds (VOC), such as trichloroethylene, tetrachloroethylene or chloroform, is very high for flow rates of up to 50 gallons per minute, the cost was US\$4-6 per 1000 gallons of the treated water [67]. The higher operating cost of portable units than that in the permanent Miami's EBRF is mainly due to transportation costs and shorter useful life [19].

The cost of the electron beam water treatment, as well as other advanced oxidation technologies, is still higher than that of conventional treatment of an average, not highly contaminated water source. Considering the cost of electron beam water treatment, it is obvious that its attractiveness has not rather been caused by economical factors yet, but it has arisen from the fact that almost all kinds of organic contamination in water can be destroyed. Bearing this in mind, it is apparent that this kind of process may be competitive in the case of water sources and wastewaters highly contaminated with organic hydrocarbons, where there is required a removal of a variety of organic compounds. An additional advantage is that a high level of water purification can be obtained without adding anything to facilitate the process. It therefore assures a high purity of the treatment. If the cost of the electron beam water treatment could be as

attractive as its performance, a great breakthrough in water treatment technology may be expected.

Little has yet been done to identify reaction by-products and intermediates in removal of different contaminants, but when complete destruction of contamination does occur the organic compounds are generally mineralized to CO₂ and H₂O (about 90% of the parent compound [54]), and salts or other harmless products depending on the kind of solute. For instance, HCl is formed in the case of electron beam treatment of trichloroethylene and chloroform aqueous solutions [68-71]; aldehydes and carboxylic acids are present in the case of electron irradiation of benzene and toluene solutions [10,72-75].

CHAPTER 3

AIM OF THE PRESENT STUDY

It may be concluded from the previous chapter that there are two ways to reduce the cost of electron beam water treatment:

1. increase in efficiency and/or decrease of cost of high voltage dc power supplies;
2. increase in efficiency of electron beam power utilization.

Recently, attempts have been made to develop a new kind of high voltage power supply operating at up to 200 kW of output power [76]. Contrary to insulated core transformers, sectionalized ferrite core is used in order to provide suitable voltage grading. Such a design improves the efficiency of high voltage generation to as high as 90%. In addition, high frequency and printed circuit board technology allow to minimize the size and to reduce the cost of the power supply and SF₆ insulation [76].

So far, an increase in efficiency of electron beam power utilization has mainly been improved by using ultra high accelerating voltages to maximize transmission and minimize energy loss of the beam passing the window. Use of low absorptivity ceramic windows can reduce the losses in the electron beam. Additionally, a proper cooling can increase power density that can be utilized at the point of action. This can be obtained if the treated water is also used as a window coolant during the treatment. Furthermore, such an arrangement eliminates an air gap between treated water stream and the window. There are therefore no additional losses due to attenuation of the beam energy

during a passage through the air gap. Using a low absorptivity window material may allow to utilize a significantly lower accelerating voltage range which otherwise could not be used due to the substantial losses of the beam power. Use of low and medium accelerating voltages within the range of 100-300 kV can reduce the size of the HV insulation and X-ray shielding system, which results in additional cost reduction of equipment, installation and maintenance of an electron beam apparatus. The power delivered to the treated water may be maintained by an increase in electron beam current density at the point of action.

All the above mentioned factors are essential in order to design and build a portable or permanent, low operating cost electron beam facility intended for purification of drinking and waste water.

The experiments presented in this thesis are focused mainly on three targets:

1. improvement of electron beam utilization with the use of boron nitride windows, so that low and medium energy electrons can be used in electron beam water purification;
2. once the above goal is obtained, it must be found out if low and medium energy electrons can be as efficient in water purification as high energy ones;
3. to investigate the dependency of removal rate of several contaminants on electron beam radiation parameters, such as: accelerating voltage, beam current, radiated and absorbed dose of electron radiation.

CHAPTER 4

EXPERIMENTAL SETUPS

4.1. Electron gun and cathode system

In electron beam technology, hot cathodes are still most frequently used as emitters for electron guns. When thermionic electron emission is used, the cathode material must have a low work function and a melting point high enough to avoid significant evaporation at working temperature (Table 4.1). The emission current density J_{eT} (the temperature determined saturation current density) of the hot cathodes obeys the Richardson-Dushman equation [77,78]:

$$J_{eT} = B \cdot T^2 \cdot e^{-W/kT}, \quad (4.1)$$

where W is the electron work function [J], i.e. the energy needed by electron to leave a cathode - it strongly depends on the cathode material, e.g. for tungsten $W=4.52$ eV and for tantalum $W=4.1$ eV (Table 4.1), k is Boltzmann's constant, T is the absolute temperature [K], and B is the Richardson constant (or universal thermionic constant) which is valid for all crystals. B , for ideal crystals, can be expressed as:

$$B = 4 \cdot \pi \cdot e \cdot \frac{m_e \cdot k^2}{h^3} = 1.2 \cdot 10^6 \left[\frac{A}{m^2 \cdot K^2} \right], \quad (4.2)$$

where e is charge of the electron, m_e is its mass, h and k are Planck's and Boltzmann's constants, respectively. For metals, work function W and thermionic constant B can be determined by measurements.

Table 4.1. Work function and melting point of materials used for electron emitters [58]

Material	Work Function [eV]	Melting Point [°C]	Material	Work Function [eV]	Melting Point [°C]
Ag	4.7	960.5	Nd	3.3	1016
Al	3.0	660.3	Ni	5.0	1453
Au	4.8	1064.6	Pt	6.0	1772
Ba	2.52	729	Rb	1.8	39.6
C	4.7	3827	Sr	2.1	768
Ca	3.2	839	Ta	4.1	3014
Cd	4.1	320.9	Ti	4.09	1670
Cs	1.8	28.5	Th	3.4	1755
Cu	4.1	1084.6	W	4.52	3407
Fe	4.7	1535	Zr	4.1	1852
Hg	4.5	-38.7	LaB ₆	2.74	2210
Ir	5.4	2443	NdB ₆	4.57	----
K	1.8	63.4	TaB	2.89	----
La	3.3	920	TaC	3.14	----
Li	2.2	180.7	ThO ₂	4.57	----
Mo	4.3	2617	TiC	3.35	----
Na	1.9	98	ZrB	4.48	----

The exponential term in the Richardson-Dushman equation is responsible for the largest part of the increase in current density as temperature is increased. The increase due to T^2 is small and not confirmed experimentally [58], because of being overshadowed by the other component. Taking tungsten as an example at 2500 K, a 1% change in temperature results in a 2% change in saturation current density because of T^2 factor, compared to a 20% increase in the exponential term. In nature, there are few effects which change as fast as the thermionic electron emission; when the temperature is doubled the J_{eT} increases 100-fold. Figure 4.1 shows saturation current density of some customary cathode materials, such as lanthanum hexaboride, tantalum and tungsten, depending on the cathode temperature. The upper limit of the useful emission current density depends on both the temperature stability and material evaporation at high cathode temperatures. For tungsten, this limit is within the range of 1-10 A/cm² [27].

The power losses during work of the hot cathode are mainly caused by thermal radiation from the cathode surface, this loss is roughly proportional to T^4 , and from thermal conduction of its support. There is also some power loss due to the fact that the cathode cools when it emits electrons, because of the work function and mean kinetic energy of the emitted electrons, Nottingham effect [58,79], but they are much lower.

According to the Richardson-Dushman equation for a given cathode temperature the saturation current density can only be achieved if the electric field strength in front of the emitting surface is high enough to extract practically all the emerging electrons;

otherwise an electron cloud will be formed in front of the cathode. This space charge then alters the electric field distribution to such an extent that further emission from the cathode becomes limited and can be estimated by using the Child-Langmuir law [58,80]. In the case of experiments presented in this thesis, the use of relatively low electron beam current (up to 1.5 mA) and accelerating voltage higher than 50 kV indicates that the emission current can be described using equation 4.1.

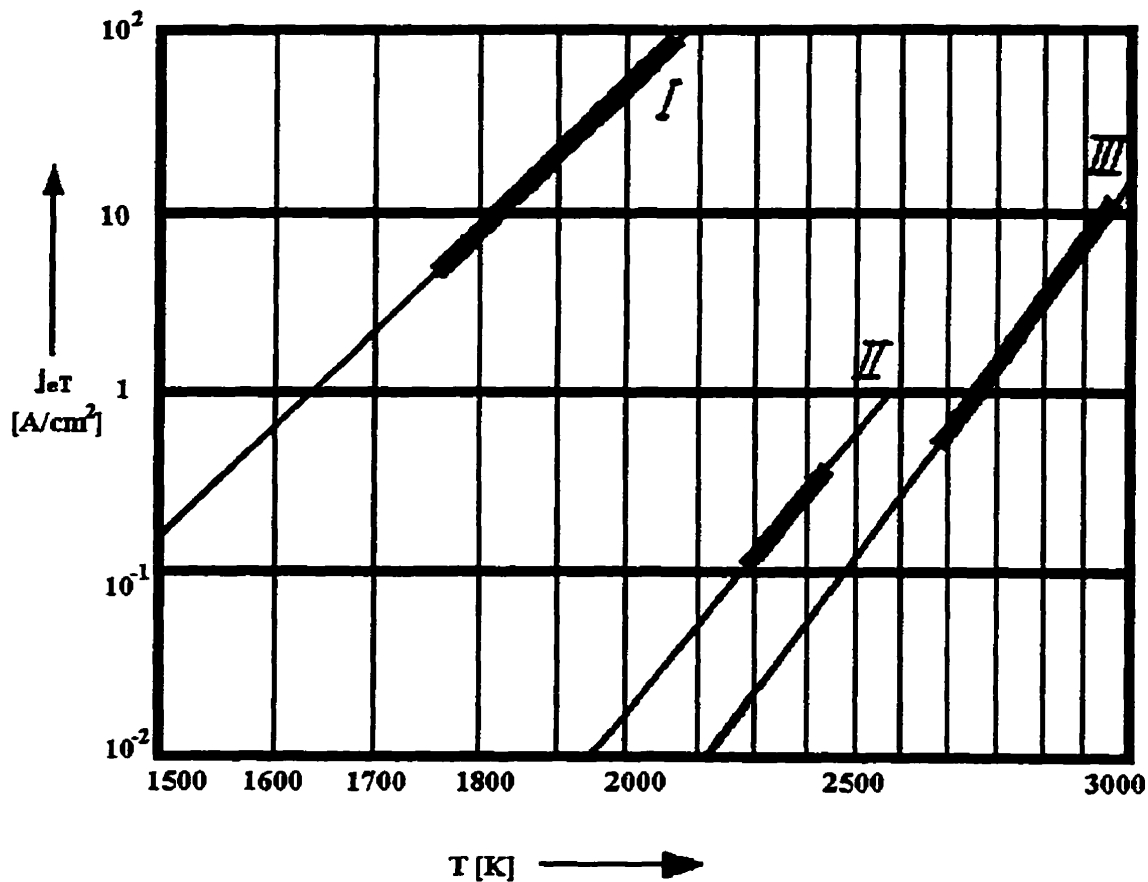


Figure 4.1. Saturation current density of some customary cathode materials versus cathode temperature: I. LaB₆ on carbonized tantalum; II. tantalum solid; III. tungsten solid. Operating ranges are indicated by bold lines [27].

The need for relatively high emission current densities at emission temperatures as low as possible leads to attempts to use activated cathodes. In electron beam technology, not too many of this kind of cathodes can cope with the arduous operating conditions. The lifetime of the cathodes is usually too short. As a result, the most common filament materials used in electron beam radiation processing are tungsten, tantalum as well as tungsten with emission-increasing alloying elements [27].

Two different types of electron guns were used in the experiment: 1. hairpin filament gun with grid electrode (Fig. 4.2); and 2. commercial dispenser cathode gun with bolt filament cathode (Fig. 4.3).

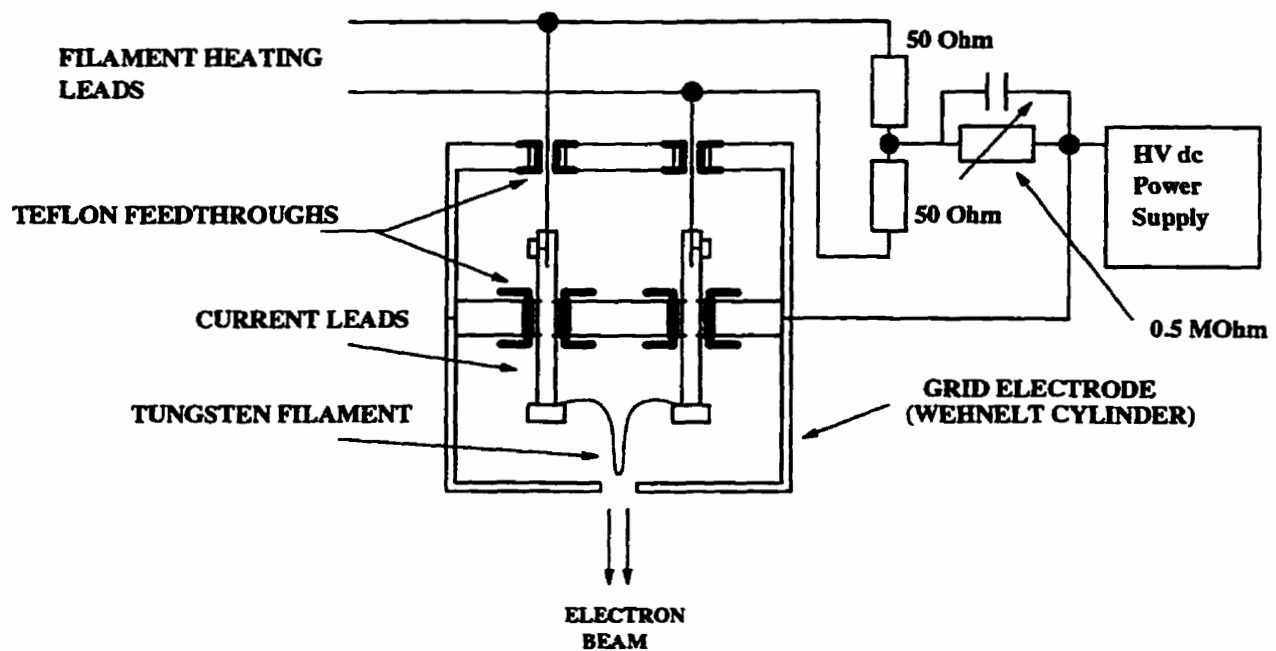


Figure 4.2. Hairpin filament electron gun with Wehnelt electrode and self-biasing circuit.

The first type of gun was mainly used to investigate the properties of the electron permeable membranes because of its limited lifetime and emission current density. This type of gun requires the use of a grid (Wehnelt) electrode in order to focus the beam properly [27,58]. The cylinder is slightly negatively polarized with respect to the filament cathode so that the electrons can leave the gun through the hole without being trapped by the grid electrode. This bias should vary depending on the beam current; higher bias voltage for higher electron beam current. Such a negative self-biasing system can be obtained by using a simple resistive circuit (see Fig. 4.2) commonly used in electron guns for electron microscopy [81-84]. In this circuit, the higher the electron beam current, the higher the bias voltage.

The dispenser cathode (or metal coated-metal surface cathode) electron gun is a low-work function bolt cathode electron source. These cathodes are used in high-power transmitting tubes since they show less crystallization than pure metals do [58]. The dispenser cathode is one that generates and maintains an excess of low work function metal or metal oxide, say barium or thorium and their oxides, at its surface and relies on that excess for its emission properties [26,58]. The dispensed low-work function material (about 1% [58]) is contained within the body of another material to provide structure and shape for the cathode, and is caused to migrate to the surface by a diffusion process. This rather complex mechanism is useful because materials with low work functions, the work function of barium is 2.52 eV and that of thorium is 3.40 eV (Table 4.1), frequently have too low melting temperature and a high bulk evaporation

rate at normal operating temperatures and therefore can not be used in their pure bulk state.

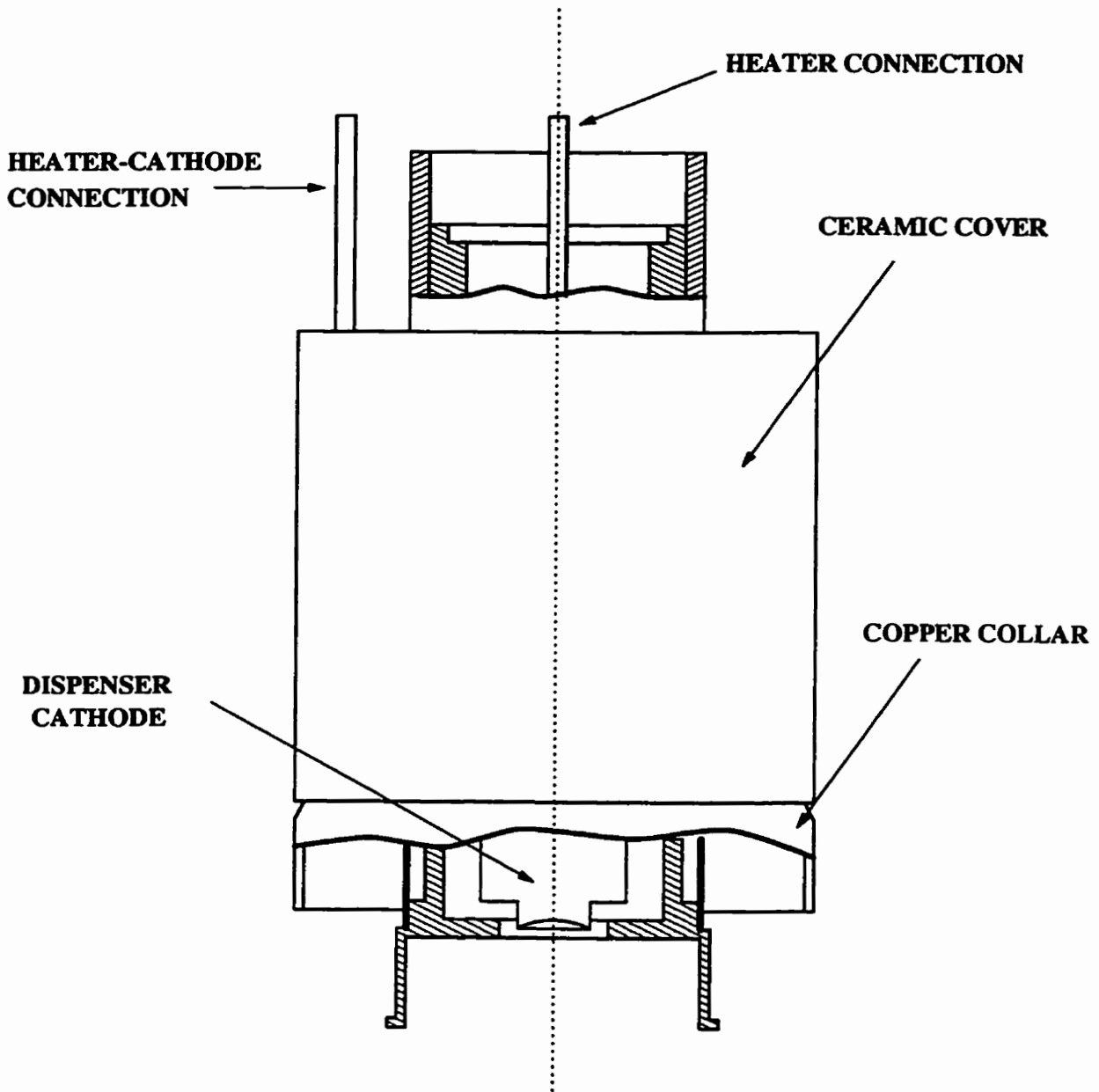


Figure 4.3. Commercial dispenser cathode electron gun.

The dispenser cathode generates what is usually taken to be a mono-molecular electropositive layer of the emitter producing a strong electric field and reducing the work function to the value that is even lower than that of dispensed material in bulk [58]. In addition, such a layer evaporates more slowly than the bulk material. Besides thorium and barium in tungsten, thorated iridium, zirconized and titanized tungsten are also sometimes used [58]. The dispenser cathode gun supplied by CPI, Ltd. was used in the experiments. For this gun, the emission current of 10 mA is obtained for voltage across the filament of 7.1 V; whereas the current flowing through the filament is 1.7 A.

The shape of the gun and the shape of the bolt filament enable to achieve a 10 mm diameter beam at the distance of 50 mm from the filament. The distance between cathode and anode in vacuum should be quite high, so that it can withstand accelerating voltage without any flashovers.

Both kinds of the guns used in the experiments were heated by the direct current flow through the filament which is the common technique in electron beam technology, except high power large surface filaments which are heated by electron bombardment [27]. The power which has to be supplied to the filament was within the range of $P_f=15-25$ W. The electron gun filaments exhibit decreased emission over time. Their lifetime depends mainly on the type of filament material, pressure inside the vacuum chamber where electrons are generated - these two factors affect sputtering rate of a cathode material - and on the reactivity of residual gas in the chamber - in the presence of residual oxygen, an oxide layer can be formed very quickly at high temperature of the

filament. This layer blocks the electron emission. Additionally, especially in the case of dispenser cathodes, the emission decreases after overloading, i.e. overheating the emitter, therefore a proper control of filament temperature is of great importance. Resistive heating of a cathode makes it possible to control the filament temperature, thereby the electron beam current by varying voltage across the filament.

4.2. Isolating transformer and filament heating

In order to control the voltage across the electron gun filament, a filament voltage supply must be properly isolated from high voltage dc supply terminal. This is usually obtained by using isolating transformers or low power motor and generator systems (motor at grounded part, generator working at high potential) connected by a shaft made of an insulating material. In the experiments, the isolating transformer depicted in Fig. 4.4 was used. The insulation problem is to design a suitable system to separate the primary and secondary windings of the transformer. The isolating transformer was built as an open core transformer and the core was made of nickel and zinc based high frequency ferrite. The primary winding (8 turns) was wound directly on the ferrite bar. This winding and the core were enclosed inside the 3/4" thick Plexiglas tube which provides a suitable high voltage insulation. The secondary winding - also 8 turns - was wound onto this tube. The accelerating negatively polarized high voltage is

applied to the one of the leads of secondary winding. The transformer output voltage is then rectified and loaded with the electron gun filament.

The whole assembly was enclosed in another insulating cylinder and filled with a transformer silicon oil in order to avoid partial and corona discharges. The tests proved that such an insulation system - oil plus Plexiglas - can quietly (without any corona activity) withstand the potential difference between secondary and primary winding of the isolating transformer up to 250 kV.

The short and open circuit tests of the transformer indicated that magnetizing to leakage reactance ratio is very low $X_m/X_L=1.2$ mainly due to an open core design. In that case, a series capacitance compensation must be used to improve efficiency of the transformer and to make the turns ratio closer to ideal $a=8/8$. The capacitive reactance must be similar to the leakage reactance measured in the short circuit test of the transformer, so that the Q factor of the circuit may be optimized. Complete resonance however should rather be avoided as the regulation of such a transformer connection system would be too high.

Two kinds of filament heating systems were used in the experiment. In both cases, a high frequency signal was used to drive the isolating transformer. In the first method depicted in Fig. 4.5, the isolating transformer was connected to the self-oscillating inverter driven by a low voltage dc supply - 30 V, 5A.

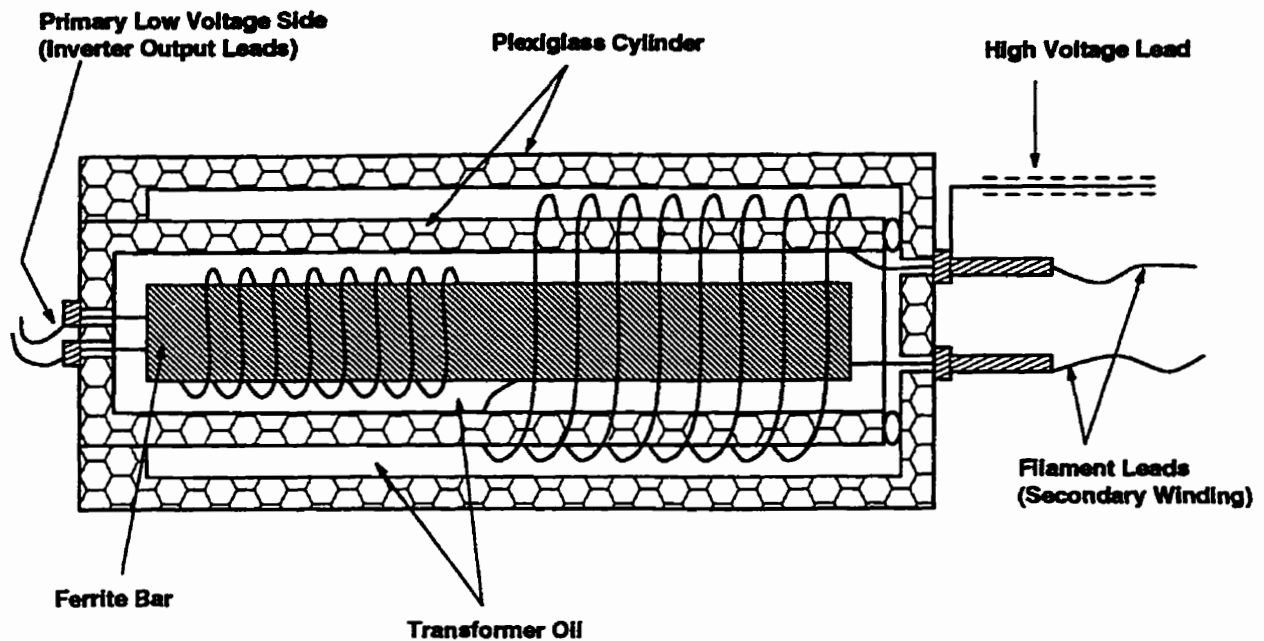


Figure 4.4. Isolating transformer.

The frequency of the signal generated from the inverter (square wave) was dependent on the inductance of the center tapped transformers used in the circuit (Fig. 4.5). This frequency could not be varied during the operation and it was about 80 kHz.

The inverter was connected with the isolating transformer through a capacitor that compensates the leakage inductance of the isolating transformer. The output voltage from the isolating transformer was rectified and applied across the cathode of the electron gun. This voltage was related to the dc voltage input of the inverter and, therefore, the low dc voltage input to the inverter can control the electron beam current. For the power that must be supplied to the cathode - up to 25 W, a very stable

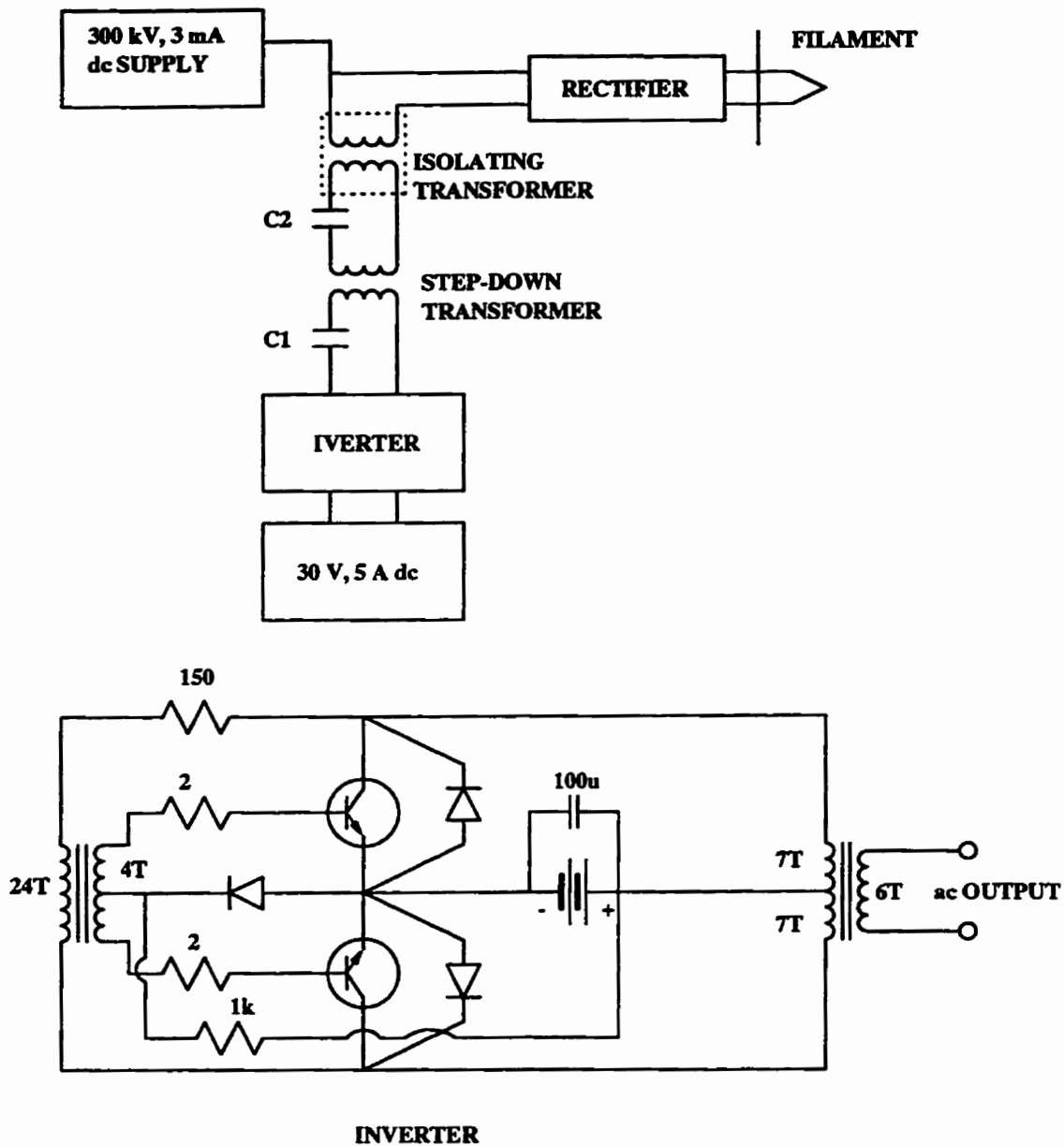


Figure 4.5. Self-oscillating inverter filament heating circuit.

and smooth control of the voltage can be obtained. The advantage of this setup is its small size (5" by 8" box) which is important in the case of the portable electron beam water treatment facilities.

The second method of direct current flow of filament heating used in the experiment is schematically shown in Fig. 4.6. Sinusoidal signal from the function generator was amplified and supplied through the step-down transformer (used for matching the rated load of an amplifier - 4Ω) to the isolating transformer again through a capacitance to compensate its leakage.

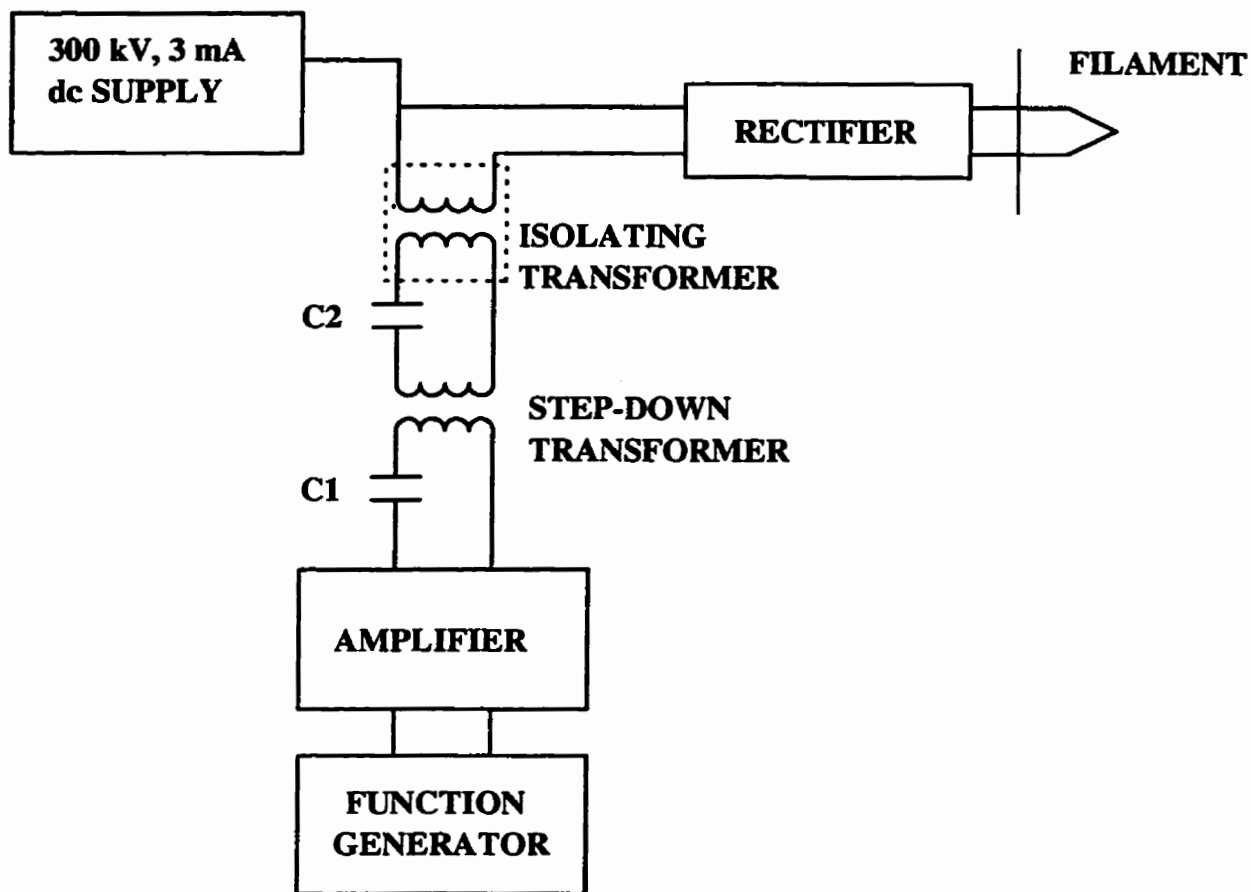


Figure 4.6. Filament heating circuit utilizing function generator and amplifier.

The signal from the isolating transformer was rectified and applied across the filament. In this case, the control of electron beam current was achieved by both ac output voltage from the amplifier and by the frequency adjusted to maximize Q factor of the circuit. The range of frequency used was between 15-17 kHz. Both methods were successfully implemented in the experiments.

4.3. Vacuum chamber and high vacuum system

The vacuum chamber was made of glass, so that it could be used as a high voltage bushing. The distance between the high voltage terminal and the edge of the grounded lead shield was about 0.56 m (Fig. 4.7). This is enough air insulation for about 300 kV. The chamber was made of two glass cylinders with metal flanges sealed to the glass for mounting the electron gun and for connection to the diffusion pump.

The X-ray shielding was made of three layers of ¼” lead sheet enclosed in the aluminum cylinder (Fig. 4.7). The layers overlap each other so that the side surface of the cylinder does not have any openings.

The operating pressure for hot cathode electron guns is usually very low $\sim 10^{-6}$ Pa. To obtain such a low pressure, two kinds of vacuum pump systems are utilized in electron beam technology: 1. turbomolecular pump with rotary roughing pump, and 2. diffusion pump with cold baffle and rotary backing pump. The latter setup was used in the experiment. Its block diagram is shown in Fig. 4.8.

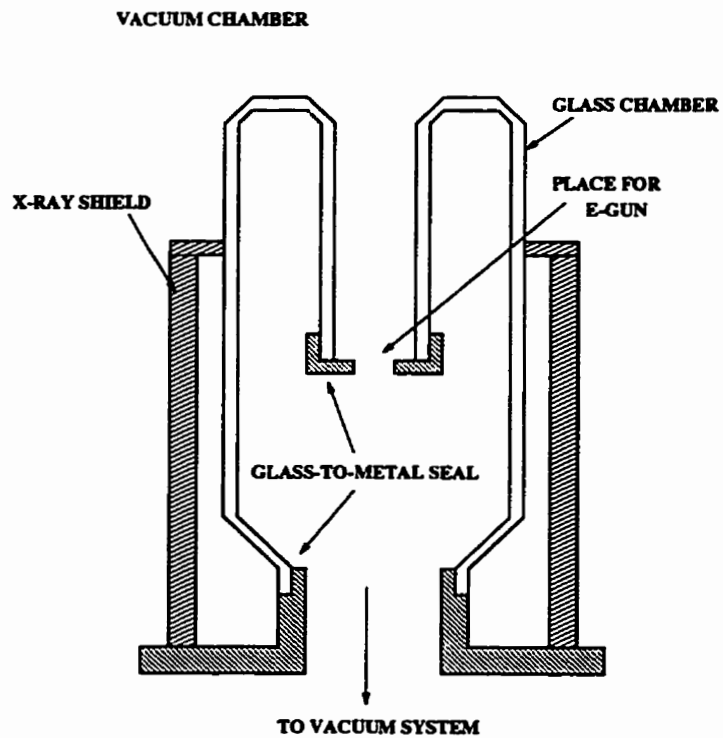
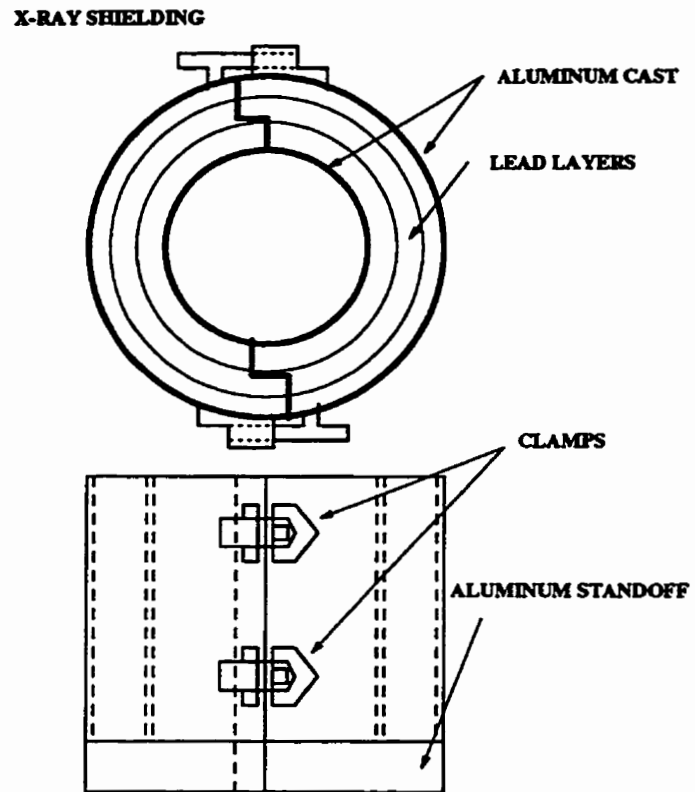


Figure 4.7. Vacuum chamber and X-ray shielding.

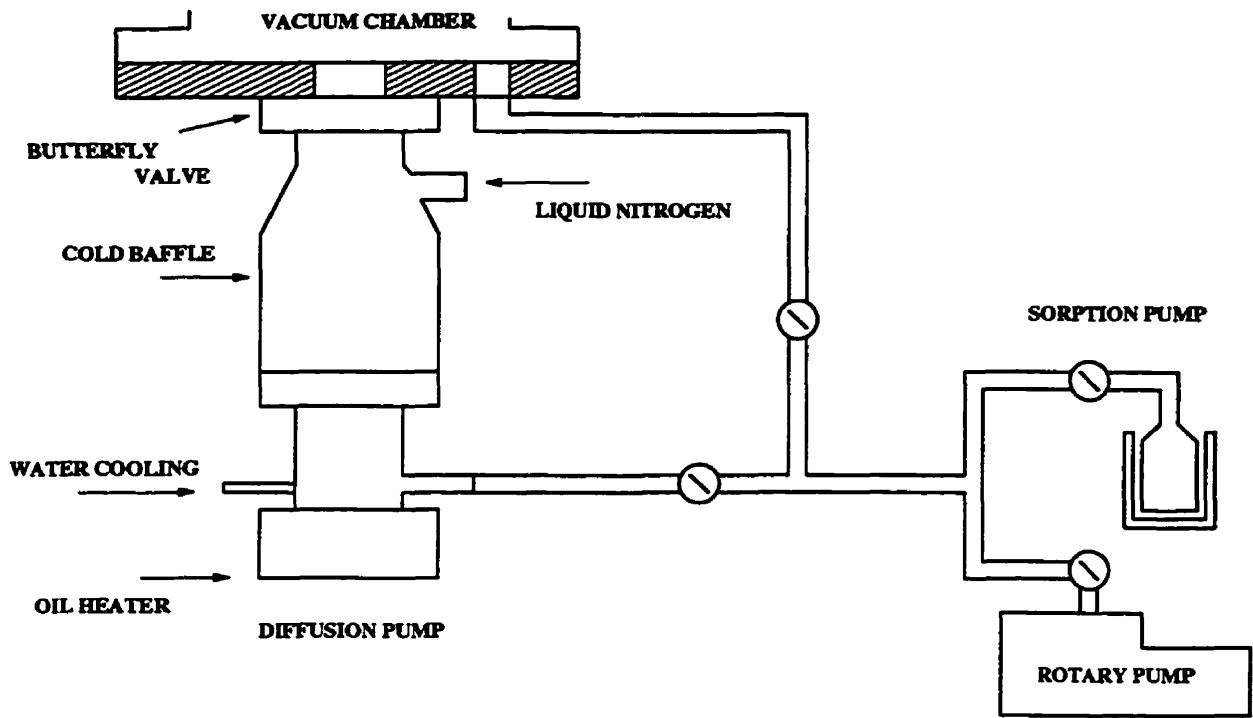


Figure 4.8. Vacuum system for electron beam water treatment apparatus.

The main drawback of this system is that the liquid nitrogen baffle should be always at a temperature of 77 K, otherwise the pressure substantially increases even up to 10^{-3} Pa and gases are adsorbed on the surface of the filament. After the gas adsorption, emission characteristics of the emitter are changed, even if the cathode is reactivated slowly in the vacuum. To secure the reliable and continuous operation, a proper liquid nitrogen dispensing system must be designed. It is important to have the lowest possible pressure so that the lifetime of the filament is quite long. If there is too much residual gas inside the chamber (pressure is too high), it will cause a quick

degradation (chemical and mechanical) of the filament - electron emitter - and eventually the total loss of electron emitting capability.

Figure 4.9 shows the measured dependence of lifetime of the hairpin tungsten filament on the pressure in the vacuum chamber. Accelerating voltage and beam current were maintained at 50 kV and 0.5 mA, respectively. In order to maintain the beam current at 0.5 mA, the heating current flowing through the filament must increase over time as the filament degradation process goes on. The four different vacuum conditions were tested at pressures $p=10^{-2}$, 3×10^{-4} , 5×10^{-6} and 2×10^{-7} Torr (10^5 Pa \approx 760 Torr). The lifetime of the tungsten filament increases significantly with lowering the pressure in the chamber (from several minutes to almost 20 hours). This is mainly due to increased sputtering rate of the filament material at higher pressures, and due to chemical degradation caused by the residual gas and enhanced by high temperature. In the case of using diffusion pump, the residual gas is probably hydrogen.

4.4. Anode (window housing) and water flow system

The anode system was designed in such a way to enable the mounting of electron permeable membranes (15 μ m and 25 μ m thick titanium, Ti, and 10 μ m thick boron nitride, BN, windows) and to adjust the distance to the electron gun. The window layer was clamped between two steel rings and sealed to the lower ring either by indium o-ring in the case of titanium window or by low vapor pressure vacuum epoxy sealant,

Torr-Seal™, in the case of boron nitride window (Fig. 4.10). These two sealants provided the system with suitable high vacuum leakproof connection.

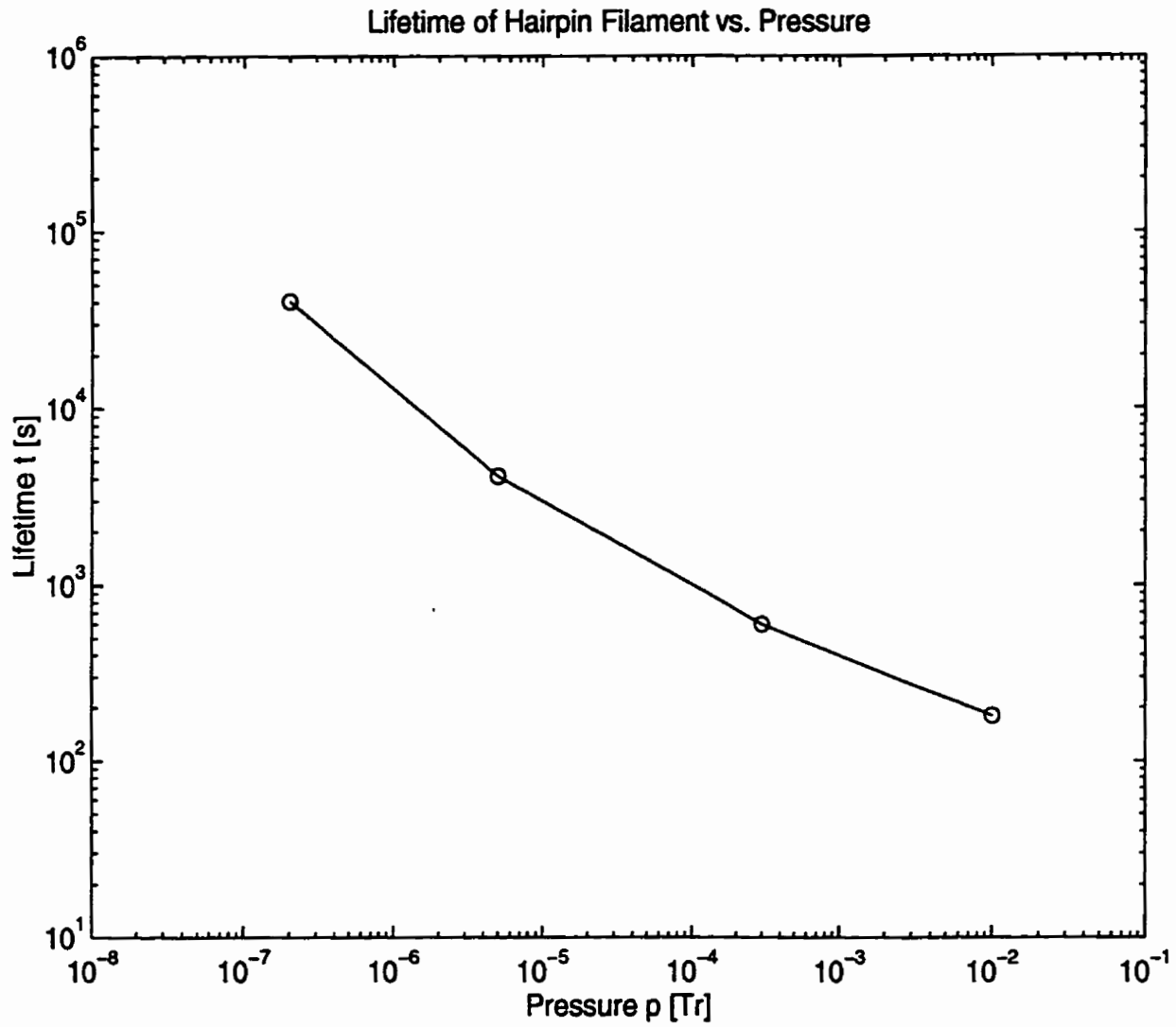


Figure 4.9. The hairpin filament (made of 0.5 mm wire) lifetime vs. pressure.

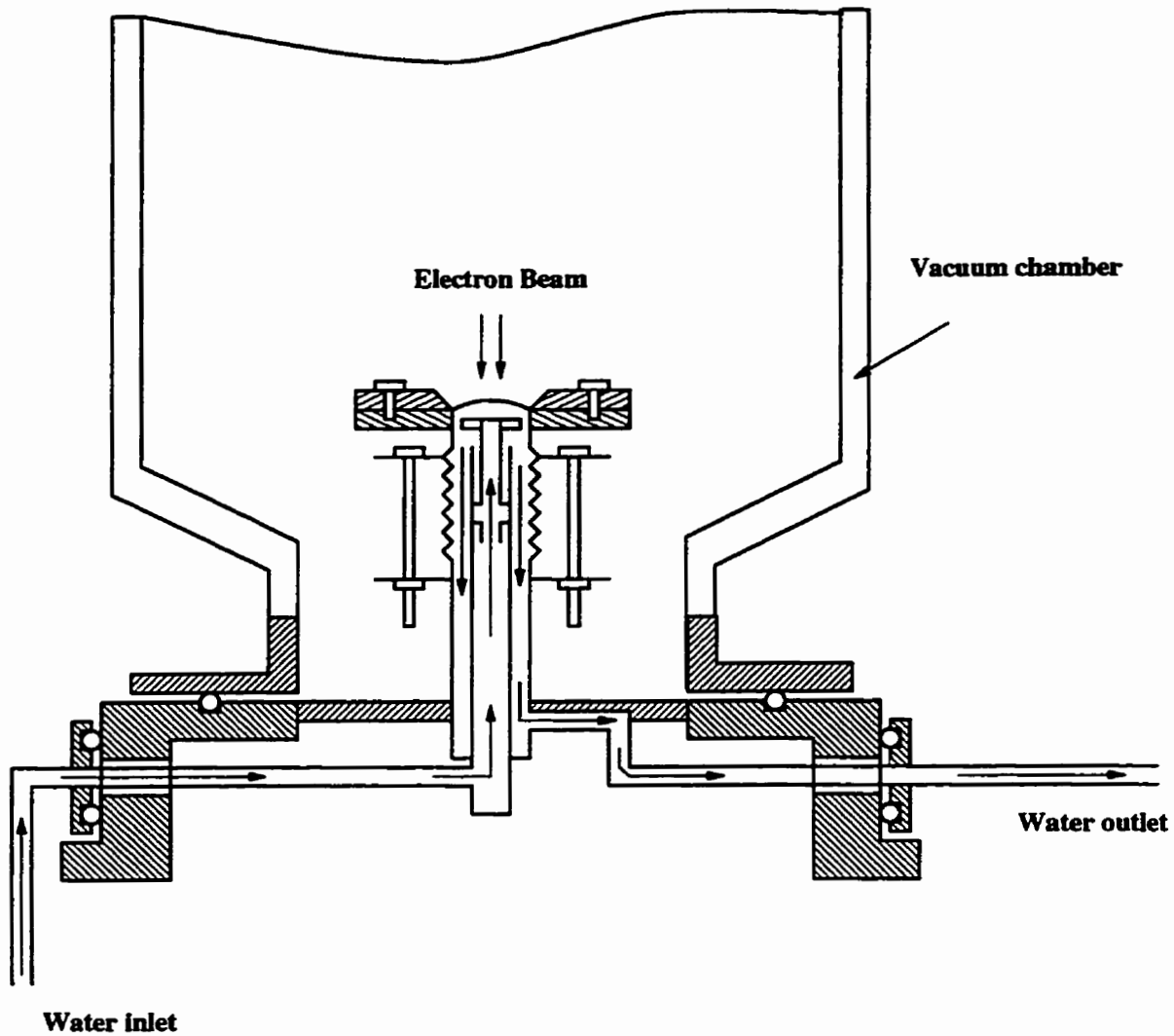


Figure 4.10. Anode with window housing and water flow system.

The diameter of the window is the same as the diameter of the hole in the upper anode ring. 5 mm- and 12 mm-diameter windows were used in the experiment. The anode was at the same time a part of the forced water flow system. Two concentric cylinders were used to guide the treated water to the window, where the electrons were injected, and the water goes back to reservoir through the space between inner and outer

tubes (Fig. 4.10). The outer tube was partly made of bellow so that the distance between electron gun and window could be adjusted and the electron beam diameter can be very close to the diameter of the window. It is important that the radiated power is spread over the whole window surface in order to avoid window implosion due to local overheating.

The exterior surface of the window (outside the vacuum chamber) was exposed to the treated water, so that the proper window cooling could be obtained. In the case of a relatively high power density, the water flow rate can not be too low, since the window may be overheated and eventually may implode, and it also can not be very high, as a high differential pressure across the membrane may cause its mechanical damage. In the experiment, the water flow rate was adjusted to be within the range of 1-5 l/min.

4.5. Titanium and boron nitride electron permeable windows

The crucial point of the electron beam water treatment setup is the electron permeable window. This is also the main device that should be improved, if efficiency of the electron beam power utilization is to be increased. In the experiments, two kinds of materials were used: titanium foil and boron nitride layers. The recent interest in boron nitride films stems from their potential applications as hard coatings [85] and from their electronic and thermal properties [86]. Cubic boron nitride (c-BN) is the

hardest known material other than diamond [86,87]. Unlike diamond, c-BN does not react with ferrous materials, and it can be used at higher temperatures before the onset of structural transformation [86]. These properties make it an excellent cutting tool material. Electronic applications of c-BN take advantage of its very wide band gap $E_g=6.4$ eV and its very high thermal conductivity ~ 70 W(m K)⁻¹ [86,87].

Boron nitride layers were prepared and supplied by Charged Injection Corporation. The desired thickness of boron nitride ceramic layer is deposited on 100 mm in diameter silicon wafer using a chemical vapor deposition (CVD) process. The wafer is then cut into the desired window shapes, e.g. 20x20 mm squares. Then the silicon substrate is chemically etched and the layers can be used. Because of the preparation process, boron nitride layers possess an internal stress (once the substrate is removed) which is an important property that must be taken into account when the window is being mounted. The direction of the differential pressure must follow the internal stress in the membrane, and one must not act against it especially for the windows with diameter greater than 5 mm.

Table 4.2 shows the comparison of certain thermal, electrical and mechanical properties of titanium and boron nitride. As can be seen, the thermal properties of boron nitride are much better with respect to their use for electron permeable membranes than those of titanium. The mechanical strength of titanium is higher at 25 °C, but its mechanical properties strongly depend on temperature, whereas boron nitride tensile strength does not decrease that rapidly with an increase in its temperature [88]. The me-

Table 4.2. Physical properties of titanium and boron nitride [85-94].

PROPERTY at 25°C	TITANIUM Ti	BORON NITRIDE BN
MASS DENSITY [g/cm ³]	4.54	~2.0
TENSILE MODULUS [GPa]	120.2	46.3-61.2
TENSILE STRENGTH [MPa]	230-460	54.4-63.3
THERMAL EXP. [1/K]	8.9x10 ⁻⁶	1.0-1.4x10 ⁻⁶
THERMAL COND. [W (K m) ⁻¹]	21.9	70.3
SPECIFIC HEAT [J (kg K) ⁻¹]	523	870
RESISTIVITY [Ω cm]	54x10 ⁻⁶	1.7x10 ¹³
DIELECTRIC CONSTANT [--]	-----	7.1

chanical strength of boron nitride layers is high enough to withstand the pressure difference that is encountered during electron beam water treatment. The only one advantage of titanium foil is its robustness arising from its elasticity. Boron nitride layers are very brittle and special care has to be taken during mounting the windows. From the electron beam application point of view, the most important thing is a relatively low mass density of boron nitride, more than two times lower than that of

titanium. It means that the absorptivity of this material is also much lower than that of titanium. This has been confirmed experimentally.

Figure 4.11 shows the fraction of the beam current transmitted through the window depending on the accelerating voltage for three membranes: 15 μm and 25 μm thick titanium windows, and 10 μm thick boron nitride layer. The incident beam current was measured by ammeter on the front panel of the high voltage dc power supply, the beam current transmitted through the window was measured by means of the collecting plate electrode placed 5 mm behind the membrane in vacuum and grounded through the 1 k Ω resistor. As can be seen, for an accelerating voltage of 100 kV approximately 95% of the beam current is transmitted through the BN window, whereas only 25% and 55% of the beam current is transmitted at 100 kV for 25 μm and 15 μm titanium foils, respectively.

While the electron beam is passing through the window, not only the current is lost but also energy of electrons is attenuated. It is very important in the case of low and medium energy electron beam, because if the window is thick and made of high density material the loss of energy may be substantial and the electron range in water is then very low. The measurements of energy loss of electron beam were carried out in a similar way to those for obtaining current transmission fraction in the vacuum. The collecting electrode was placed 50 mm behind the window and was grounded through the 1 k Ω resistor. The grid (mesh) electrode was placed midway between the window and the collector. The negative dc voltage within the range of 0-100 kV was applied to

the grid electrode and adjusted to the value for which the collector current was approximately equal to zero. This value of voltage multiplied by charge of an electron gives the actual value of electron beam energy.

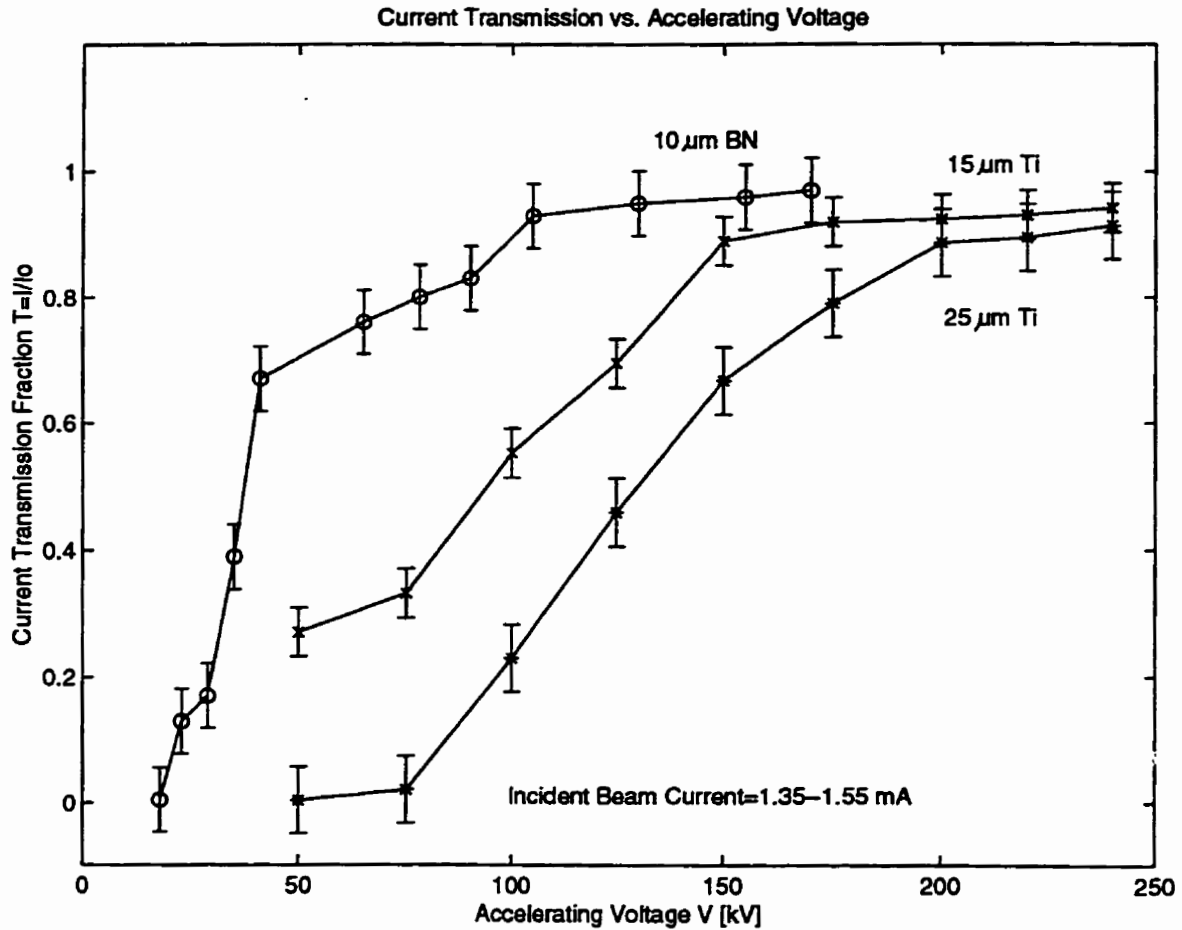


Figure 4.11. Current transmission fraction vs. accelerating voltage for three types of windows: 15 and 25 μm thick titanium, and 10 μm thick boron nitride.

Figure 4.12 shows energy loss of electron beam depending on accelerating voltage after passing through 10 μm thick boron nitride window. The results show that only about 5 keV is lost for the 100 keV incident beam which passes through the 10 μm boron nitride layer. It is low energy loss, e.g. for 25 μm titanium foil, approximately 80% of incident beam energy is lost for accelerating voltage of about 120 kV [27].

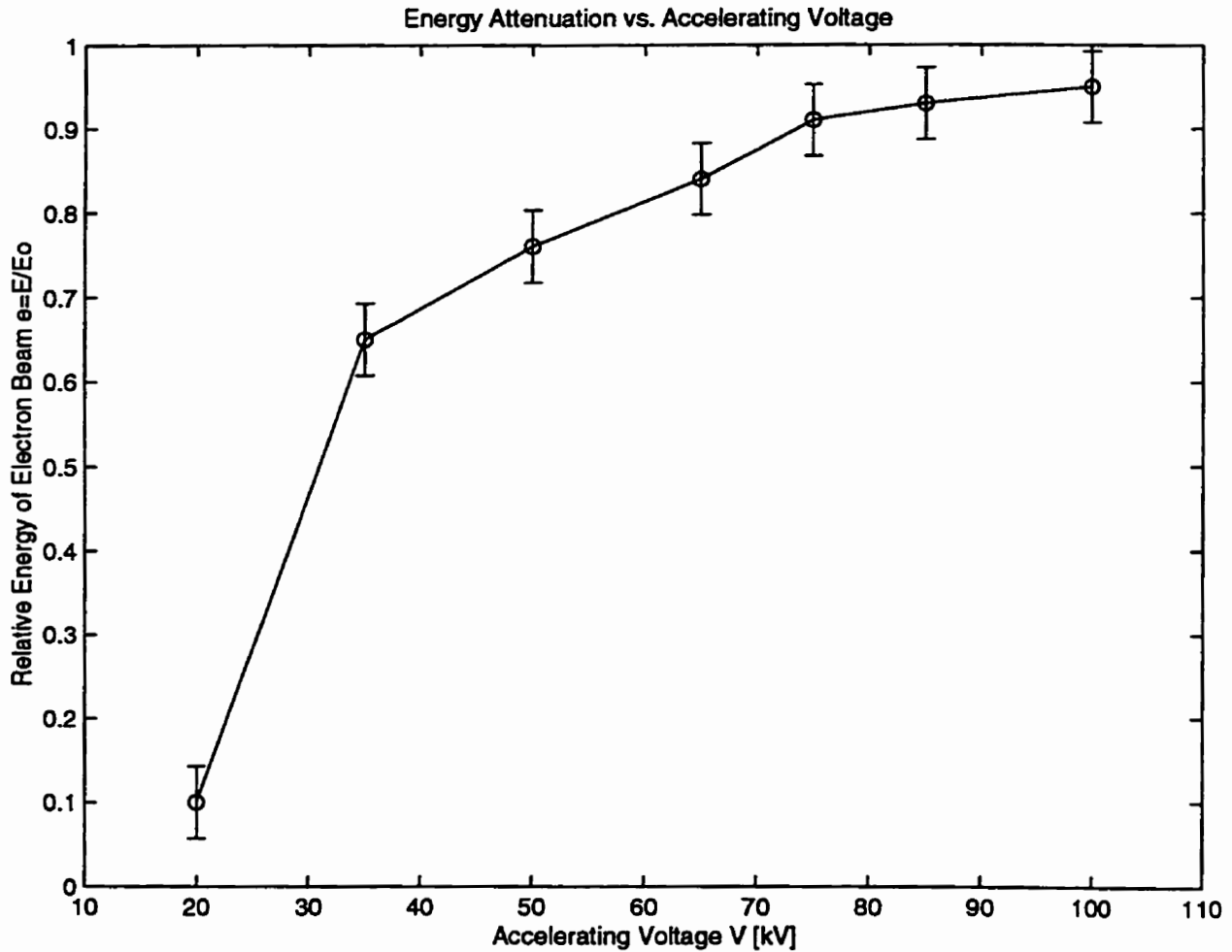


Figure 4.12. Energy loss of electron beam for 10 μm thick boron nitride window.

The efficiency of electron beam passage through the window can be calculated on the basis of energy loss and current transmission fraction measurements. For the radiated power of 100 W - 100 kV and 1 mA, the power after passing through the 10 μm boron nitride window is equal to 95 kV multiplied by 0.95 mA, about 90.25 W. It means that the efficiency at 100 kV and 1 mA is about 90%. Of course, as the energy loss decreases and transmission fraction increases with an increase in accelerating voltage, the efficiency will also increase with an increase in energy of electron beam.

Because the window has a diameter of only 12 mm, it is important that the fraction of power absorbed within the window is efficiently dissipated in order to avoid window implosion due to local overheating of the membrane. Very good thermal conductivity of both boron nitride and titanium is an advantage in this case. Usually, the titanium window is air cooled in commercial facilities which allows to apply about 0.5-1.5 mA per centimeter of window length [27]. The most important parameter in this case is the maximum power density that can be safely applied, without an implosion of the window.

To find out an approximate maximum power density, four kinds of windows were investigated for implosion: 25, 15 and 10 μm titanium and 10 μm boron nitride membranes. In these measurements the windows were not being cooled. The voltage was fixed at 100 kV and the current was varied from 0-2 mA. Diameter of the windows under investigation was 5 mm. The conditions (voltage and current) at which the window imploded after a maximum 2 minutes of continuous work were used to estimate

maximum power density which can be used without cooling. As it is shown in Table 4.3, almost ten times higher power can be applied to the boron nitride window than that applied to the 25 μm titanium window at 100 kV. It is of course related to the current and energy loss of the beam. The difference would be smaller in the case of higher electron energies - higher accelerating voltages.

Table 4.3. Power density at the time of implosion for four different membranes.

Window Material	Thickness [μm]	Implosion at:		Power Density [W/cm^2]
		Voltage [kV]	Current [mA]	
Ti	25	100	0.12	61.1
Ti	15	100	0.31	157.9
Ti	10	100	0.58	295.4
BN	10	100	1.12	570.4

Use of treated water to cool the window causes a remarkable increase in an average power dissipated. This power dissipated by 25 μm water cooled titanium window is about 78 W/cm^2 [66]. Only 3 W/cm^2 can be dissipated in the case of the air cooled window [66]. Because of the very good thermal properties of both titanium and boron nitride, if the window is cooled by treated water, one can expect the maximum power density to be at least one order of magnitude higher than the value included in the

Table 4.3. The power density will also depend on window thickness and size, and on the water flow rate.

Throughout the experiments concerning boron nitride windows, it turned out that the most difficult part in dealing with the membranes is a way of mounting them in the anode. Special care has to be taken to maintain the mechanical stability of the layers during window assembly due to brittleness and internal stress arising from the method of preparation, after the silicon substrate is etched. In addition, the window should be assembled in a charge-free environment because of being a very good dielectric (see Table 4.2) which can easily trap a surface charge - all the tools and even hands must be grounded. The charge built up on the layer would interfere with electrons and negatively affect transmission properties of the layer and efficiency of beam passage. Figure 4.13 shows two methods of mounting boron nitride layers. The first method (Fig. 4.13a) in which the boron nitride layer is placed between two steel rings can be used for the windows with diameter not greater than 5 mm. In this case the boron nitride window seems to be robust enough to be forced and clamped between the rings. A high-vacuum leakproof connection was obtained by using Torr-Seal low vapor pressure epoxy.

The second method (Fig. 4.13b) was used for the windows having a diameter of 12 mm. The boron nitride layer was put on the steel ring with the groove which was filled with Torr-Seal epoxy sealant. The sealant curing time is about 2 hours. After that time, the high vacuum leakproof connection is obtained. Such windows can withstand a

differential pressure across the membrane of up to 1.5 atmosphere. Their lifetime depends mainly on the pressure and beam power.

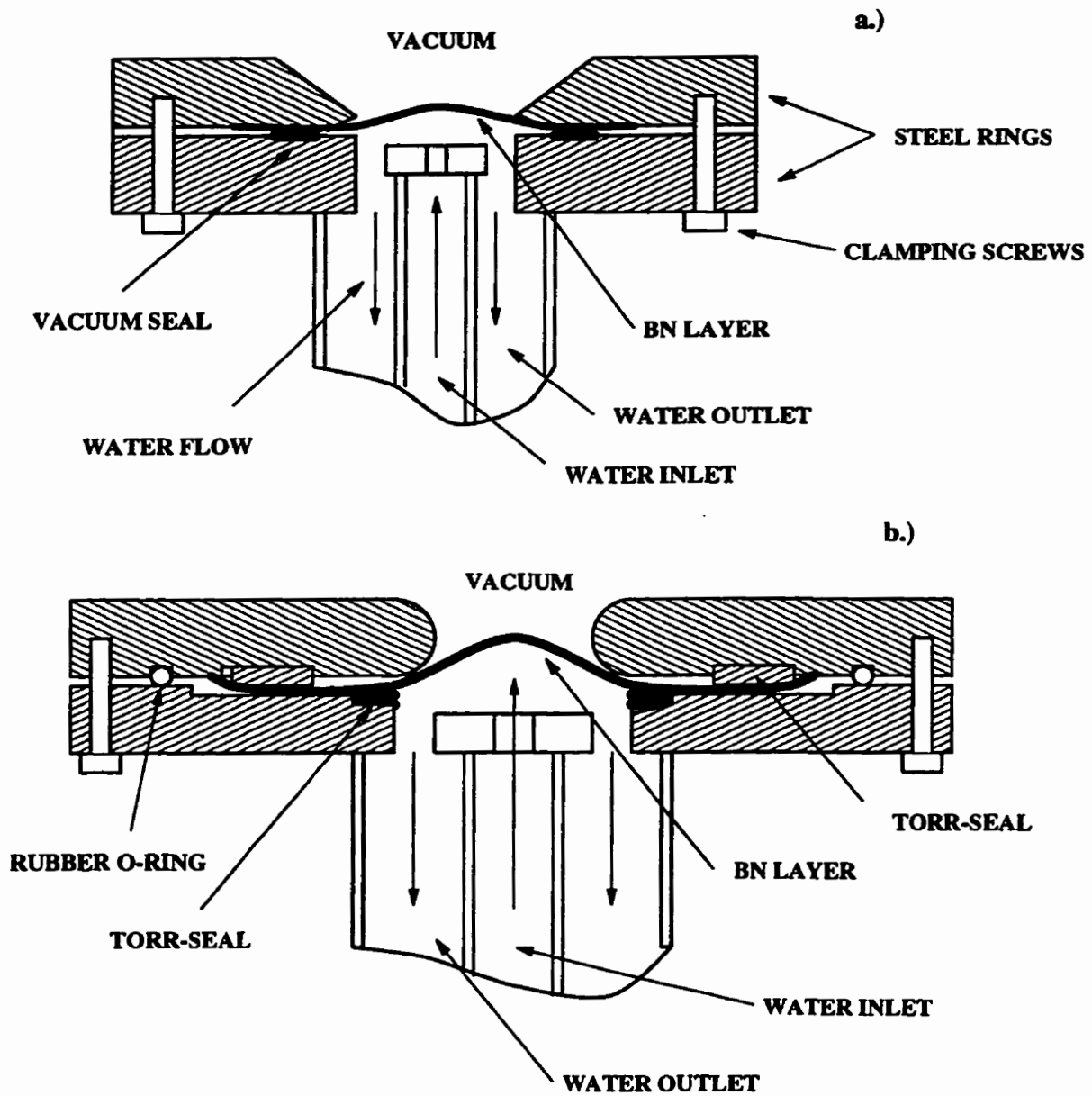


Figure 4.13. Methods of mounting 10 μm thick boron nitride membranes in anode: a) windows with diameter less than 5 mm; b) windows with diameter greater than 5 mm.

The use of 10 μm thick boron nitride layers for electron permeable membranes significantly improves efficiency of electron beam power utilization. This kind of material should be used especially for low and medium energies of electron beam.

4.6. Electron beam laboratory scale apparatus for water purification

The schematic diagram of the lab scale electron beam water treatment apparatus is presented in Figure 4.14. The photograph of the setup is presented in Figure 4.15. The electron beam is generated in a vacuum chamber (pressure is $<10^{-5}$ Pa) made of glass, which also serves the role of high voltage bushing. Electrons are emitted by thermionic emission from the hot cathode (either hairpin filament or dispenser cathode) which is heated by direct current flow. The emitter is at negative dc high potential and electrons, once they leave filament material due to acquired thermal energy, are accelerated in the high electric field. The accelerated electrons bombard very thin electron permeable membrane (window) and pass it through into water stream. The exterior of the window is exposed to the treated water, so that the water stream is used as the window coolant.

In order to control the beam current, the isolating transformer is used to separate the control panel from high potential.

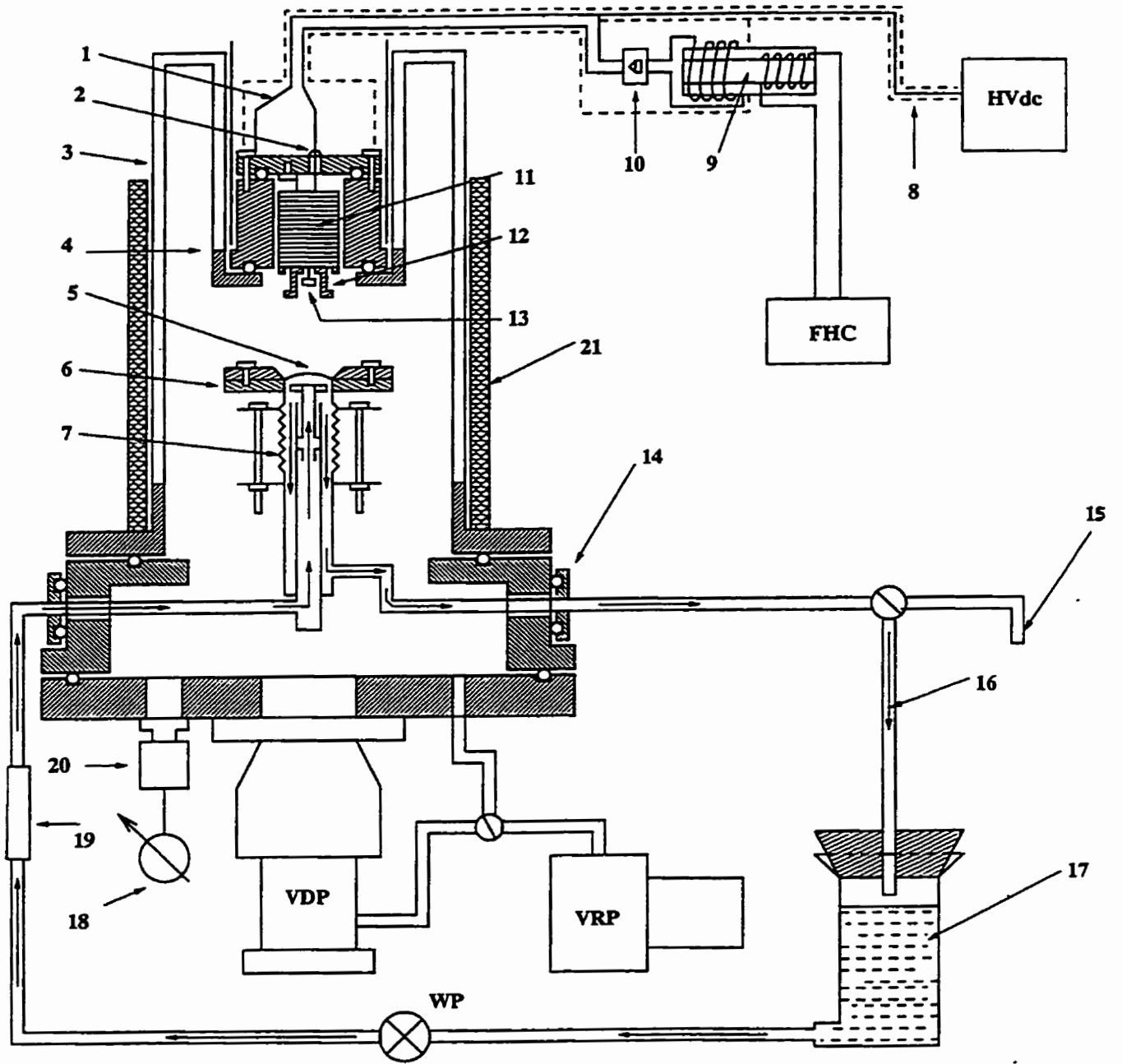


Figure 4.14. The schematic diagram of electron beam water treatment apparatus.

The meaning of symbols and numbers in Fig. 4.14:

HVdc - negatively polarized high voltage dc power supply (Voltronics, maximum power 1 kW, voltage 300 kV);

FHC - filament heating control (either self-oscillating inverter or amplified signal from function generator);

VDP - vacuum diffusion pump (Edwards);

VRP - vacuum rotary backing pump (Edwards);

WP - water diaphragm pump (up to 5 l/min);

1. heater-cathode connection of electron gun;

2. heater connection of electron gun;

3. glass vacuum chamber;

4. glass-to-metal seal for high voltage terminal of the apparatus;

5. electron permeable window;

6. anode rings - window housing;

7. adjustable bellow;

8. high voltage (300 kV dc) shielded cable;

9. isolating transformer;

10. rectification of isolating transformer output signal;

11. electron gun assembly;

12. electron gun high voltage electrode;

13. dispenser cathode of electron gun;

14. high vacuum liquid feedthroughs (Ceramaseal);
15. water sample outlet;
16. water outlet from the apparatus;
17. water reservoir;
18. high vacuum meter (Penning gauge controller);
19. water flow meter;
20. Penning gauge head;
21. X-ray shielding.

An X-ray shielding, 25 mm-thick lead cylinder, is placed around the vacuum chamber. Its side area is completely closed due to the overlapping arrangement of lead layers closed in the aluminum cast. The X-radiation dose during the operation of the apparatus at 200 kV and 2.0 mA was measured and it never exceeded 0.02 mR/h (milliroentgens per hour) which is far below the maximum safe exposure limit $SE=0.6$ mR/h [22,23,36], and the annual permissible dose of 5 rem is never exceeded even if very long working hours are assumed. The anode with the window and water system was designed in a way that enables a regulation of the distance to electron gun. This allows spread of the electron beam over the whole window surface, so that the power of the beam is evenly distributed over the window surface. The diameter of the beam at the point of action is about 10 mm (the window diameter is about 12 mm). The increment

of the gun-anode distance by 10 mm causes the increase in the beam diameter by about 2 mm.

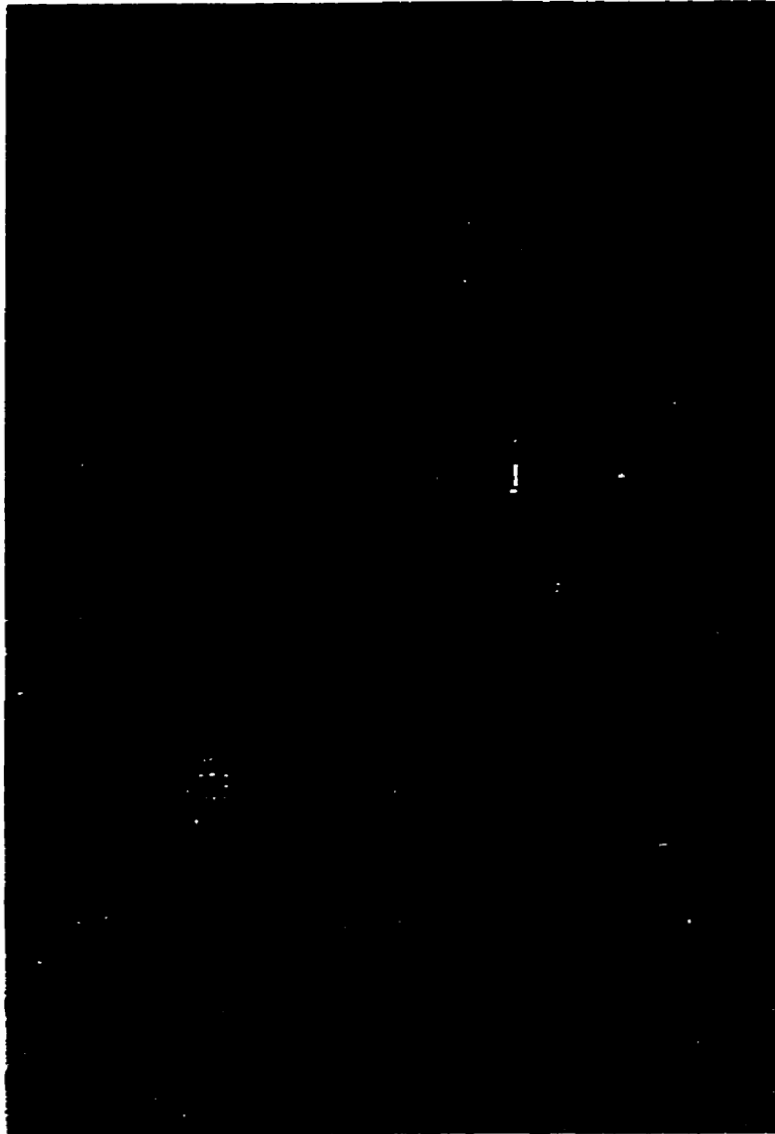


Figure 4.15. The photograph of electron beam apparatus used for water purification.

CHAPTER 5

RESULTS - REMOVAL OF VOLATILE ORGANIC COMPOUNDS

The main criterion for choosing the volatile organic compounds for investigation was the frequency of their presence at 546 Superfund* Sites [19]. Trichloroethylene can be found at 33% of the sites (the most frequently identified substance) [19]. Toluene, benzene and chloroform can be found in 28%, 26%, and 20% of the sites, respectively [19]. All these compounds are within the top six of the most frequently identified substances at the Superfund Sites - toluene is the third, benzene is the fourth, and chloroform is the sixth. These contaminants have different chemical structures. Benzene is an aromatic hydrocarbon C_6H_6 ; toluene is also an aromatic hydrocarbon but it has additional aliphatic side chain $C_6H_5 - CH_3$; trichloroethylene has two carbon aliphatic chain $CHCl=CCl_2$; chloroform is the simplest halogenated aliphatic hydrocarbon $CHCl_3$ and the most difficult to be removed among trihalomethanes [3].

5.1. Removal of benzene, toluene and trichloroethylene

The dependencies of the relative content, c , of contaminants ($c=C/C_0$ where C is the concentration of contaminant after the treatment and C_0 is its initial concentration)

* So called Superfund program was enacted in 1980. Its goal has been to fund a clean up of the worst toxic waste sites in USA. United States Environmental Protection Agency has governed its realization.

on the total radiated dose and absorbed dose were measured [95-97]. Because of the limited solubility of the compounds in water, the deionized water solutions contained only up to 12 ppm (12 mg/liter) of the contaminant. The volume of water to be treated was spiked by the required amount of contaminant and stirred over an extended period of time - from 3 to 24 hours - in a closed container (to avoid air stripping of the volatile compounds). Concentration of both compounds before and after the treatment was measured by means of microextraction to hexane technique and gas chromatography measurements [98,99]. A Hewlett Packard HP 5890 Series II gas chromatograph was used in these measurements. A Hewlett Packard HP-624 column with the following parameters: 1. Length – 30 m; 2. Diameter – 0.53 mm; 3. Film thickness – 3 μm ; and 4. Phase ratio – 40, was used. A carrier through the column was helium at a flow rate of 4.4 ml/min. An oven temperature was initially adjusted to 35⁰C, and then it was ramped up to 120⁰C at a rate of 15⁰C/min. After ramping up, a final time of the run was 2 minutes, and total run time was 14 minutes. Split ratio of injection was 1:50, and FID detector was used. The accuracy of these measurements was equal to about 1%.

In the experiment, special attention should be paid to air stripping and absorption of the contamination in the water system. The use of stainless steel and Teflon™ tubing prevents the excessive absorption of hydrocarbons, which takes place while Tygon™ tubing is used. The use of closed water circulation system should prevent an excessive aeration of the treated solution and, therefore, the part of volatile contaminant stripped to the air is negligible. After 60 minutes of circulation, 10% of TCE, 6% of toluene and

5% of benzene disappeared without electron beam treatment from initial concentrations of each contaminant of about 10 ppm. These values were used to estimate an initial concentration of the contamination depending on the time of the water circulation, so that only the removal caused by the electron beam could be taken into account.

5.1.1. Effect of beam power utilization

As it has been shown in Chapter 1, efficiency of electron beam power conversion into absorbed dose contributes significantly in an overall efficiency of electron radiation processes. The main factors that can cause the electron beam power utilization to increase are: 1. use of a relatively high accelerating voltage and 2. use of low absorptivity electron permeable membranes. Figures 5.1, 5.2 and 5.3 show the results of the experiment concerning removal of TCE, toluene and benzene, respectively, for the three different types of windows - 15 and 25 μm thick titanium foil and 10 μm thick boron nitride layer. The dependency of relative concentration of contaminant $c=C/C_0$ on radiated dose is shown.

The radiated dose was calculated as incident beam power over water flow rate multiplied by the number of exposures of the treated volume of water during the period of water circulation. The radiated dose was varied by the time of water circulation. The circulating water was treated over a certain period of time within the range of 10-50 minutes. The water flow was adjusted to be 1 kg/min and the volume of treated water

was 2 liters. The accelerating voltage and electron beam current were 125 kV and 0.6 mA, respectively.

As can be seen in Fig. 5.1, the differences in a degree of the removal of trichloroethylene as a function of total radiated dose come from the loss of the beam power during the passage through the window. The performance of the boron nitride layer seems to be the best for low energy electron beam. The removal of TCE for the maximum radiated dose $D=31.5$ kGy ($Gy=J/kg$) was: 83%, 53% and 32% for 10 μm thick boron nitride window, 15 μm and 25 μm thick titanium windows, respectively.

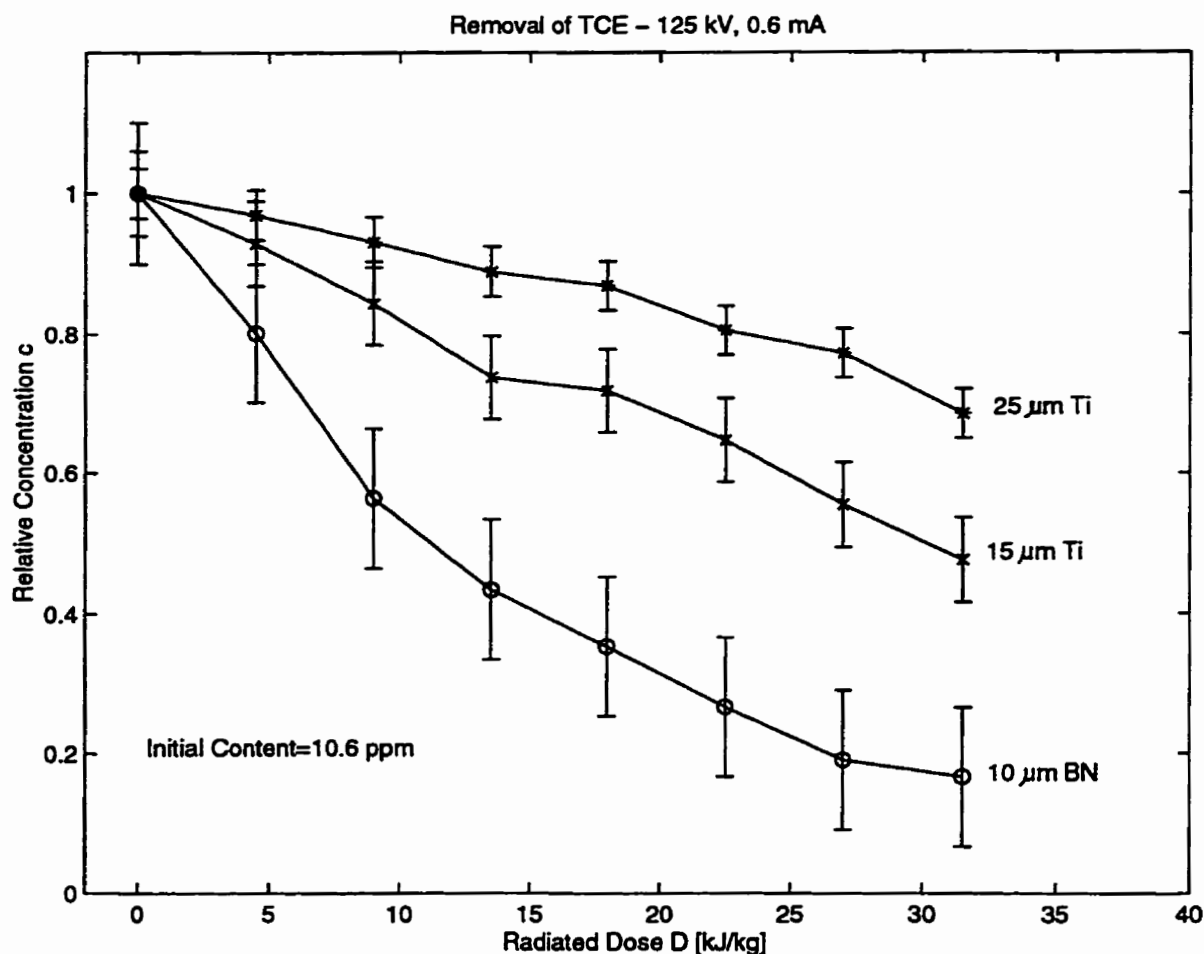


Figure 5.1. Relative concentration of TCE vs. radiated dose for three different windows.

The same measurements were carried out for toluene and benzene. Figure 5.2 shows the dependence of the relative content of toluene depending on the total radiated dose for three different types of electron permeable windows. The removal efficiency of toluene is lower than that of TCE. For the radiation dose $D=36$ kGy, the removal was 64%, 42 % and 30% for 10 μm thick boron nitride window, 15 μm and 25 μm thick titanium windows, respectively. Again, it seems that the amount of the contaminant removed depends on the losses in the window which are the highest for 25 μm titanium.

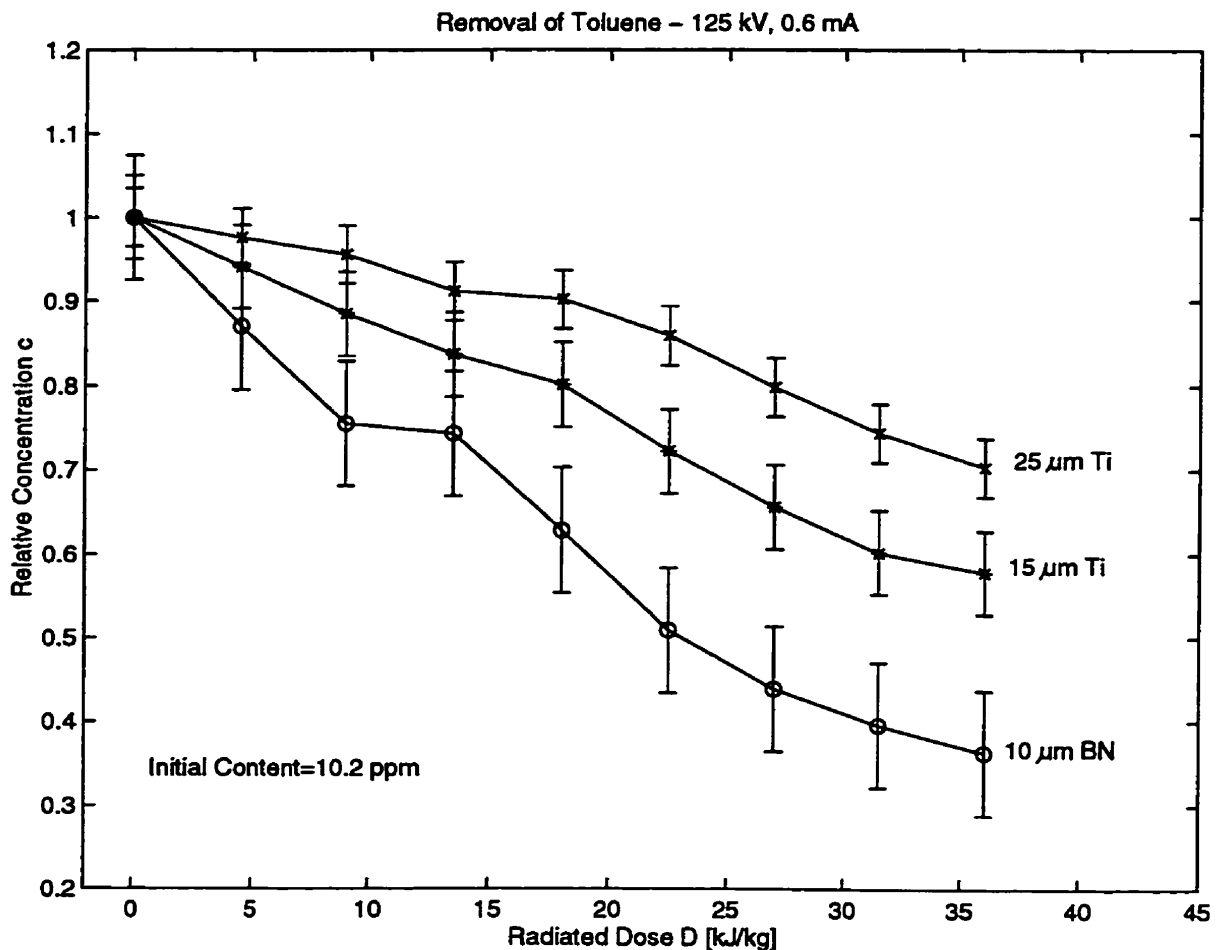


Figure 5.2. Relative concentration of toluene vs. radiated dose for different windows.

Figure 5.3 shows the dependence of the relative content of benzene depending on the total radiated dose of electrons. For the radiation dose $D=36$ kGy, the removal was 62%, 40 % and 25% for 10 μm thick boron nitride window, 15 μm and 25 μm thick titanium windows, respectively. The removal of benzene was similar to that of toluene (about 5% lower), which can be expected because of the similar chemical structure of both chemicals.

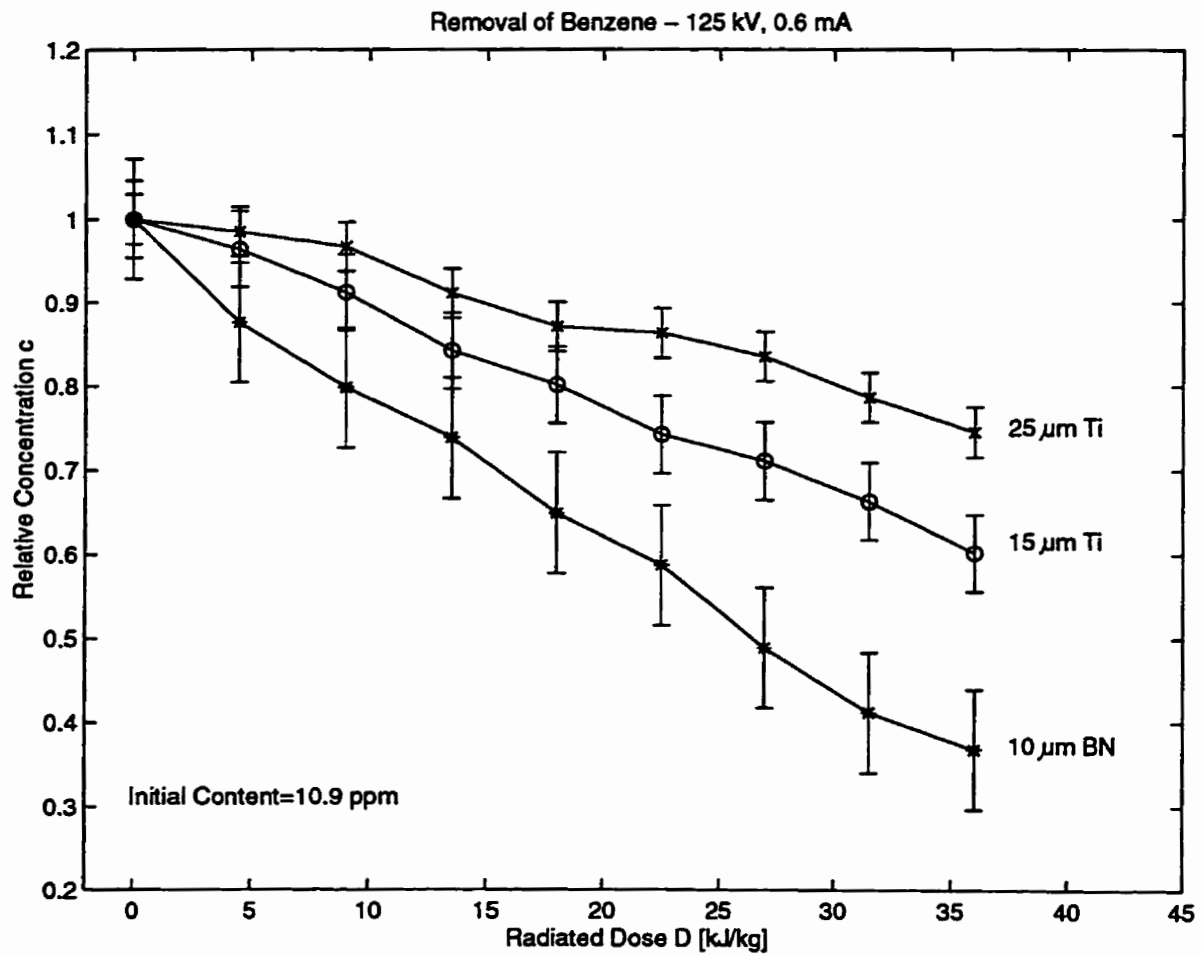


Figure 5.3. Relative concentration of benzene vs. radiated dose for different windows.

In each case the initial concentration was about 10 ppm=10 mg/liter which is a substantial amount. The Electron Beam Research Facility in Miami carries out its research for the initial concentrations of contaminants being less than 1.5 ppm. This amount is similar to the level that usually can be found in ground- and wastewater treatment. In the case of drinking water, the maximum contaminant level for example for chlorination by-products is between 25-125 $\mu\text{g/liter}$. A more efficient decomposition can be expected while the initial concentration is lower, although it is claimed that relative removal does not depend on the initial concentration if it is below 1.5 ppm [3].

5.1.2. Effect of accelerating voltage and electron beam current

The electron beam power is one of the major parameters of the electron irradiation technique. Accelerating voltage, electron beam current and exposure time (water flow rate) are major variables that shall influence the efficiency of contaminant decomposition.

Figure 5.4 shows the dependence of the relative concentration of benzene on the radiated dose for two different values of accelerating voltage 125 kV and 175 kV. The incident beam current was equal to 0.8 mA. The water flow was adjusted to be 1 l/min and the volume of treated water was 2 liters. The dose was controlled by water circulation time - longer circulation time is required for lower beam power (lower accelerating voltage) in order to maintain the same radiated dose. The boron nitride

window was used in the experiment, so that the losses in the beam are not a major factor influencing the removal of benzene. According to the results presented in Figures 4.11 and 4.12, the approximate beam power loss in the window is about 9% in the case of $V_A=125$ kV, and approximate power loss in the case of $V_A=175$ kV is about 6%. The initial concentrations of benzene dissolved in deionized water were $C_0=10.1$ ppm and $C_0=9.5$ ppm in the case of $V_A=175$ kV and $V_A=125$ kV, respectively.

The obtained results (Figure 5.4) show that, for the same radiated energy density, the rate of benzene removal is higher in the case of higher accelerating voltage. The 90% removal of benzene takes place at approximately $D=24$ kJ/kg and $D=31$ kJ/kg for $V_A=175$ kV and 125 kV, respectively. This difference can arise from the fact that at higher electron energies, the larger volume of water can be penetrated due to an increased electron range in water.

The electron beam current has even stronger influence on the removal rate of benzene. The dependence of the relative concentration of benzene on the radiated dose for two different values of incident electron beam current $I=0.8$ mA and 1.12 mA is presented in Fig. 5.5. The accelerating voltage was equal to 125 kV. The water flow was again adjusted to be 1 l/min and the volume of treated water was 2 liters. The dose was controlled by water circulation time - longer circulation time is required for lower beam power (lower beam current) in order to maintain the same radiated dose. The boron nitride window was used in the experiment, so that the power losses in the beam are not a major factor influencing the removal of the contaminant. The initial

concentrations of benzene dissolved in deionized water were $C_0=13.0$ ppm and $C_0=12.9$ ppm in the case of $I=1.12$ mA and $I=0.8$ mA, respectively.

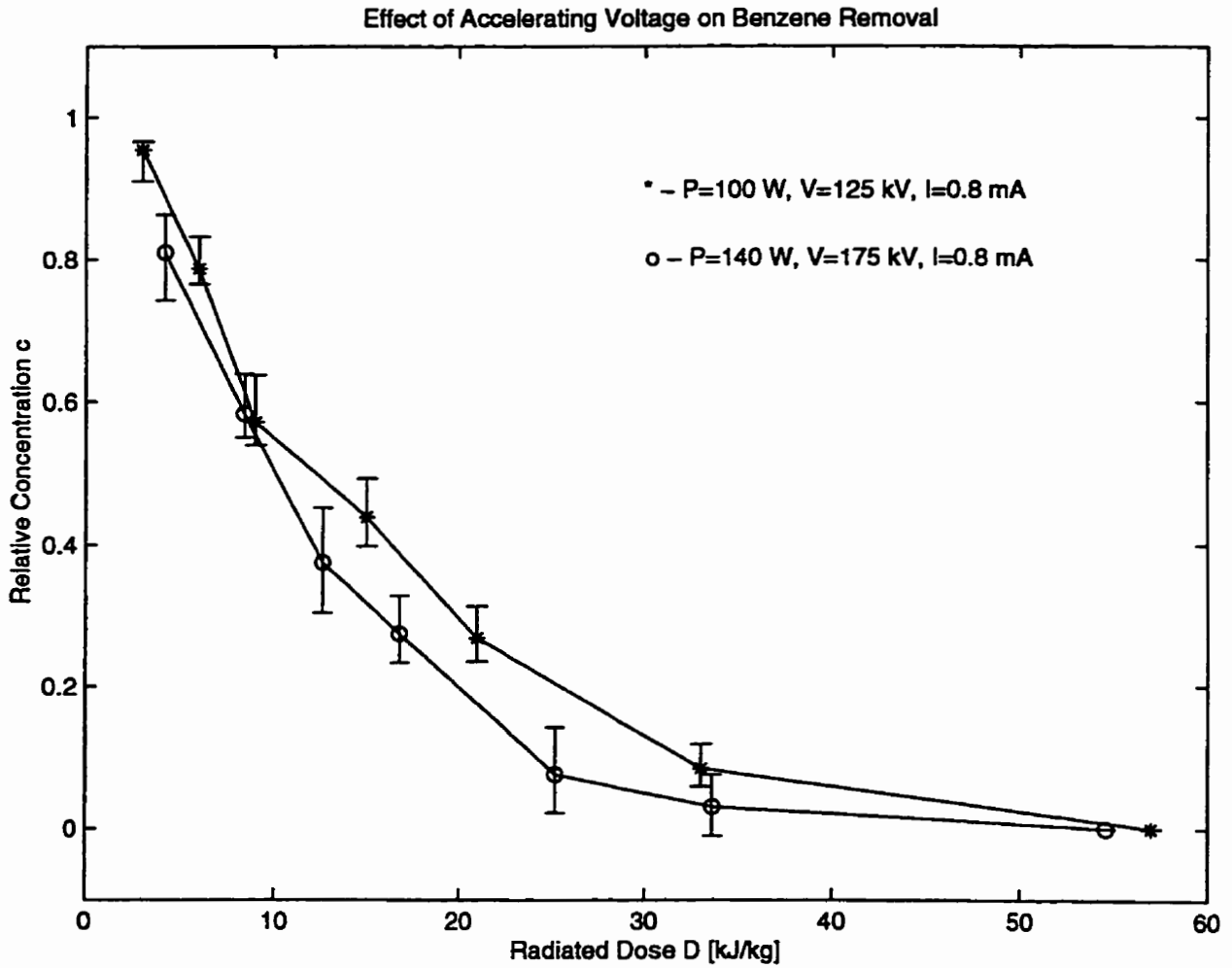


Figure 5.4. Relative concentration of benzene vs. radiated dose for two different values of accelerating voltage: 125 kV ($C_0=9.5$ ppm) and 175 kV ($C_0=10.1$ ppm).

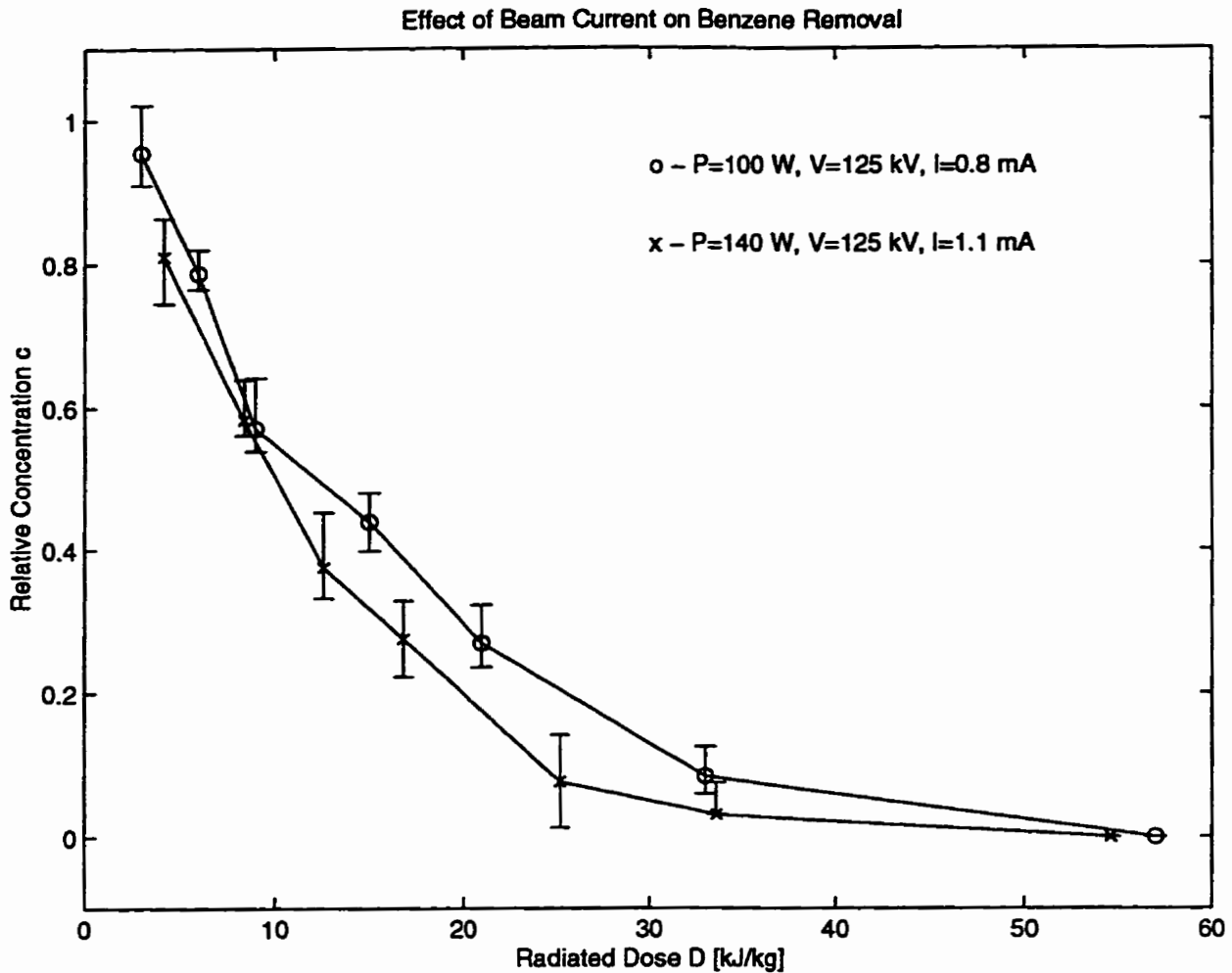


Figure 5.5. Relative concentration of benzene vs. radiated dose for two different values of incident electron beam current: 0.8 mA ($C_0=12.9$ ppm) and 1.12 mA ($C_0=13.0$ ppm).

The obtained results (Fig. 5.5) show that for the same radiated energy density, the rate of benzene removal is higher in the case of higher incident beam current. The 90% removal of benzene takes place at approximately $D=20$ kJ/kg and $D=32$ kJ/kg for 1.12 mA and 0.8 mA, respectively. This difference can be caused by higher power

absorbed per unit volume in the case of higher current density at the point of action as it is explained in Section 2.1, page 15-16.

5.2. Removal of chloroform

Chloroform was found to be the most resistant among trihalomethanes in electron beam water treatment [3]. The method of sample preparation was the same as in the case of the other volatile organic compounds investigated in the experiments; however, due to very high volatility of this compound, the part stripped to air during the experiment was not negligible. After 60 minutes of mixing in the water system without electron beam radiation, the stripped part of chloroform is within the range of 15-32% depending on the initial concentration (10-100 ppm). In order to correctly estimate the actual content of chloroform, which is decomposed by electron beam treatment, it is necessary to take into account the loss due to aeration. Figure 5.6 shows the dependence of relative concentration of chloroform on radiated dose. The experiment was performed using 25 μm thick titanium window, therefore the total radiated dose is significantly higher than that in the case of the rest of the investigated volatile compounds (see section 3.1.1). In this experiment [97,99], the water flow rate was 2 l/min and the volume of treated solution was 1 liter. The initial concentration of chloroform was $C_0=89.2$ ppm. The power of the incident beam was equal to $P=187$ W

($V_A=170$ kV, $I_B=1.1$ mA). The radiated dose was controlled by the circulation time of the water.

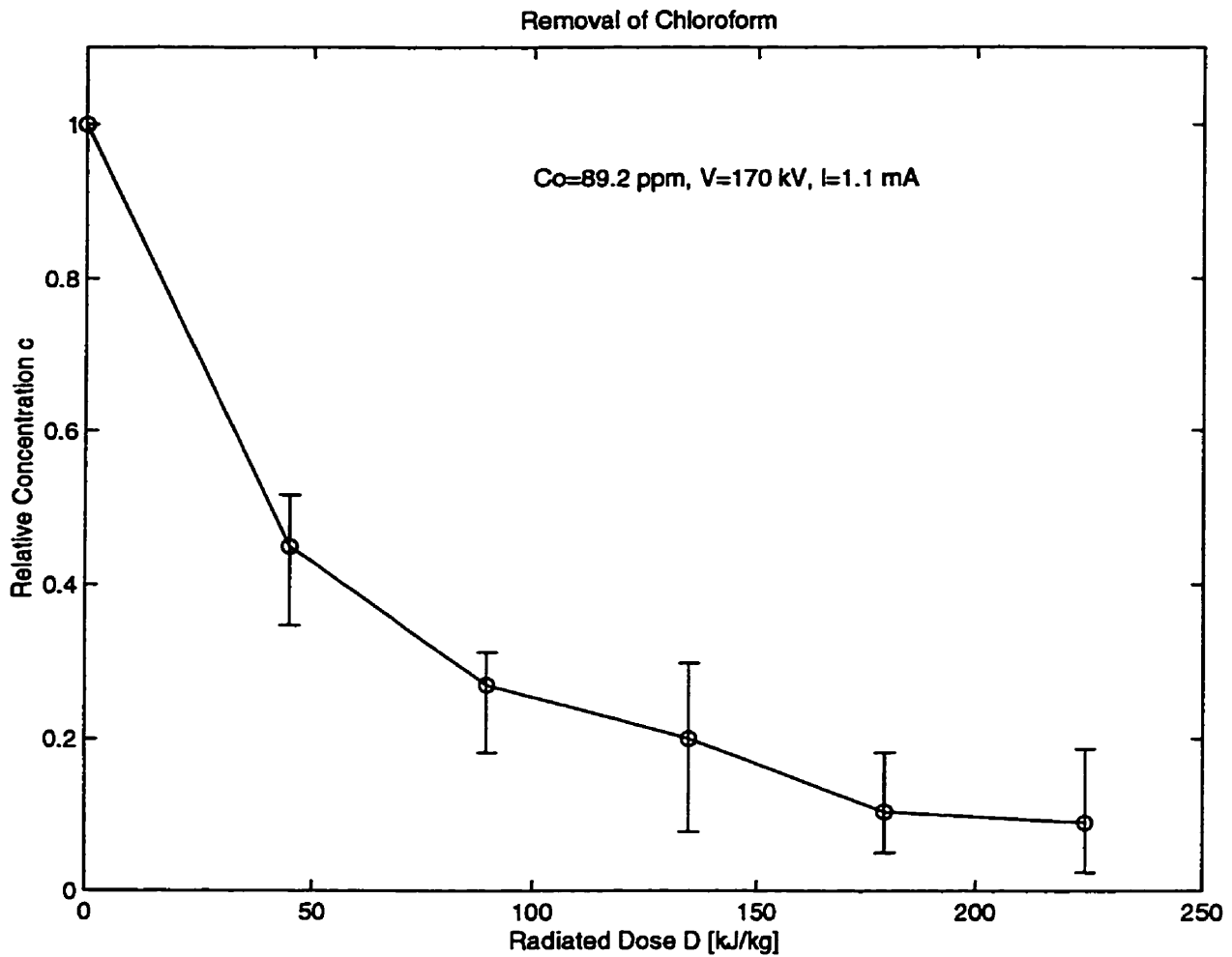


Figure 5.6. The dependence of the relative content of chloroform on the radiated dose for 25 μm thick Ti window using electron beam at $V_A=170$ kV and $I=1.1$ mA.

The 90% of chloroform removal is obtained at the radiated dose of $D=224.4$ kJ/kg which corresponds to the treatment time $t=10$ min. One has to bear in mind that

only a small fraction of the radiated dose was absorbed by the solution due to the use of a relatively thick titanium window. The part of chloroform stripped to air during a control run for a similar initial concentration was taken into account in the results presented in Fig. 5.6.

5.3. Removal of volatile organic compounds depending on absorbed dose

Absorbed energy density (absorbed dose) is only a fraction of the radiated dose. In the case of using a low accelerating voltage, the significant power loss of the electron beam can take place, especially when titanium windows are used, due to beam current and energy losses in the window (see Fig. 2.4, Fig. 4.11 and Fig. 4.12). The most common approach undertaken to estimate the absorbed dose is to measure the temperature rise associated with injection of the electron beam power at certain water flow rate [3,10,13-24,27,31,32,54]. Such measurements are accurate only for a semi-adiabatic system, for instance if the water stream is irradiated in air. In the case of the described experiment, when the window and the whole anode assembly is in contact with the treated water, such a measurement would not give a reasonable outcome.

The average absorbed dose can be estimated on the basis of the knowledge of the following: 1. the beam power losses in the window; 2. the electron range in water (equations 2.1, 2.2 and 2.3); 3. the energy absorption pattern over the electron range

(equation 2.5 and Fig. 2.2). Knowing all the above, it is possible to deduce an empirical formula to estimate the average absorbed dose A :

$$A = 0.75 \cdot \frac{R_e}{h_w} \cdot \eta(I) \cdot \eta(E) \cdot P_0 \cdot \frac{t}{m} \cdot n, \quad (\text{J/kg}) \quad (5.1)$$

where, R_e - penetration depth in mm calculated for a given accelerating voltage with the use of one of the equations 2.1, 2.2 and 2.3, h_w - distance between the titanium foil and internal anode in mm (height of the water stream - in our case $h_w=1-3$ mm), $\eta(I)$ - the transmission efficiency of the electron beam current, depending on the window material and thickness, at a given accelerating voltage (Fig. 2.4 and Fig. 4.11), $\eta(E)$ - the attenuation of the electron beam energy, depending on the window material and thickness, at a given accelerating voltage (Fig. 2.4 and Fig 4.12), P_0 - the incident electron beam power in W, t is the treatment time in s (water circulation time), m is the mass of treated water in kg, n is the number of exposures of the treated water of mass m during the treatment time t . The ratio R_e/h_w estimates the volume of water through which the incident electrons penetrate. The constant 0.75 is used to account for the average power absorbed within the penetration depth (see equation 2.5 and Fig. 2.2):

$$P_{av} = \frac{1}{R_e} \cdot \int_0^{R_e} 1 - \frac{9}{4} \left(\frac{z}{R_e} - \frac{1}{3} \right)^2 dz \cdot P_{max} = 0.75 \cdot P_0, \quad (5.2)$$

assuming that the incident beam power P_0 is equal to maximum power P_{max} , which is a reasonable assumption for low mass density materials, such as aqueous solutions.

Figure 5.7 shows the dependence of the relative content of TCE on the absorbed dose calculated by using equation 5.1, for two independent experiments: 1. with the use of 10 μm thick boron nitride window; 2. with the use of 25 μm thick titanium window. The initial concentration of trichloroethylene was equal to $C_0=12.5$ ppm and $C_0=13.5$ ppm in the case of using BN and Ti windows, respectively. Accelerating voltage and beam current were nearly the same in both cases - $V_A=170$ kV and $I=0.9$ mA for Ti window; $V_A=170$ kV and $I=0.85$ for boron nitride window.

The results shown in Fig. 5.7 indicate an exponential decrease in TCE concentration with an increase in the absorbed dose. Although two different windows were used for two independent measurements, the data seem to follow the same trend. The disappearance of TCE in deionized water below the detection level (0.001 ppm or 1 $\mu\text{g/liter}$) takes place at the absorbed dose of $A=7.5$ kJ/kg, but it has to be noted that the radiation dose required to remove the contaminant may vary with initial concentration, especially at a relatively high level, i.e. more than 2 ppm. For example, the reported absorbed dose (based on the temperature rise measurements) for 99% removal of TCE for the initial concentration being within the range of 5.2-7.6 ppm is barely equal to 1.07 kJ/kg [54]. The difference is probably caused by the differences in initial concentration of contaminants, in accelerating voltage (1.5 MV) and beam current ($I=50$ mA), and by the different way of absorbed dose estimation (temperature rise measurements).

Figure 5.8 shows the dependence of relative concentration of chloroform on the absorbed dose of electron radiation for two independent experiments. The experiments were performed using 25 μm thick titanium window. In this experiment [97,99], the water flow rate was 2 l/min and the volume of the treated solution was 1 liter. The initial concentrations of chloroform were $C_0=49.9$ ppm and $C_0=89.2$ ppm for the incident beam powers of $P=63$ W ($V=115$ kV, $I=0.55$ mA) and $P=187$ W ($V_A=170$ kV, $I=1.1$ mA), respectively. The radiated dose was controlled by the water circulation time.

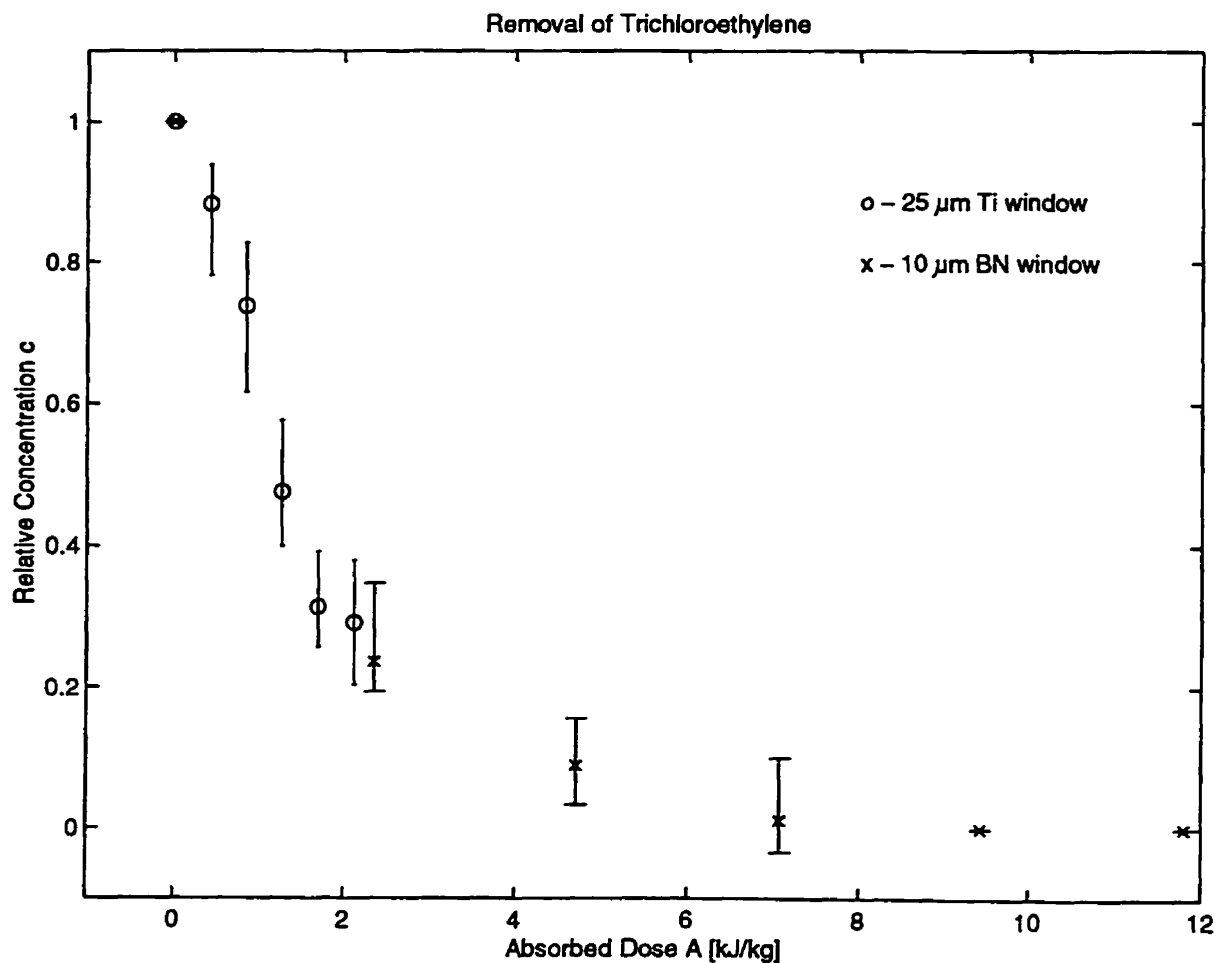


Figure 5.7. The dependence of the relative concentration of trichloroethylene vs. the estimated absorbed dose for two kinds of electron permeable windows.

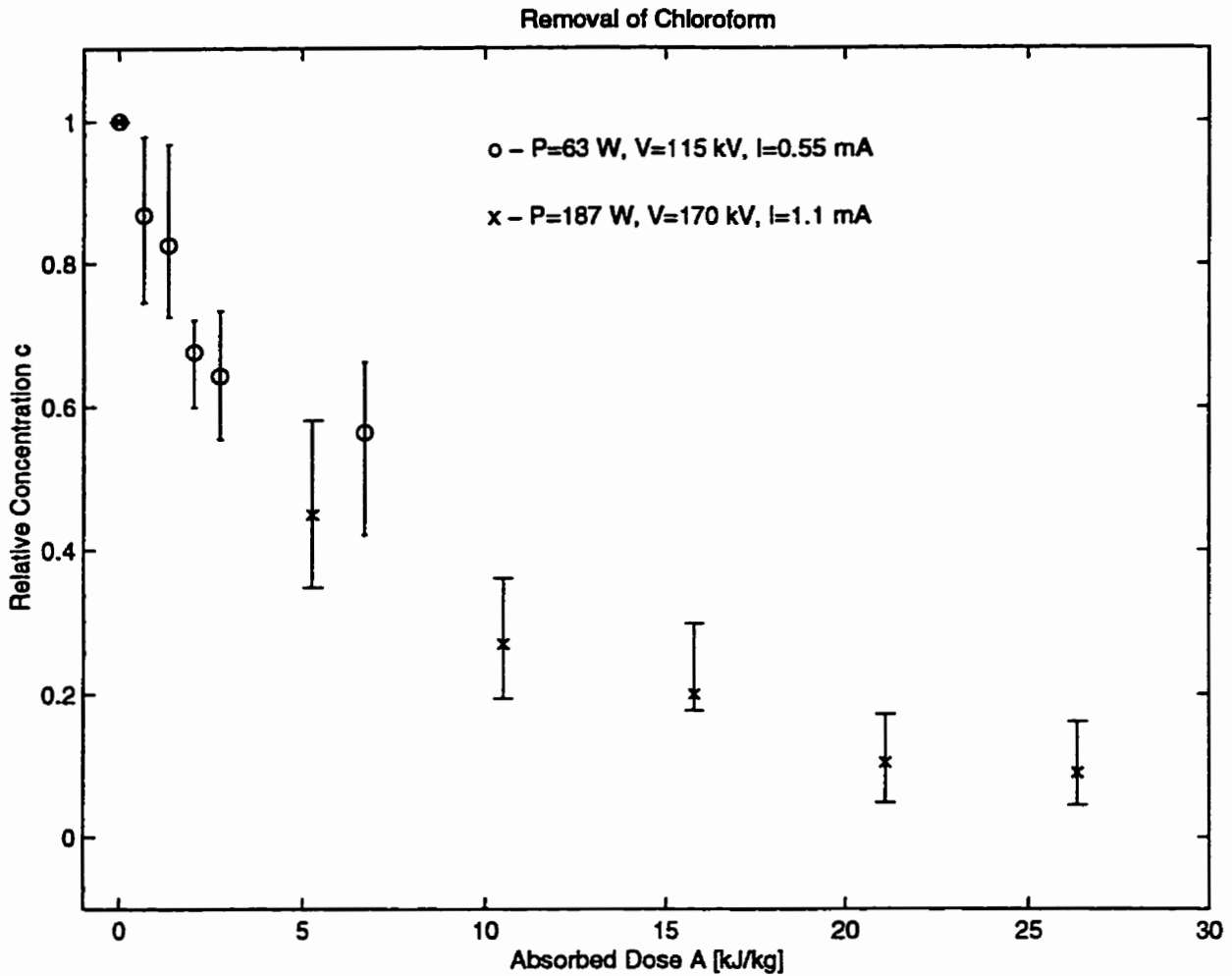


Figure 5.8. The dependence of the relative content of chloroform on absorbed dose for two different values of the incident beam powers: $P_0=63$ W, $V=115$ kV, $I=0.55$ mA, and $C_0=49.8$ ppm; and $P_0=187$ W, $V=170$ kV, $I=1.1$ mA, and $C_0=89.2$ ppm.

The 90% of chloroform removal is obtained for the absorbed dose of $A \approx 26$ kJ/kg. Similar to the results obtained in the case of TCE, the relative content of chloroform seems to decrease exponentially with an increase in the absorbed dose of electron radiation, in spite of different initial concentrations.

The absorbed doses needed for at least 90% removal of benzene and toluene have also been estimated. Figures 5.9 and 5.10 show the dependence of relative contaminant concentration depending on the absorbed dose (estimated using equation 5.1) for benzene and toluene, respectively.

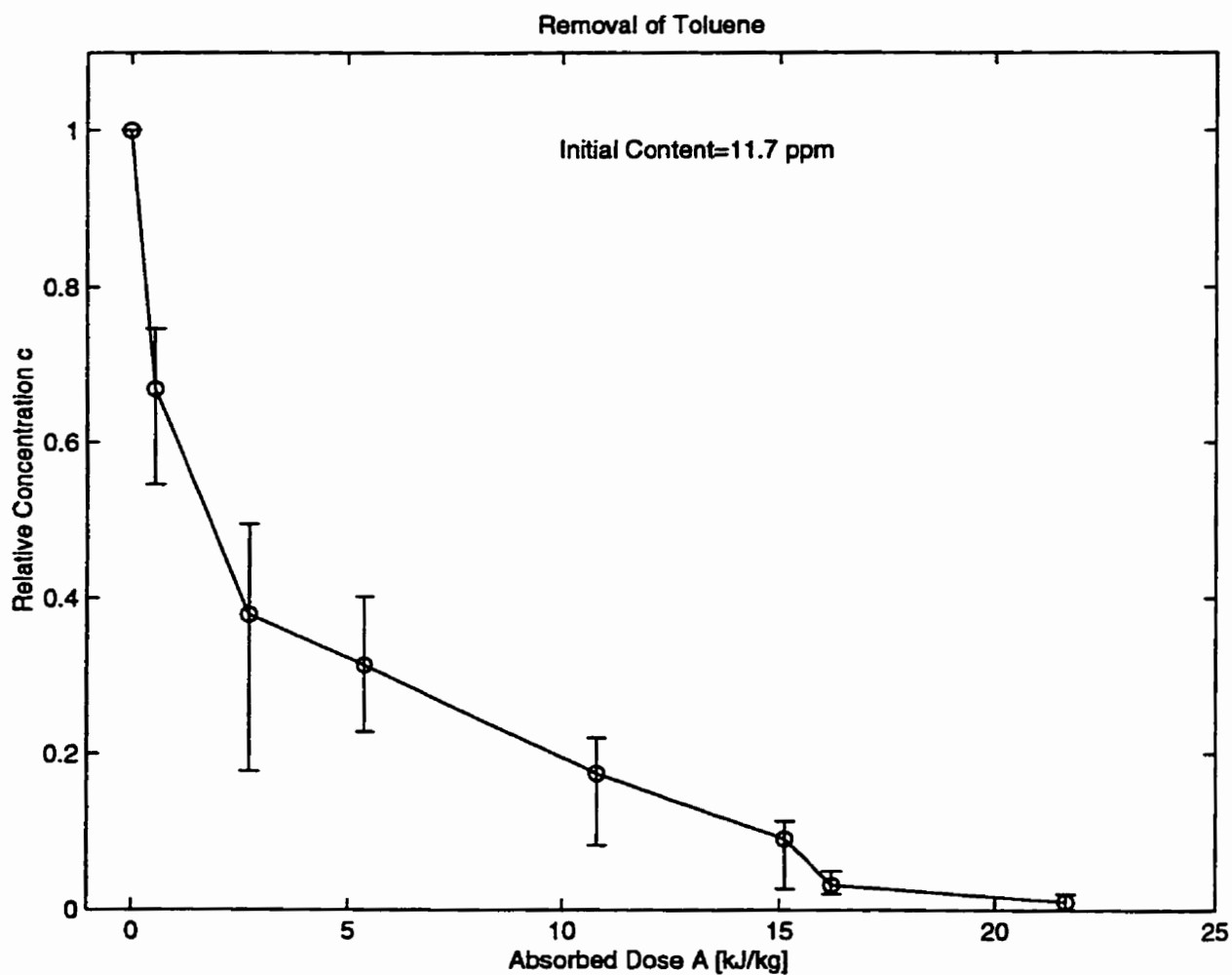


Figure 5.9. Relative content of toluene vs. absorbed dose of electron radiation.

In both experiments, the 10 μm thick boron nitride window was used. Mass of the treated water was equal to $m=2$ kg and the water flow rate was $\text{FR}=1$ kg/min. Electron beam power used in either case was equal to $P=70$ W (accelerating voltage $V_A=100$ kV and beam current $I_B=0.7$ mA). The initial concentration of toluene was $C_0=11.7$ ppm and the initial concentration of benzene was $C_0=12.9$ ppm.

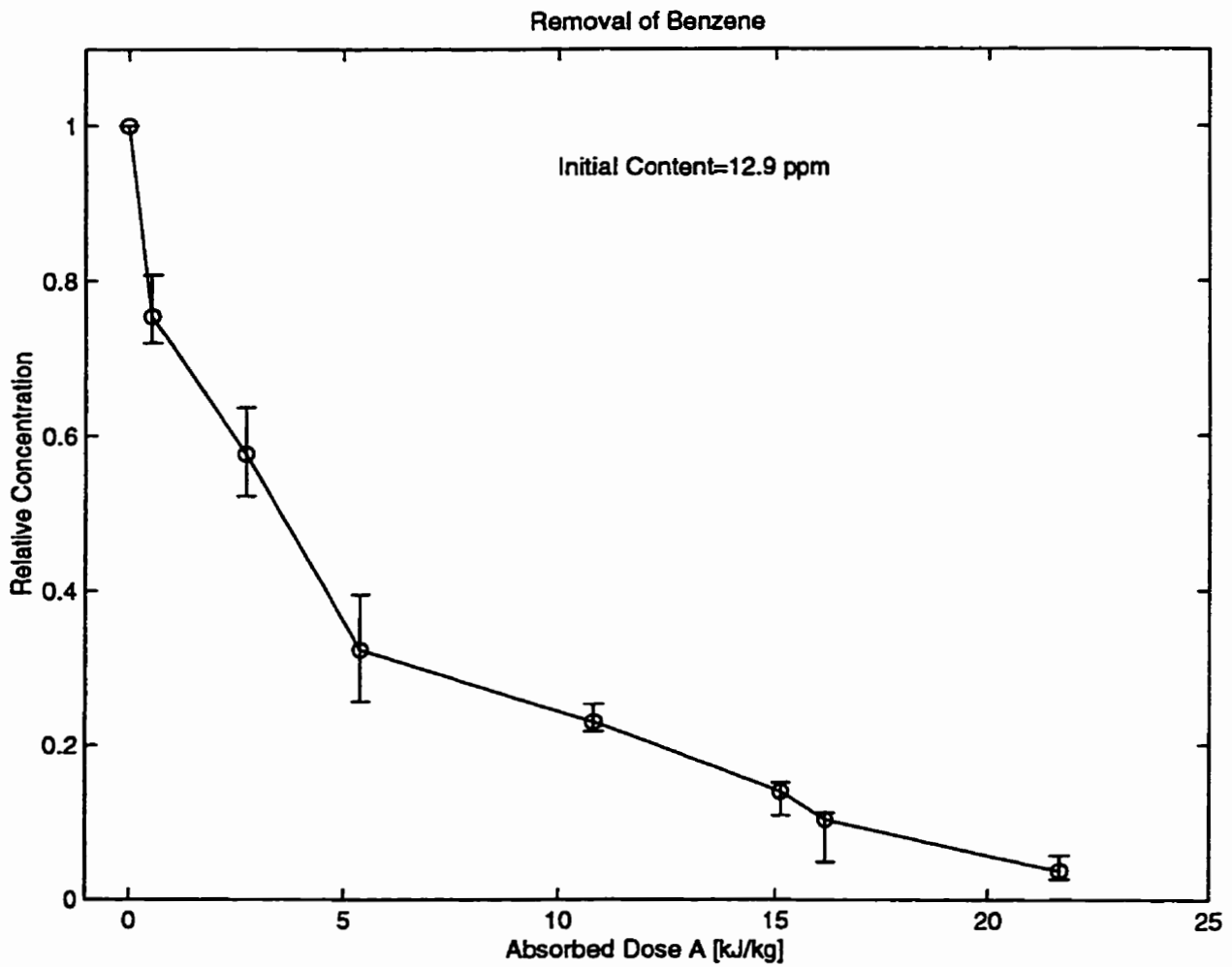


Figure 5.10. Relative concentration of benzene vs. absorbed dose of electron radiation.

The estimated absorbed doses required to decompose 90% of toluene and benzene are equal to $A \approx 14.8$ kJ/kg and $A \approx 16.2$ kJ/kg, respectively (Fig. 5.9 and 5.10). The similar values of the absorbed doses of electron radiation needed for 90% removal of both contaminants are due to their similar chemical structures as it has been reported in works [10,20,54].

The relative concentration of the investigated compounds decreases exponentially with increased absorbed dose, which has been confirmed in several independent measurements (Fig. 5.7-5.10). It is therefore obvious that the absorbed dose of radiation being a function of accelerating voltage, beam current, exposure time, and beam power conversion efficiency, is the main parameter upon which the relative removal depends. The exponential decrease in contaminant concentration can be expressed as a first order chemical reaction kinetics, and in the case of electron beam water treatment it can simply be described by using the formula [10]:

$$C = C_0 e^{-kA} \quad (5.3)$$

where, C (mole/liter) is the solute concentration at any absorbed dose A (J/kg), C_0 (mole/liter) is the initial solute concentration, and k (kg/J) is the dose constant representing the reaction rate, i.e. the amount of solute reduced per unit of the radiation energy absorbed. The constant k can be calculated on the basis of the measurements; however, it would have to be taken into account that this constant depends on various parameters, such as initial concentration, temperature, water pH, and alkalinity, etc.

5.4. By-products and intermediates during e-beam benzene removal

Electron beam water treatment of benzene aqueous solutions leads to the formation of several intermediates. It is claimed that during the electron beam oxidation process, phenolic, aldehyde and carboxylic acid intermediates are formed [10,22,40,41,54,72-75]. Phenols and aldehydes are harmful and their amount should be limited to a very low level. Recognition of the amount of the by-products depending on the radiation dose was the main purpose of this experiment.

The experiment was performed in cooperation with the NSERC Chair in Water Treatment, Civil Engineering Department, University of Waterloo, where all the chemical analysis to recognize the intermediates was performed. The initial concentration of benzene was equal to $C_0=9.9$ mg/liter. The accelerating voltage and the beam current were equal to 100 kV and 0.5 mA, respectively. The volume of the treated water was 4 liters and the water flow rate was equal to 1 liter/min. The total treatment time of the sample was equal to 140 min.

Figure 5.11 shows the dependence of benzene and total phenol concentrations on the calculated absorbed dose of electron radiation. The total phenol was calculated as a sum of the measured concentration of the following compounds: phenol, the total amount of which makes up almost 80% of the total phenolic intermediates, catechol, hydroquinone, and resorcinol. The maximum amount of the total phenol (1.91 mg/liter) appears at the absorbed dose of about 16 kJ/kg, which at the same time is the absorbed

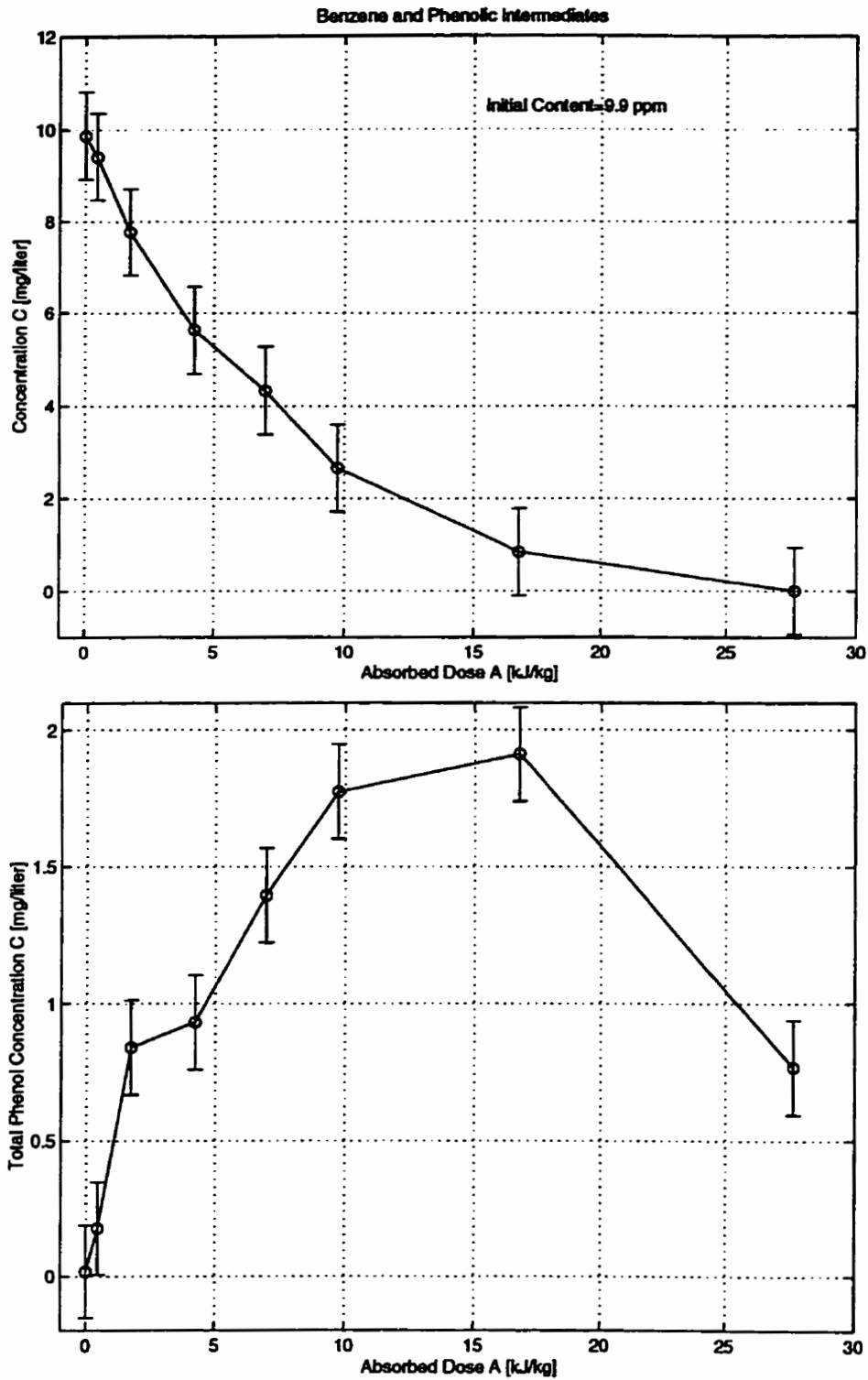


Figure 5.11. The dependence of benzene and total phenol concentrations on the estimated absorbed dose of electron beam radiation.

dose required for the decomposition of almost 90% of the initial amount of benzene. At the end of the experiment (the absorbed dose of about 27 kJ/kg), the total phenol concentration was barely 0.77 mg/liter. It can therefore be seen that, in the electron beam treatment, the radiation dose, which is required for total removal of the phenols, is higher than that needed for the total disappearance of benzene. It means that water streams containing benzene must be treated by the radiation doses that are required for the total disappearance of phenols formed during the oxidation.

Figure 5.12 shows the dependence of concentrations of benzene and total aldehydes on the calculated absorbed dose of electron radiation. The total aldehydes were calculated as a sum of measured concentrations of formaldehyde, the total amount of which makes up to 46% of the total aldehydes, acetylaldehyde, which totally contributes in 26% of the total aldehyde intermediates, glyoxal, and methylglyoxal. Although some aldehyde intermediates are considered to be carcinogens, their very low concentration (peak is 42 $\mu\text{g/liter}$ at the dose of about 16 kJ/kg) should not affect the attractiveness of electron beam water treatment. Again, the dose required for the complete removal of the aldehydes is higher than that needed for the complete decomposition of benzene. At the absorbed dose of 27 kJ/kg at which the benzene was not found, the concentration of the total aldehyde intermediates was 30 $\mu\text{g/liter}$.

Figure 5.13 shows the dependence of concentrations of benzene and total carboxylic acid intermediates on the calculated absorbed dose of electron radiation.

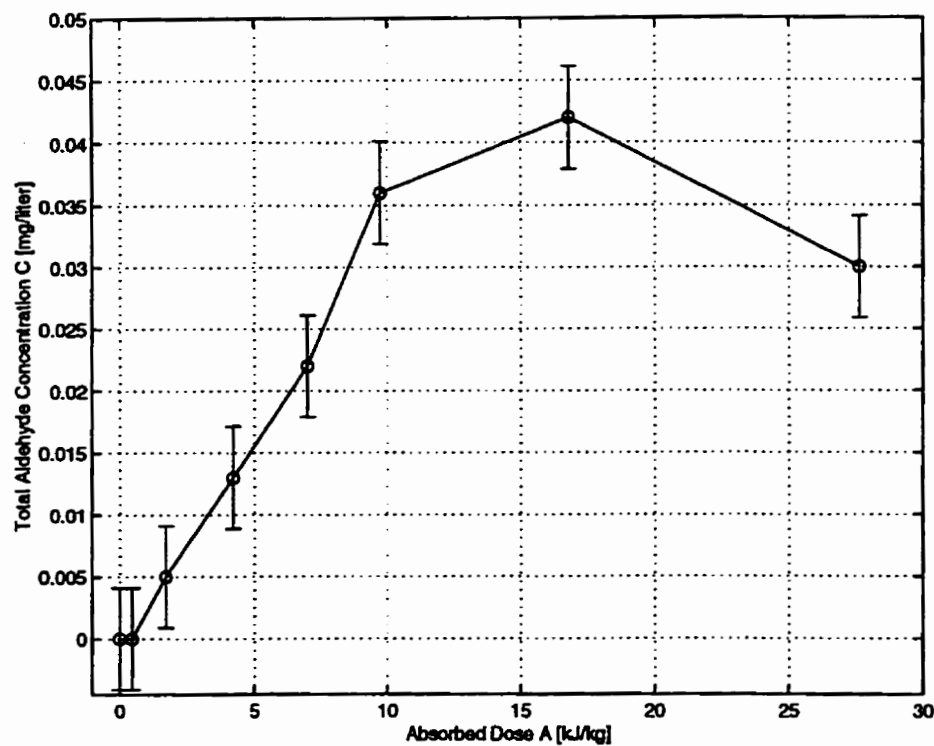
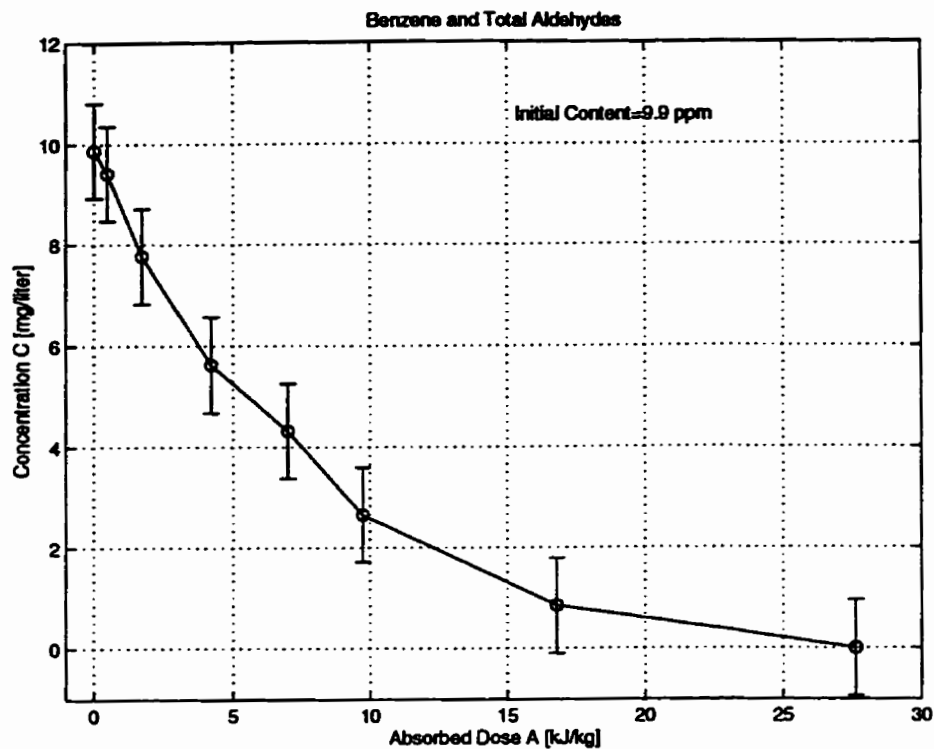


Figure 5.12. The dependence of the concentrations of benzene and total aldehydes on the estimated absorbed dose of electron beam radiation.

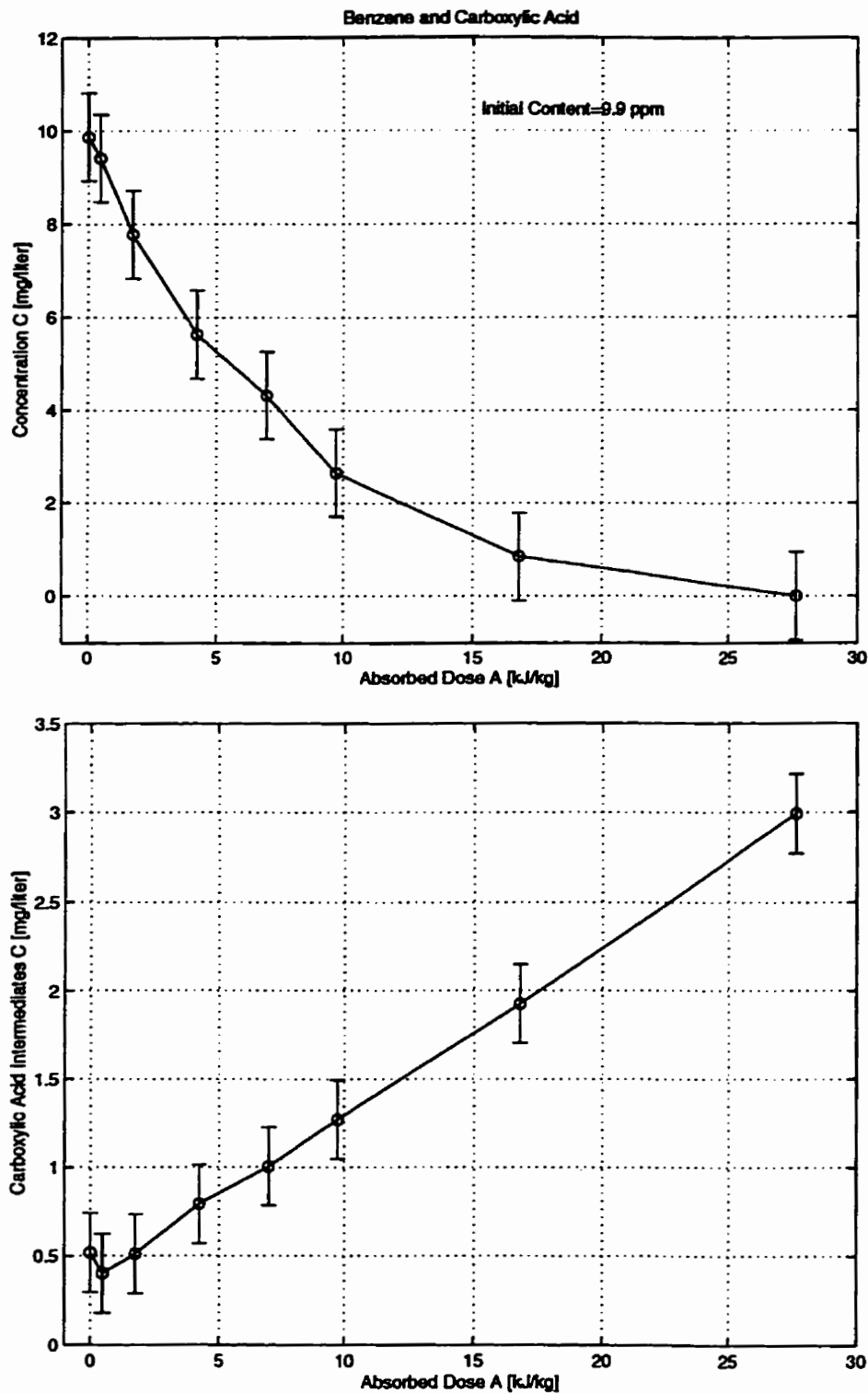


Figure 5.13. The dependence of the concentrations of benzene and total carboxylic acids intermediates on the estimated absorbed dose of electron beam radiation.

The concentration of the total carboxylic acid intermediates was calculated as the sum of the measured contents of the following compounds: hydroxybutyrate, acetate, glycolate, formate, pyruvate, ketobutyrate, and oxalate, which makes up almost 75% of the total concentration. It can be seen that the concentration of the carboxylic acid intermediates does not reach its peak within the range of the applied doses (up to 27 kJ/kg). It therefore suggests that this harmless product is most likely to appear when the electron beam oxidation is complete, i.e. when there are neither the phenolic nor the aldehyde intermediates present in the water. Although the carboxylic acid intermediates do not pose a direct threat to human health, their presence in water distribution system is a food source for some bacteria and facilitates a regrowth of pathogens that escape disinfection in a drinking water treatment plant. In a drinking water treatment therefore, the dose of the electron beam radiation should be as high as it is needed to completely decompose the carboxylic acid intermediates.

CHAPTER 6

RESULTS - REMOVAL OF NITROBENZENE

Nitrobenzene is a significant component of systems, which are used for radioactive waste extraction, for instance, in nuclear plants for extraction of cesium [100,101]. It is therefore important to search for a technology that can efficiently remove nitrobenzene and its radiolysis products from nuclear fuel reprocessing wastewater. To date, gamma-radiation has been used for this purpose [100,101]. Although nitrobenzene used in water for nuclear fuel reprocessing is exposed to partial autoradiolysis due to gamma radiation arisen from nuclear waste, the doses required for its removal are very high [101]. In other words, the exposure (treatment) time is long and volume of the treated water is small, e.g. 0.05 liters of water require about 15 minutes of treatment to remove approximately 150 ppm of nitrobenzene [101]. Nitrobenzene is also very resistant to chemical and biological degradation [100]. The air stripping process can not be used for nitrobenzene removal due to its very low volatility. Conventional water treatment processes, such as oxidation by chlorine or ozone and filtration/adsorption, can decompose this contaminant with a very limited efficiency [1,11,22].

For the first time, the electron beam radiation technique was used in the experiment concerning nitrobenzene removal. The 10 μm thick boron nitride window was used in the experiment. The mass of the treated water was equal to $m=2$ kg and the

water flow rate was $FR=1$ kg/min. The incident beam power was relatively low $P=40$ W ($V_A=100$ kV and $I_B=0.4$ mA), and the radiated dose of $D=72$ kJ/kg could be achieved per one hour of water circulation during the treatment. Figure 6.1 shows the dependence of the relative content of nitrobenzene depending on the absorbed dose estimated with the use of equation 5.1. The initial concentration of nitrobenzene was equal to $C_0=30.1$ ppm. The concentration of the contaminant before and after treatment was measured by using high purity liquid chromatography (HPLC) method. The HPLC analysis was performed on a 3.9 by 300 mm μ Bondapak™ C18 column (Waters, Milford, MA). The apparatus consists of two Shimadzu LC-600 pumps, a Shimadzu SPD-6A UV spectrophotometric detector, and a sample injector 7125 (all components from Shimadzu Corp., Kyoto). Sample (15 μ l) was injected and eluted with methanol and milliQ water (0.1% acetic acid). Solvents were delivered at the rate of 0.55 (methanol) and 0.45 (milliQ water) ml/min. The contaminant was monitored at UV A_{254nm} .

The obtained results (Fig. 6.1) show that about 80% of nitrobenzene can be decomposed for the absorbed dose of electron radiation being equal to $A\approx 24$ kJ/kg. It is higher than the doses obtained in the case of the volatile organic compounds. After the treatment, the treated solution still had a very bad odor and an even worse color than the initial solution. Because the radiolysis of the contaminant was not complete, it is believed that the formation of intermediates causes the negative changes in the treated water - mainly nitrophenols [22,101]. It is also believed that nitrophenols are more capable of being decomposed using biodegradation than nitrobenzene itself, therefore

the electron beam combined with the biodegradation could be much more efficient in the decomposition of this contaminant.

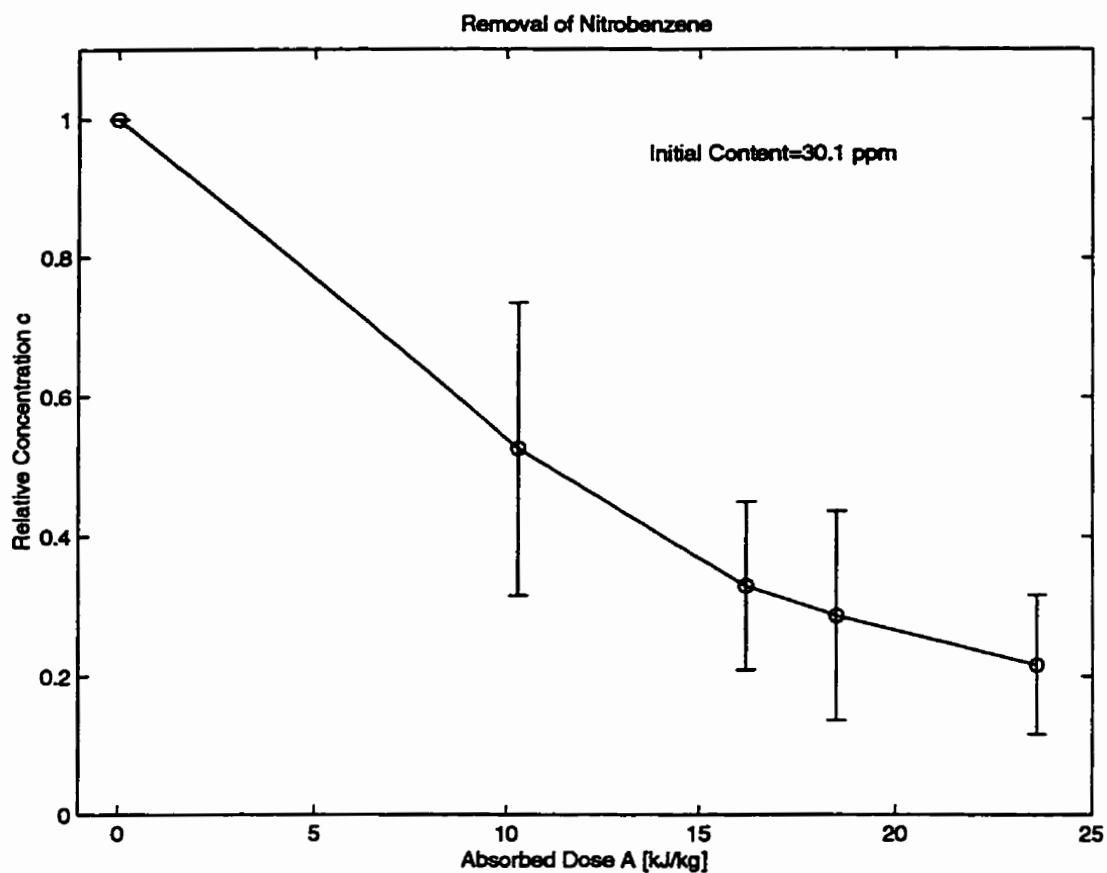


Figure 6.1. The dependence of the relative concentration of nitrobenzene vs. the estimated absorbed dose for 10 μm thick BN window and incident beam power $P=40\text{ W}$ (accelerating voltage $V_A=100\text{ kV}$ and electron beam current $I_B=0.4\text{ mA}$).

CHAPTER 7

DISCUSSION AND CONCLUSION

The volatile organic contaminants: trichloroethylene, toluene, benzene, chloroform, and, for the first time, nitrobenzene were removed from deionized water using electron beam irradiation technique at relatively low accelerating voltages (100-200 kV). For each compound investigated, the removal efficiency was relatively high (80-99%) even though the initial concentrations (10-100 ppm) were substantial. It has been found that the absorbed dose of radiation depending on accelerating voltage, beam current, exposure time and beam power conversion efficiency, should be thought as the main parameter on which the relative removal of contaminants depends. The average absorbed dose was calculated on the basis of the electron beam power utilization, equation 5.1. The formula used for calculations of the absorbed dose was confirmed for two different types of windows (Fig. 5.7) and for two different values of electron beam power (Fig. 5.8). In both cases, the relative contaminant concentration decreases exponentially with a rise in absorbed energy density. The exponential decrease in contaminant concentration with an increase in the absorbed dose is the common feature of the removal kinetics of all the investigated compounds (Fig. 5.5-5.10 and Fig. 6.1), even though their chemical structure and initial concentrations were different. The kinetics can be expressed as a first order reaction kinetics with the use of equation 5.3.

Table 7.1 shows the calculated values of the dose constant k (equation 5.3 – $C/C_0=e^{-kA}$).

The estimation was based on the results presented in Fig. 5.5-5.10 and Fig. 6.1.

Table 7.1. Estimated values of the rate constant k for the investigated contaminants.

Contaminant	Initial Content [mg/liter]	Rate Constant k [kg/kJ]	Fitting Coefficient R^2
Trichloroethylene	12.5-13.5	0.551	0.924
Toluene	11.7	0.232	0.934
Benzene	12.9	0.189	0.829
Chloroform	49.9-89.2	0.099	0.894
Nitrobenzene	30.1	0.065	0.948

The following pattern of the contamination removal in electron beam water treatment has been indicated on the basis of the obtained results: 1. TCE is the easiest to be decomposed - it is removed completely for the absorbed dose being equal to about 6.5 kJ/kg (Fig. 5.7); 2. toluene and benzene are moderately easy to remove from water - the required absorbed doses of radiation for 90% of the removal of both compounds are similar, approximately 14.8 kJ/kg and 16.2 kJ/kg, respectively (Fig. 5.9 and 5.10). The similarity in required dose for removal of benzene and toluene arises from a similarity in chemical structures of these compounds; 3. chloroform is the volatile organic compound that is the most resistant to electron beam decomposition - for 90% of its disappearance, the required absorbed dose is equal to 26 kJ/kg (Figure 5.8); 4.

nitrobenzene is more difficult to remove than all the investigated volatile chemicals - the absorbed dose of 24 kJ/kg is needed to decompose 80% of the compound (Fig. 6.1). The pattern obtained in the experiment, which is TCE<toluene<benzene<chloroform, is somewhat different than the theoretical pattern (TCE<chloroform<benzene<toluene) based on radiation chemistry [22,40,41,54,69-71]. The theoretical pattern is derived on the basis of the differences in chemical structures, bonds, properties, and in the sequence of, initiated by free radicals, chain reactions of the compounds in the case of the radiation induced oxidation. On the other hand, this pattern agrees with the experimental results presented in works [14-18,20,54] from the EBRF in Miami. The difference between the experiment and the theory can result from the fact that there is also a significant reducing action involved in the chemistry of the electron beam water treatment process.

In the work [3], it has been shown that chloroform has the most resistance for the removal using electron beam technique as far as chlorination by-products are considered. The remarkable reduction in chloroform concentration obtained in the studies suggests that the other trihalomethanes formed during chlorination can be decomposed by means of low and medium energy electron beam radiation. This means that the electron beam radiation can be efficiently used in drinking water treatment.

The results have also shown that it is possible to use electron beam to decompose nitrobenzene in water. The absorbed dose of electron radiation needed for an efficient decomposition of this contaminant is much higher than that in the case of volatile

organic compounds. Such a difficulty can be expected on the basis of the results concerning γ -ray radiation of nitrobenzene solutions presented in works [100,101], as the similar radiolysis process is associated with both treatments. In order to improve efficiency of the nitrobenzene removal in the future, the process may be combined with biodegradation or other processes with the use of which a removal of nitrophenolic intermediates is quite feasible.

The level of decomposition of the contaminants does not necessarily increase with an increase in incident electron beam energy; however the energy must be high enough to allow electrons to pass through the window and to penetrate reasonably deeply into the water stream. As the current transmission ratio of the window materials used in the experiment saturates at relatively low accelerating voltages (approximately 90 kV, 140 kV and 190 kV for 10 μm thick BN, 15 μm and 25 μm thick Ti windows, respectively, Fig. 4.11), the advantage of using a very high energy electron beam (over 1 MeV) in water treatment is to reduce relative loss of energy and enhance the penetration depth of electrons. The use of extra high accelerating voltage makes it possible to treat (penetrate) large volumes of water and therefore to reduce cost per unit volume of water, which typically is about US\$ 2.9 per 1000 gallons. At the same time, if the current is not increased, using a high accelerating voltage actually reduces the power absorbed per unit volume of the treated water, especially for low and medium accelerating voltages - equations 2.9, 2.10 and 2.11. As it is shown in Fig. 5.5, the power absorbed per unit volume of the water seems to have a significant effect on the

efficiency of the contamination removal. The increase in water throughput capacity and the reduction in cost per unit volume of water can also be achieved by increasing the electron beam current density at the point of action. Alternatively, power injection into water can be increased by increasing the power density that can be transmitted through the window without any implosion of electron transparent layer. This can be achieved by the choice of either the area of the window or the window material (such as boron nitride) and proper window cooling (similar to the one adopted in this experiment using the treated water as a coolant).

The use of a low absorptivity boron nitride window makes it possible to obtain a significant removal of hazardous contaminants using a relatively low voltage (~100 kV). This is because of a remarkable improvement in efficiency of electron beam power conversion into a power absorbed per unit volume of the treated water (Fig. 5.1-5.3). Although penetration depth of electrons at this level of voltage is limited to about 0.2 mm [22,23,26,27], the electron beam method is still quite efficient. This is important as far as design factors of water treatment facilities using electron beam radiation technique are concerned. The size of such facilities utilizing a low and medium accelerating voltage can be substantially reduced due to the facts that both insulation and X-ray shielding systems will be considerably simplified and their size will be reduced. A portable unit, which can actually be brought to various water sources, may therefore be built.

A high level of water throughput capacity for low energy electron beam water treatment can be obtained by an increase in radiation dose using higher current of electron beam. Some additional research is required to estimate the size of the window needed for higher beam power so as to prevent window implosion due to too high power density absorbed by the window. Considering high power operation (about 50-100 kW), the area of a water cooled boron nitride window would have to be of about 50-100 cm². It is possible to make such a layer on silicon wafer, but, even if the layer is thicker than 10 μm, it is yet very difficult to frame the BN layer in the way which would successfully allow the window to physically withstand the differential pressure encountered in operation. Assuming that the system would be designed in the similar way to the lab scale apparatus (Fig. 4.14 and 4.15), a solution to this problem could be a use of several small area (about 5 cm²) BN windows for parallel electrical and hydraulic operation. This would require the use of several low current electron guns and a high power, high voltage dc supply to provide the suitable overall current. An accelerating voltage of such a design could be within the range of 100-300 kV to maintain the compact size of the whole apparatus.

The designed lab scale electron beam water treatment apparatus can also be used to determine reaction kinetics for a variety of contaminants. Results obtained by using this apparatus could be very useful to estimate radiation doses required for a given level of contaminant decomposition. Once the needed dose is known, the proper scaling for high power equipment and high water flow rates can be done on condition that the

power absorbed per unit volume of a treated water is the same in both the lab scale and the high power commercial processes.

The obtained results concerning by-products distribution during benzene removal (Fig. 5.11-5.13) seem to confirm the fact that the fully completed radiation oxidation of benzene results in its decomposition into water, carbon dioxide, and harmless carboxylic acid. It has to be noted that the measured intermediates occur typically during an oxidation of benzene by hydroxyl radical. More research is required to identify the by-products and intermediates which can occur in the electron beam treatment due to its reducing action, since the reducing radicals are also formed during the electron beam water treatment. The obtained results provide us with a very important conclusion. They show that certain by-products and intermediates, such as the total phenolic and aldehyde intermediates in the case of benzene, do not disappear from the treated water at the same time as the parent compound does (Fig. 5.11 and 5.12). This fact has to be taken into account when a commercial use of electron beam in water treatment is considered. In such a case, the required dose would have to be established on the basis of intermediate distribution, especially if such products pose a potential threat to environment, not at the point of the total decomposition of a parent compound.

Much more research is required to identify the by-products and intermediates in the case of the other compounds. This is especially important in the case of electron beam irradiation of chloroform and nitrobenzene aqueous solutions, as these compounds are fairly resistant to the radiation and high doses are required for their

complete removal. Not only could the identification of the by-products and intermediates during electron beam process be used to verify and establish the dose required to purify a given water stream, but it would also allow one to choose the most efficient combination between electron beam water treatment and any other suitable water purification technology to increase the efficiency of the clean-up.

REFERENCES

- [1] Getoff N., "Advancements of Radiation Induced Degradation of Pollutants in Drinking and Waste Water", *Applied Radiation and Isotopes* 7(1989)585-594
- [2] Montgomery J. M., Inc., *Water Treatment: Principles and Design*, John Wiley & Sons, Wiley Interscience, New York, 1985
- [3] Cooper W. J., Cadavid E.-M., Nickelsen M. G., Lin K., Kurucz C. N., Waite T. D., "Removing THMs from Drinking Water Using High-Energy Electron Beam Irradiation", *Journal of American Water Works Association* 9(1993)106-113
- [4] Metcalf and Eddy, Inc., *Wastewater Engineering - Treatment/Disposal/Reuse*, 3rd Edition, McGraw-Hill, New York, 1991
- [5] American Water Works Association (AWWA), *Water Quality and Treatment*, 4th Edition, 1990
- [6] ASCE-AWWA, *Water Treatment Plant Design*, 2nd Edition, 1990
- [7] Benefield L. D., Judkins J. F., Weand B. L., *Process Chemistry for Water and Wastewater Treatment*, Prentice Hall, New Jersey, 1982
- [8] Glaze B., "The Chemistry of Water Treatment Processes Involving Ozone, H₂O₂ and UV", *Ozone Science and Engineering* 9(1987)335-352
- [9] Buxton G. V., Greenstock C. L., Helman W. P., Ross A. B., "Critical Review of Rate Constants for Reactions of Hydrated Electrons, Hydrogen atoms and Hy-

**droxyl Radicals in Aqueous Solution”, Journal of Physical Chemistry
17(1988)513-886**

- [10] Nickelsen M. G., Cooper W. J., Kurucz C. N., Waite T. D., “Removal of Benzene and Selected Alkyl-Substituted Benzenes from Aqueous Solution Utilizing Continuous High-Energy Electron Irradiation”, Environmental Science and Technology 26(1992)144-152**
- [11] Getoff N., “Radiation and Photoinduced Degradation of Pollutants in Water. A Comparative Study”, Radiation Physics and Chemistry, 37(1991)673-680**
- [12] Gehringer P., Eschweiler H., Szinovatz W., Fiedler H., Steiner R., Sonneck G., “Radiation-Induced OH Radical Generation and Its Use for Groundwater Remediation”, Radiation Physics and Chemistry 12(1992)71-714**
- [13] Waite T. D., Cooper W. J., Kurucz C. N., “Recent Advances in Electron Beam Irradiation of Wastewater and Hazardous Waste”, Proceedings of the American Society of Civil Engineers, National Conference of Environmental Engineering, Washington DC, July 1990**
- [14] Kurucz C. N., Waite T. D., Cooper W. J., Nickelsen M. G., “High Energy Electron Beam Irradiation of Water, Wastewater and Sludge”, Advances in Nuclear Science and Technology 22(1991)1-43**
- [15] Waite T. D., Cooper W. J., Kurucz C. N., Nickelson M., “Wastewater Treatment Utilizing Electron Beam Technology. Water Quality Changes and Toxin De-**

- struction”, National Conference on Environmental Engineering, ASCE, NY USA, 1990, pp. 55-61
- [16] Farooq S., Kurucz C., Waite T. D., Cooper W. J., Mane S. R., Greenfield J. H., “Treatment of Wastewater with High Energy Electron Beam Irradiation”, *Water Science and Technology*, 26(1992)1265-1274
- [17] Mane S., Greenfield J., Narbaitz R., Bhatt T., Cooper W., Waite T. D., Kurucz C., “Electron Beam Irradiation of Wastewater”, National Conference on Environmental Engineering”, ASCE, NY USA, 1990, pp. 901-902
- [18] Cooper W. J., Nickelsen M. G., Meacham D. E., Waite T. D., Kurucz C. N., “High Energy Electron Beam Irradiation. An Advanced Oxidation Process for the Treatment of Aqueous Based Organic Hazardous Wastes”, *Pollution Research Journal of Canada*, 27(1992)69-95
- [19] Kurucz C. N., Waite T. D., Cooper W. J., Nickelsen M. G., “Full-Scale Electron Beam Treatment of Hazardous Wastes - Effectiveness and Costs”, 45th Purdue Industrial Waste Conference Proceedings, 1991, pp. 539-545
- [20] Nickelsen M. G., Cooper W. J., Lin K., Kurucz C., Waite T. D., “High Energy Beam Generation of Oxidants for the Treatment of Benzene and Toluene in the Presence of Radical Scavengers”, *Water Research* 5(1994)1227-1237
- [21] Farooq S., Kurucz C. N., Waite T. D., Cooper W. J., “Disinfection of Wastewaters: High Energy Electron vs. Gamma Irradiation”, *Water Research* 7(1994)1177-1184

- [22] Woods R. J., Pikaev A. K., *Applied Radiation Chemistry: Radiation Processing*, John Wiley & Sons, New York, 1994
- [23] Bradley R., *Radiation Technology Handbook*, Marcel Dekker, New York, 1984
- [24] Siddiqui M., Amy G., Nickelsen M. G., "Bromate Ion Removal by HEEB Irradiation", *Journal of the American Water Works Association*, 10(1996)90-97
- [25] Vysotskaya N. A., Bortun L. N., Derbaremdiker P. Z., "Use of Radiation Treatment for Decoloration of Sewage Containing Dyes", *Khimiya i Tekhnologiya Vody* 15(1993)31-37
- [26] Bakish R., *Introduction to Electron Beam Technology*, John Wiley & Sons, New York - London, 1962
- [27] Sciller S., Heisig U., Panzer S., *Electron Beam Technology*, A Wiley Interscience Publication, John Wiley & Sons, New York, 1982
- [28] Simonis, P. J. C. A., *Handbook of Electron Beam Processing*, Vol. IND-001. Burlington, Mass.: High Voltage Engineering Corp., 1979
- [29] Du Plessis T. A., De Hollain G., "Electron Beam Curing of Coatings", *J. Oil Col. Chem. Assoc.* 62(1979)239-245
- [30] Stolz W., *Strahlensterilisation*, Leipzig: J. Ambrosius-Barth-Verlag, 1972
- [31] Abstracts of *The First International Conference on Advanced Oxidation Technologies for Water and Air Remediation*, London, Ontario, Canada, June, 1994
- [32] Abstracts of *The Third International Conference on Advanced Oxidation Technologies for Water and Air Remediation*, Cincinnati, Ohio, USA, October, 1996

- [33] Dolin P. I., Shubin V. N., Brusentseva S. A., *Radiation Purification of Water*, Nauka, Moscow, 1973
- [34] Grosswendt B., Roos M., "Electron Beam Absorption in Solid and in Water Phantoms: Depth Scaling and Energy-Range Relations", *Physics in Medicine and Biology*, 34(1989)509-518
- [35] von Ardenne M., *Tabellen zur Angewandten Physik*, Vol. 1, 2nd edition, VEB Dtsch. Verlag d. Wissenschaft, Berlin, 1962
- [36] Holmes-Siedle A., Adams L., *Handbook of Radiation Effects*, Oxford University Press, Oxford-New York-Tokyo, 1993
- [37] Ziegler J. F., Biersack J. P., Littmark, *The Stopping Power and Range of Ions in Solids*, Pergamon Press, Oxford, 1985
- [38] Kelly A. J., U.S. Patent No. 5,478,266, Dec. 1995
- [39] Kelly A. J., "On the statistical, quantum and practical mechanics of electrostatic atomization", *Journal of Aerosol Science* 6(1994)1159-1177
- [40] Draganic I. G., Draganic Z. D., *The Radiation Chemistry of Water*, Academic Press, New York and London, 1971
- [41] Pikaev A. K., *Pulse Radiolysis of Water and Aqueous Solutions*, Indiana University Press, Bloomington & London, 1967
- [42] Buxton G. V., "Pulse Radiolysis Studies of Aqueous Solutions" in *Pulse Radiolysis* edited by Yoneho Tabata, CRC Press, Boca Raton-Ann Arbor-Boston, 1991

- [43] Buxton G. V., "Radiation Chemistry of the Liquid State: (1) Water and Homogeneous Aqueous Solutions" in *Radiation Chemistry* edited by Farhatziz and M. A. J. Rogers, VCH, New York, 1987
- [44] Kaindl K., Graul E. H., *Strahlenchemie*, Heidelberg, A. Huethig-Verlag, 1967
- [45] Kalashnikov N. A., Kalinichenko B. S., Shvetsov I. K., "Influence of Reagent Phase State, Form and Dose Rate Irradiation on Efficiency of Radiolytic Decomposition of Water and Carbon Dioxide", *Atomnaya Energiya* 72(1992)47-53
- [46] Terrissol M., Beaudre A., "Simulation of Space and Time Evolution of Radiolytic Species Induced by Electrons in Water", *Radiation Protection Dosimetry* 31(1990)175-177
- [47] Ushakov W. Ya., *Impulsnyî Elektricheskiî Proboî Zhidkosteî*, Izdatelstvo Tomskovo Universiteta, Tomsk, 1975
- [48] Adamczewski I., *Ionization, Conductivity and Breakdown in Dielectric Liquids*, Taylor & Francis Ltd., London, 1969
- [49] Alkhimov A. P., Vorob'ev V. V., Klimkin V. F., Ponomarenko A. G., Soloukhin R. I., "The Development of Electrical Discharge in Water", *Soviet Physics - Doklady* 15(1971)959-961
- [50] K. A. Naugolnykh, N. A. Roy., *Elektricheskie Razryady v Vode*, Moscow, Izdatelstvo Nauka, 1971

- [51] Yanshin E. V., Ovchinnikov I. T., Vershinin Yu. N., "Mechanism of the Pulsed Electrical Breakdown of Water", Soviet Physics - Doklady, Technical Physics 19(1974)95-96
- [52] Kuskova N. I., "Mechanisms of Electrical Breakdown in Water", Soviet Technical Physics Letters 15(1989)936-937
- [53] Srebrov B. A., Dishkova L. P., Kuzmanova F. I., "Electrical Breakdown of a Small Gap Filled with Distilled Water", Soviet Technical Physics Letters 16(1990)70-71
- [54] Cooper W. J., Waite T. D., Kurucz C. N., Nickelsen M. G., Lin K., "An Overview of the Use of High Energy Electron Beam Irradiation for the Destruction of Toxic Organic Chemicals from Water, Wastewater and Waters Containing Solids", manuscript of the paper submitted for consideration in: Emerging Technologies for Hazardous Waste Management, 1992
- [55] Dorfman L. M., Adams G. E., "Reactivity of the Hydroxyl Radical in Aqueous Solution", National Standards Reference Data Series of National Bureau of Standards (USA) 46(1973)1-59
- [56] Mak F. T., Zele S. R., Cooper W. J., Kurucz C. N., Waite T. D., Nickelsen M. G., "Kinetic Modeling of Carbon Tetrachloride, Chloroform and Methylene Chloride Removal from Aqueous Solution Using the Electron Beam Process", Water Research 2(1997)219-228

- [57] Marton L., El-Kareh A. B. (eds), *Electron Beam and Laser Technology*, Academic Press, New York and London, 1968
- [58] Sedlacek M., *Electron Physics of Vacuum and Gaseous Devices*, A Wiley-Interscience Publication, John Wiley & Sons, Inc., 1996
- [59] Amboss K., "The Design of Large Area Beam Guns", in *Electron Beam and Ion Beam Science and Technology, 6th International Conference, San Francisco, California, 1974*, edited by R. Bakish. Electrochemical Society, Princeton, NJ, 1974, pp.482-517
- [60] Cleland M. R., Thompson C. C., Malone H. F., "The Prospects for Very High-Power Electron Accelerators for Processing Bulk Materials", *Radiation Physical Chemistry* 9(1977)547-566
- [61] Cleland M. R., Morgenstern K. H., Thompson C. C., "High Power DC Electron Accelerators for Industrial Applications", *Proceedings of the 3rd All-Union Conference on Applied Accelerators, Leningrad, USSR, June 26-28, 1979*
- [62] Cleland M. R., "Electron Beam Processing, Future Markets/Future Equipment", *RDI Technical Information Series TIS 80-3*, March, 1980
- [63] Cleland M. R., "Electron Beam Technology for Environmental Applications", *Proceedings of the MIT/NSF Seminar on Electron Disinfection of Municipal Sludge for Beneficial Disposal, MIT, June 23-24, 1980*
- [64] Becker R.C., Bly J. H., Cleland M. R., Farrel J. P., "Accelerator Requirements for Electron Beam Processing", *Radiation Physical Chemistry* 14(1979)353-375

- [65] Yost K. W., "UV Peroxidation: An Alternative Treatment Method for Organic Contamination Destruction in Aqueous Waste Streams", Proceedings of the 43rd Purdue Industrial Waste Conference, West Lafayette, IN, 1988
- [66] Shuetz M., "Design and Testing of Semi-Portable Electron Accelerators Specifically Intended for the Treatment of Aqueous Streams", The First International Conference on Advanced Oxidation Technologies for Water and Air Remediation, Abstracts, London, Ontario, June 25-30, 1994
- [67] Alvarez F., Topudurti K., Keefe M., Petropoulou C., Schlichting T., "Demonstration of HVEA High-Voltage Electron Beam Technology", The Third International Conference on Advanced Oxidation Technologies for Water and Air Remediation, Abstracts, London, Ontario, June 25-30, 1994
- [68] Dickson L. W., Lopata V. J., Toft-Hall A., Kremers W., Singh A., "Radiolytic Removal of Trihalomethanes from Water", Proceedings from the 6th Symposium on Radiation Chemistry, 1986, pp.173-182
- [69] Gehringer P., Proksch E., Szinovatz W., "Radiation-Induced Degradation of Trichloroethylene and Tetrachloroethylene in Drinking Water", International Journal of Applied Radiation and Isotopes 36(1985)313-330
- [70] Gehringer P., Proksch E., Szinovatz W., Eschweiler H., "Radiation Induced Decomposition of Aqueous Trichloroethylene Solutions", Applied Radiation and Isotopes 39(1988)1227-1231

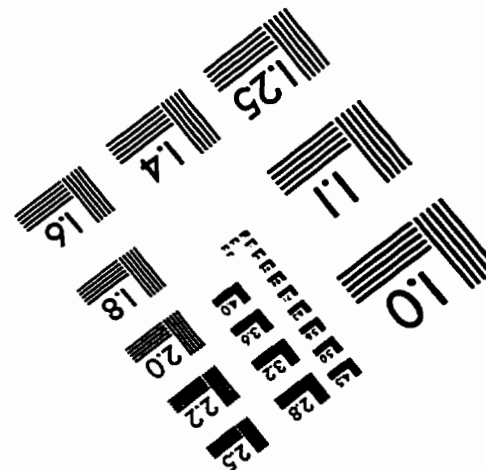
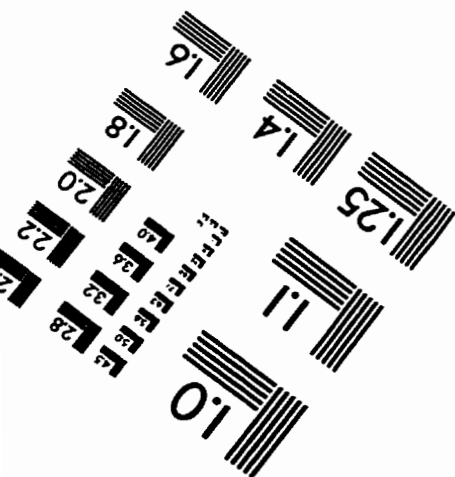
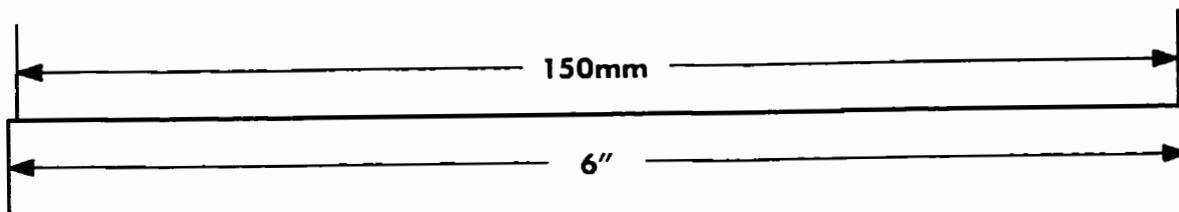
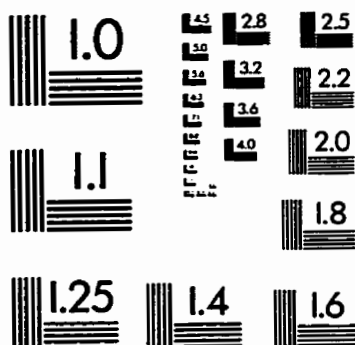
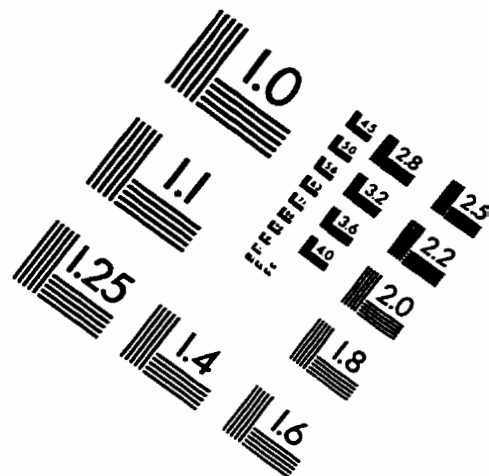
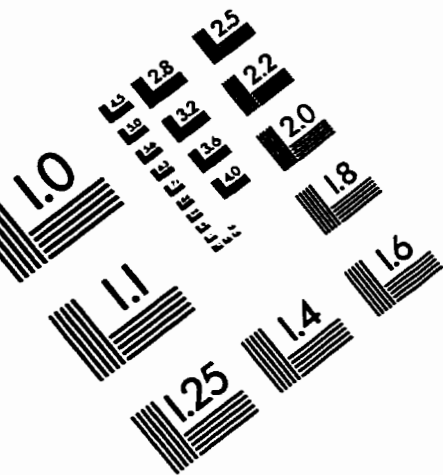
- [71] Getoff N., "Radiation Induced Decomposition of Biologically Resistant Pollutants in Water", *Applied Radiation and Isotopes* 37(1986)1103-1120
- [72] Dorfman L. M., Taub I. A., Buehler R. E., "Pulse Radiolysis Studies. I. Transient Spectra and Reaction-Rate Constants in Irradiated Aqueous Solutions of Benzene", *Journal of Chemical Physics* 36(1962)3051-3061
- [73] Michael B. D., Hart E. J., "The Rate Constants of Hydrated Electron, Hydrogen Atom and Hydroxyl Radical Reactions with Benzene, 1,3-Cyclohexadiene, 1,4-cyclohexadiene and cyclohexene", *Journal of Physical Chemistry* 74(1970)2878-2884
- [74] Schested K. H., Corfitzen H, Christensen H. C., Hart E. J., "Rates of Reaction of O, OH and H with Methylated Benzenes in Aqueous Solution. Optical Spectra of Radicals", *Journal of Physical Chemistry* 79(1983)310-315
- [75] Getoff N., Solar S., "Radiation Induced Decomposition of chlorinated Phenols in Water", *Radiation Physics and Chemistry* 31(1988)121-130
- [76] J. D. Cross, High Voltage Power Supply, US Patent, 5,631,815, May 1997
- [77] Richardson O. W., "The Electrical Conductivity Imparted to a Vacuum by Hot Conductors", *Phil. Trans. Roy. Soc.*, A201(1903)497-508
- [78] Dushman S., "Electron Emission from Metals as a Function of Temperature", *Physical Review*, 21(1923)623-636
- [79] Nottingham W. B., "Thermionic Emission from Tungsten and Thorated Tungsten Filaments", *Physical Review* 49(1936)78-87

- [80] Langmuir I., "The Effect of Space Charge and Residual Gases on Thermionic Currents in High Vacuum", *Physical Review* 2(1913)450-461
- [81] Hall C. E., *Introduction to Electron Microscopy*, 2nd Edition, McGraw-Hill Book Company, New York, 1966
- [82] Thomas G., *Transmission Electron Microscopy of Metals*, John Wiley & Sons, Inc., New York, 1962
- [83] Zworykin V. K., Morton G. A., Ramberg E. G., Hillier J., Vance A. W., *Electron Optics and the Electron Microscope*, New York: John Wiley & Sons, Inc., London: Chapman & Hall, Limited, 1945
- [84] Haine M. E., Cosslett V. E., *The Electron Microscope: The Present State of Art*, Interscience Publishers, New York, 1961
- [85] Noaker P. M., "Hard Facts on Hard Turning", *Manufacturing Engineering*, February 1992, pp.43-46
- [86] Kester D. J., Alley K. S., Lichtenwainer D. J., Davis R. F., "Growth and Characterization of Cubic Boron Nitride Films", *Journal of Vacuum Science and Technology* 12(1994)3074-3081
- [87] Zhou D. S., Chen C. L., Mitchell T. E., Hackenberger L. B., Messier R., "Thin Films of Cubic Boron Nitride on Silicon", *Philosophical Magazine Letters* 3(1995)163-166

- [88] Knott J. F., "Metals and Ceramics - Mechanical Properties", in *Future Developments of Metals and Ceramics* edited by J. A. Charles, G. W. Greenwood, G. C. Smith, The Institute of Materials, London, UK, 1992
- [89] *Materials Science and Engineering Handbook*, edited by J. F. Shackelford, W. Alexander, J. S. Park, CRC Press, Boca Raton, Ann Arbor, London, Tokyo, 1994
- [90] *Ceramic Raw Materials*, edited by D. J. DeRenzo, Noyes Data Corp., Park Ridge, NJ, USA, 1987
- [91] *Handbook of Chemistry and Physics*, edited by D. R. Lide, H. P. R. Fredrikse, CRC Press, Boca Raton, New York, London, Tokyo, 1995/96
- [92] "Boron", *Supplement to Mellor's Comprehensive Treatise on Inorganic and Theoretical Chemistry*, Volume V, Longman, London and New York, 1980
- [93] Goodfellow Products, Catalogue 1996/97
- [94] Schwartz M. M., *Handbook of Structural Ceramics*, Mc Graw-Hill, Inc., 1992
- [95] Lubicki P., Cross J. D., Jayaram S., "Decomposition of chloroform and trichloroethylene in water with the use of low voltage electron beam", Proceedings of 12th International Conference on Conduction and Breakdown in Dielectric Liquids, Rome, Italy, July 15-19, 1996, pp. 442-445
- [96] Lubicki P., Cross J. D., Jayaram S., Zhao J. S., Ward O., "Removal of nitrobenzene and volatile organic compounds using electron radiation", 1997 IEEE Annual Report - Conference on Electrical Insulation and Dielectric Phenomena, Minneapolis, Minnesota, USA, October 19-22, 1997, Volume 2, pp.698-701

- [97] Lubicki P., Cross J. D., Jayaram S., "Removal of volatile organic compounds in water using electron beam", accepted to be published in IEEE Transactions on Dielectrics and Electrical Insulation, 1998.
- [98] American Society for Testing and Materials-ASTM, "Standard Practice for Micro-Extraction of Water for the Analysis of Volatile and Semivolatile organic Compounds", Designation: D5241-92, Sept. 1992
- [99] American Society for Testing and Materials-ASTM, "Proposed Test Method for Determination of Semivolatile Organic Compounds in Water by Gas Chromatography/Mass Spectrometry (GC/MS)", Designation: D-19, Proposal P241, Feb. 1994
- [100] Kuruc J., Sahoo M. K., Locaj J., Hutta M., "Radiation Degradation of Waste Waters. I. Reverse Phase-High Performance Liquid Chromatography and Multi-component UV-VIS Analysis of Gamma-Irradiated Aqueous Solutions of Nitrobenzene", Journal of Radioanalytical and Nuclear Chemistry. Articles 1(1994)99-107
- [101] Cechova S., Macasek F., Cech R., "Radiation Yields of Phenol Derivatives in Nitrobenzene-Water Systems", Radiation Physics and Chemistry 2(1987)119-123

IMAGE EVALUATION TEST TARGET (QA-3)



APPLIED IMAGE, Inc
1653 East Main Street
Rochester, NY 14609 USA
Phone: 716/482-0300
Fax: 716/288-5989

© 1993, Applied Image, Inc., All Rights Reserved